

Appendix A

Westinghouse Owners Group and PNNL Flawed Weld Specimens

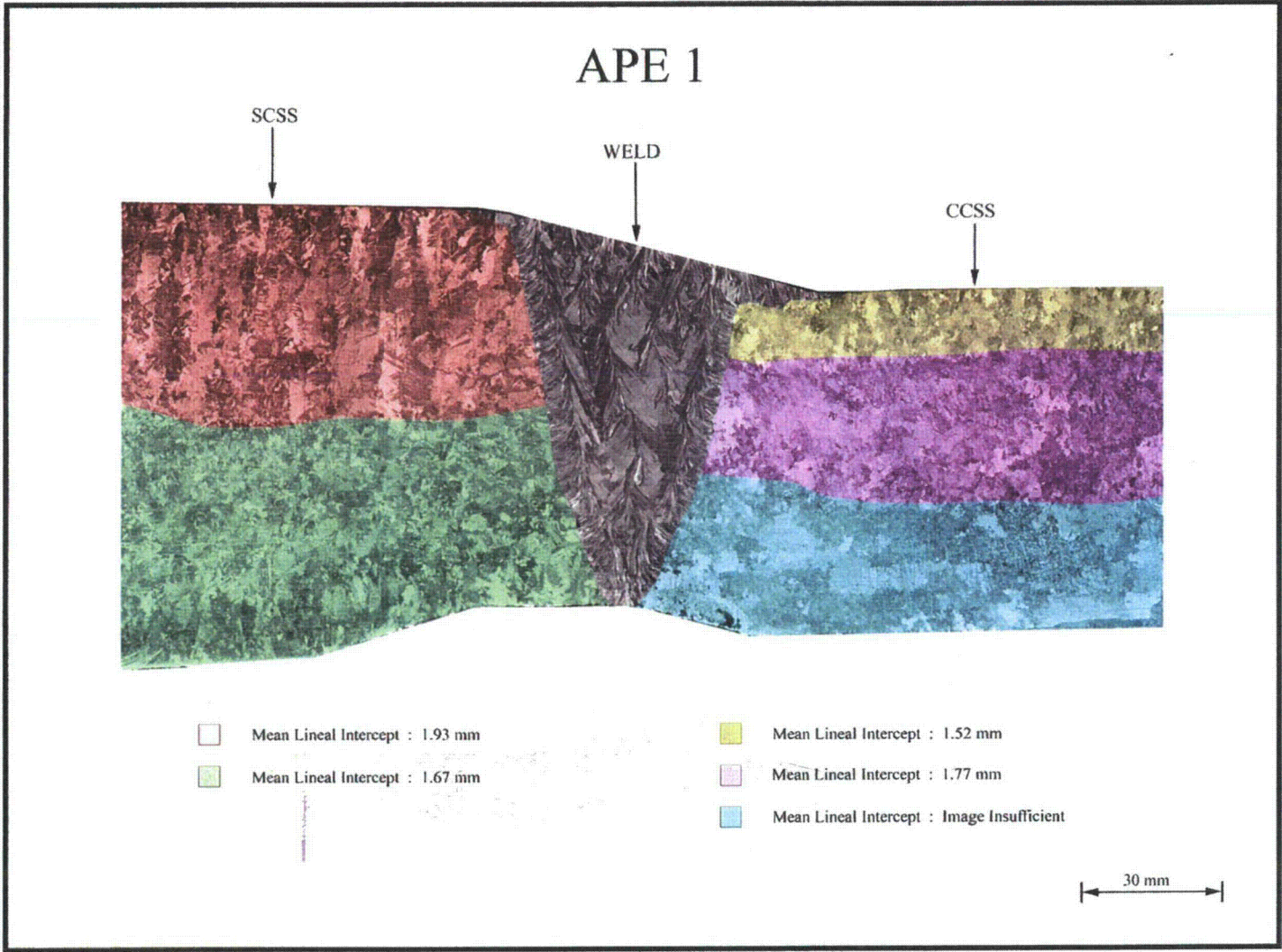


Figure A.1 Axial-Radial Cross Section of WOG Specimen APE-1, Showing Outside and Inside Diameter Geometry, and Grain Size, Typical of APE Configuration

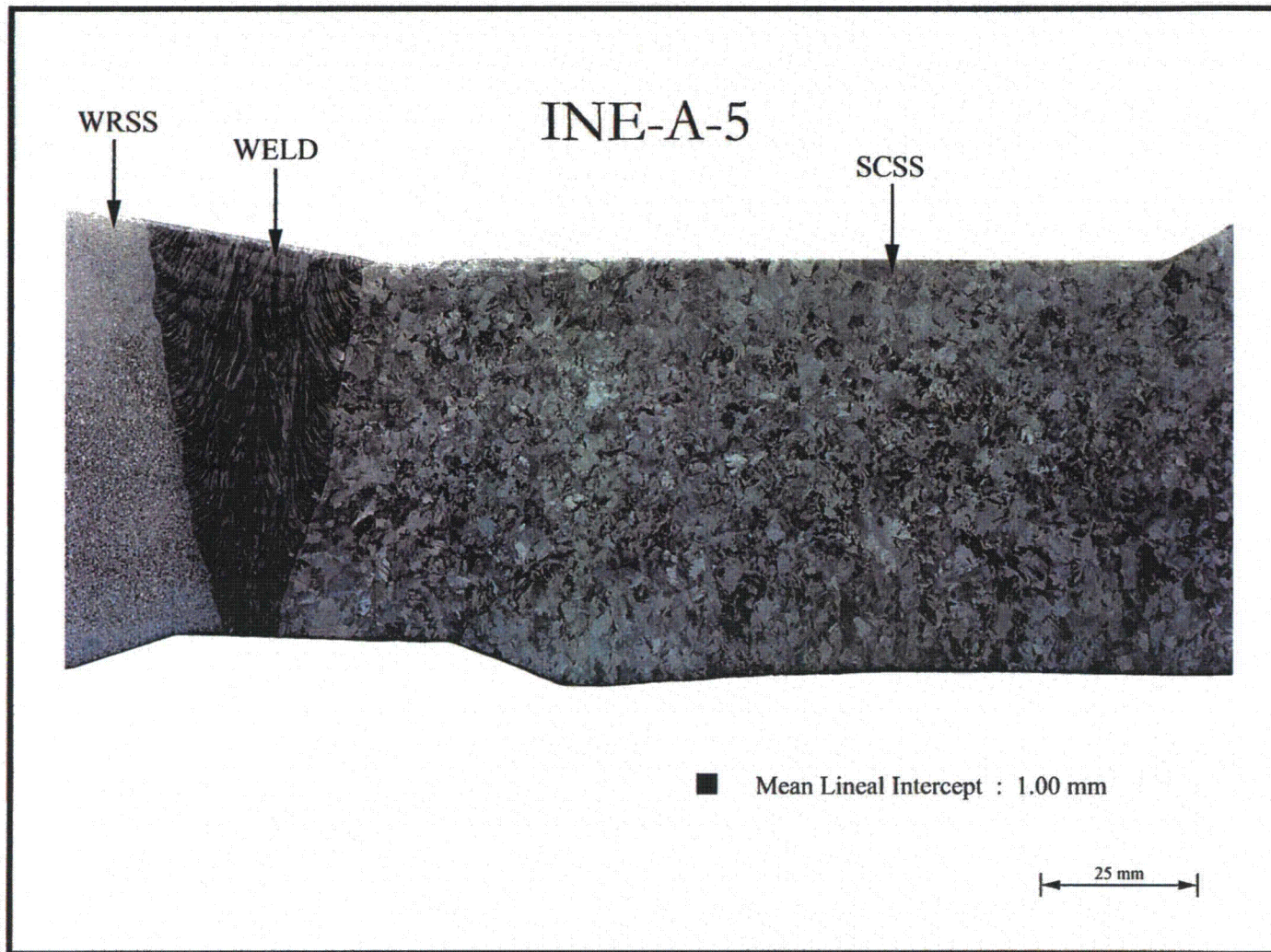
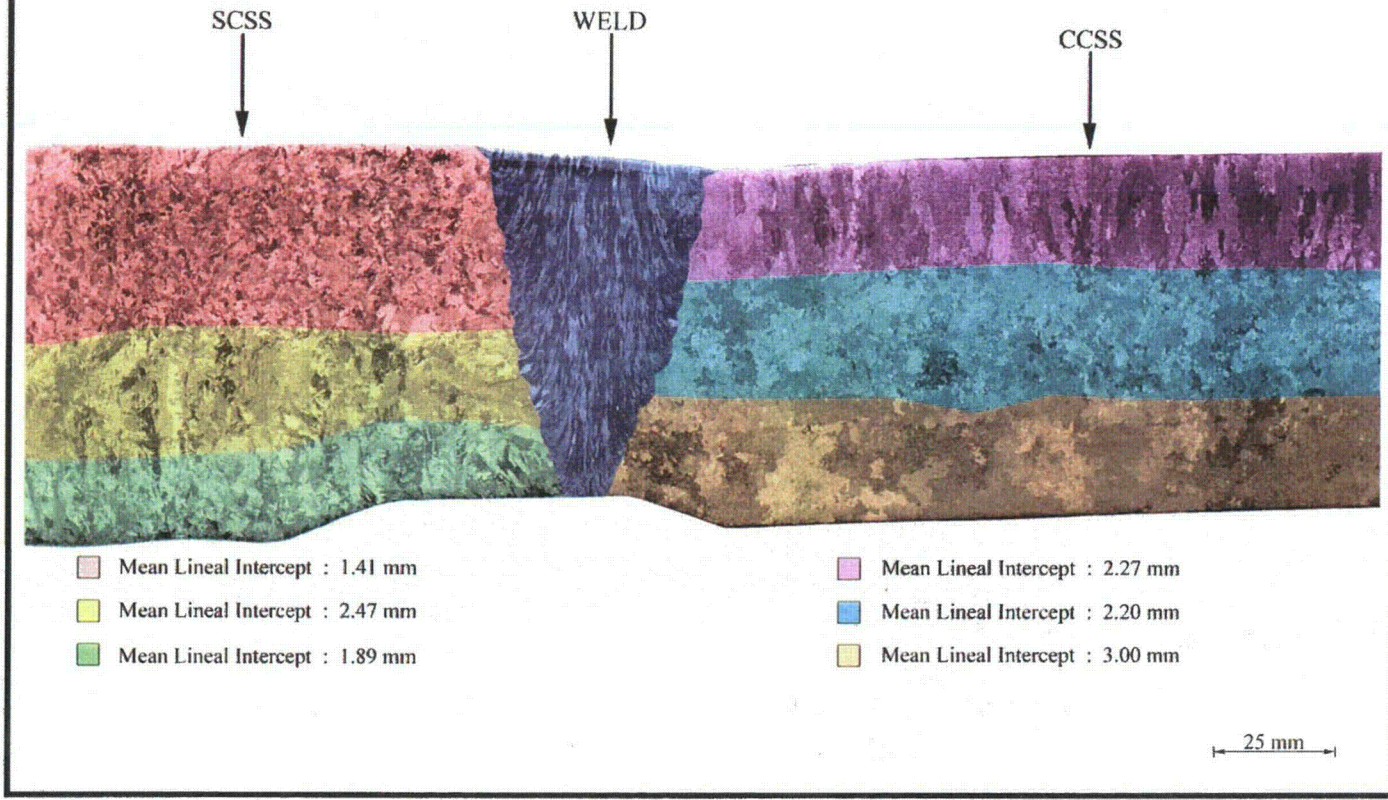


Figure A.2 Axial-Radial Cross Section of WOG Specimen INE-A-5, Showing Outside and Inside Diameter Geometry, and Grain Size, Typical of INE-A Configuration

MPE 06



A.3

Figure A.3 Axial-Radial Cross Section of WOG Specimen MPE-06, Showing Outside and Inside Diameter Geometry, and Grain Size, Typical of MPE Configuration

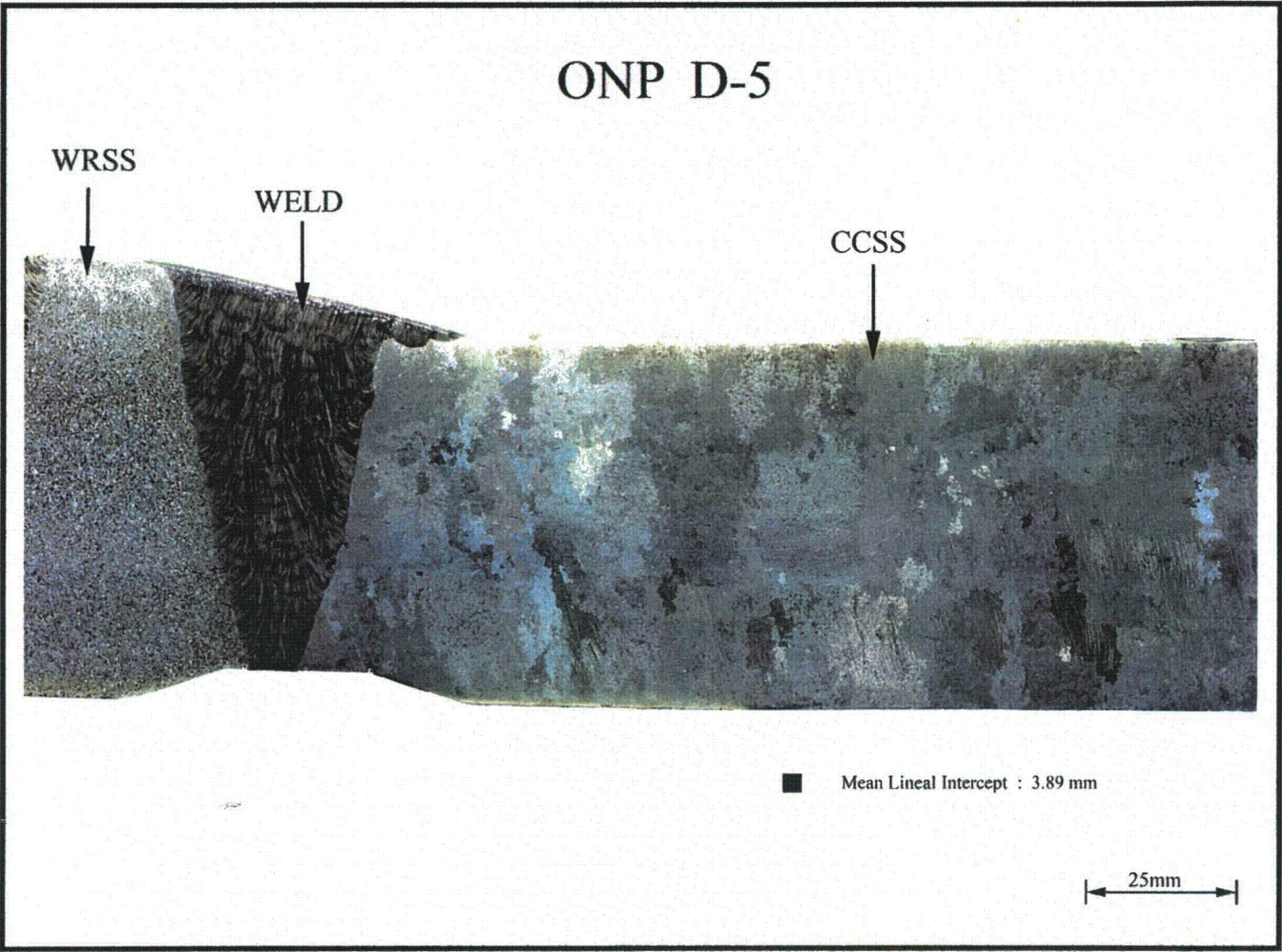


Figure A.4 Axial-Radial Cross Section of WOG Specimen ONP-D-5, Showing Outside and Inside Diameter Geometry, and Grain Size, Typical of ONP-D Configuration

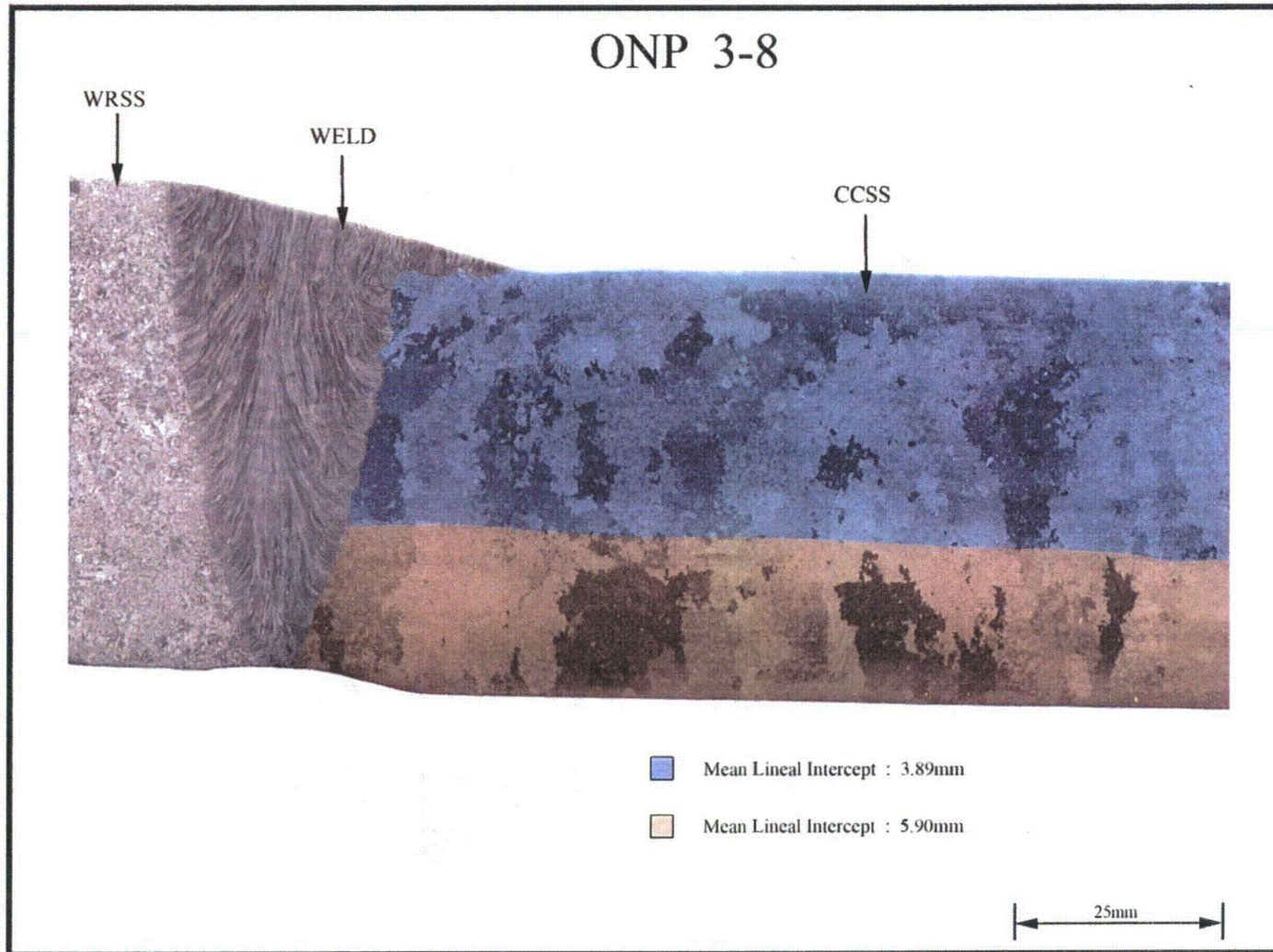


Figure A.5 Axial-Radial Cross Section of WOG Specimen ONP-3-8, Showing Outside and Inside Diameter Geometry, and Grain Size, Typical of ONP Configuration

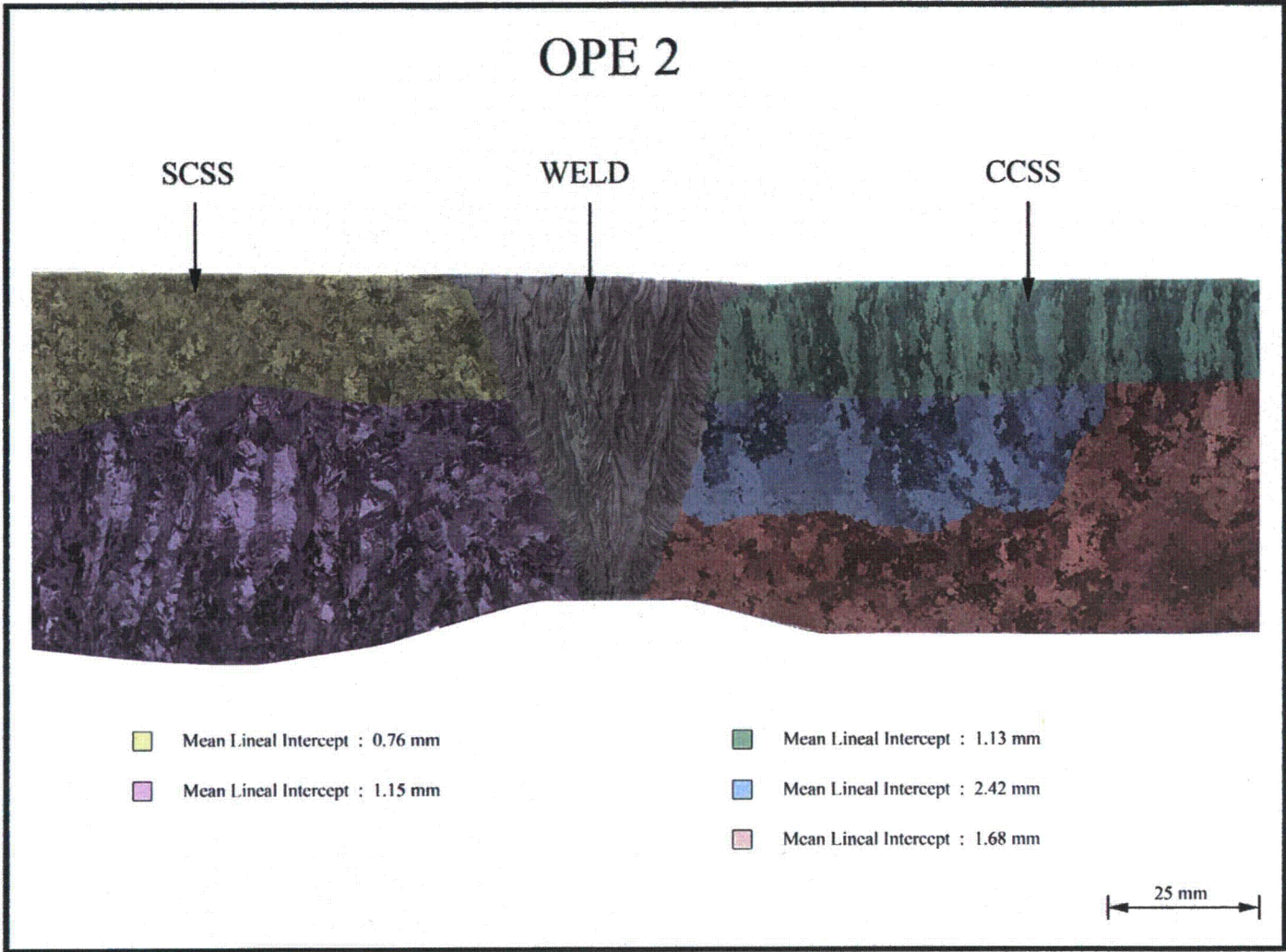


Figure A.6 Axial-Radial Cross Section of WOG Specimen OPE-2, Showing Outside and Inside Diameter Geometry, and Grain Size, Typical of OPE Configuration

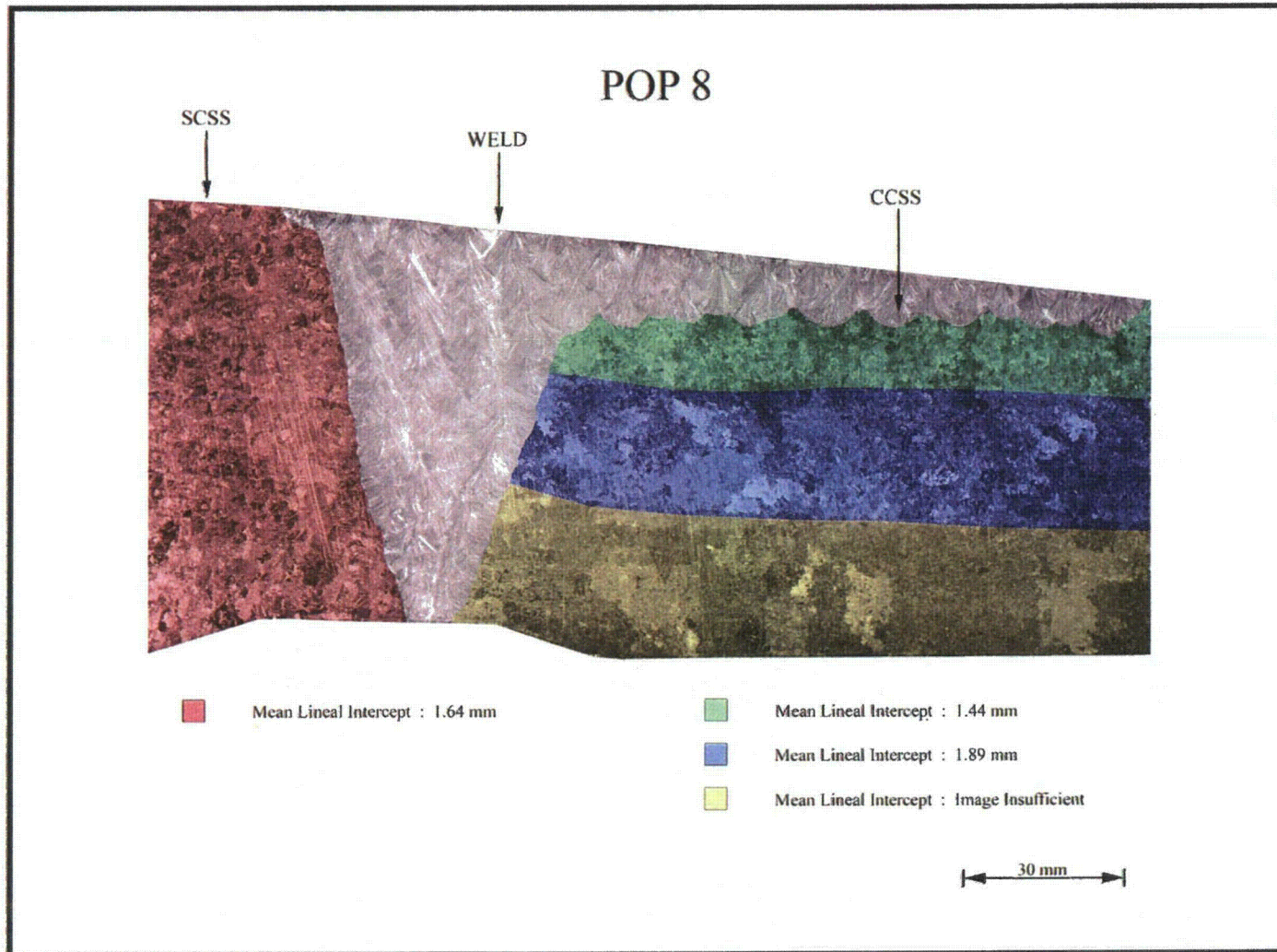


Figure A.7 Axial-Radial Cross Section of WOG Specimen POP-8, Showing Outside and Inside Diameter Geometry, and Grain Size, Typical of POP Configuration

A.8

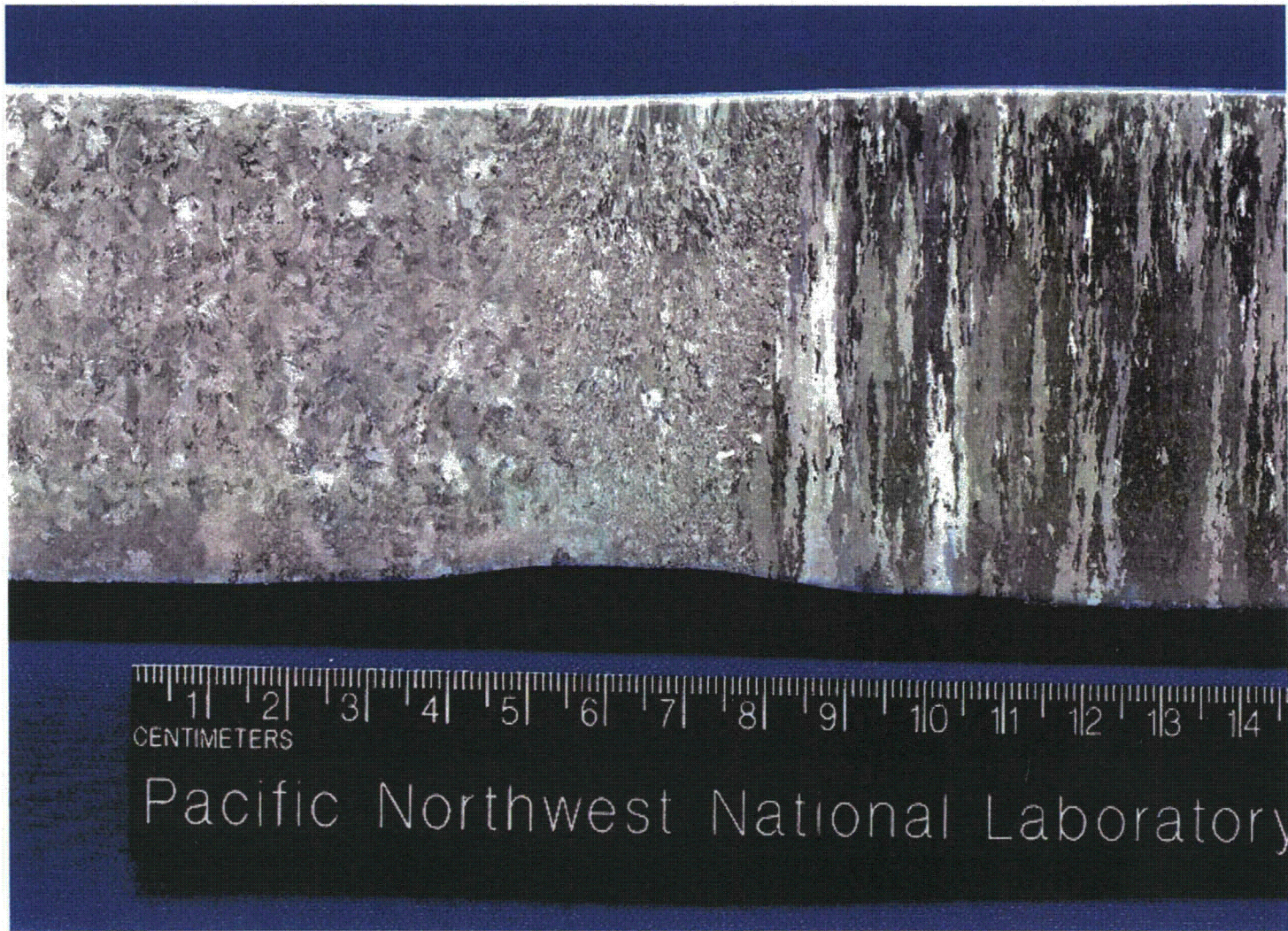


Figure A.8 Axial-Radial Cross Section of PNNL Specimen B515, Showing Outside and Inside Diameter Geometry, and Grains Typical of PNNL Specimens. The equiaxed CCSS grains on the left have a mean linear intercept of 2.34 mm and the columnar CCSS grains on the right have a mean linear intercept of 2.48 mm.

Appendix B

Phased Array and Low Frequency Data from the Corner Signal from CCSS Base Metal for Signal-to-Noise Characterization

(All scales are in inches.)

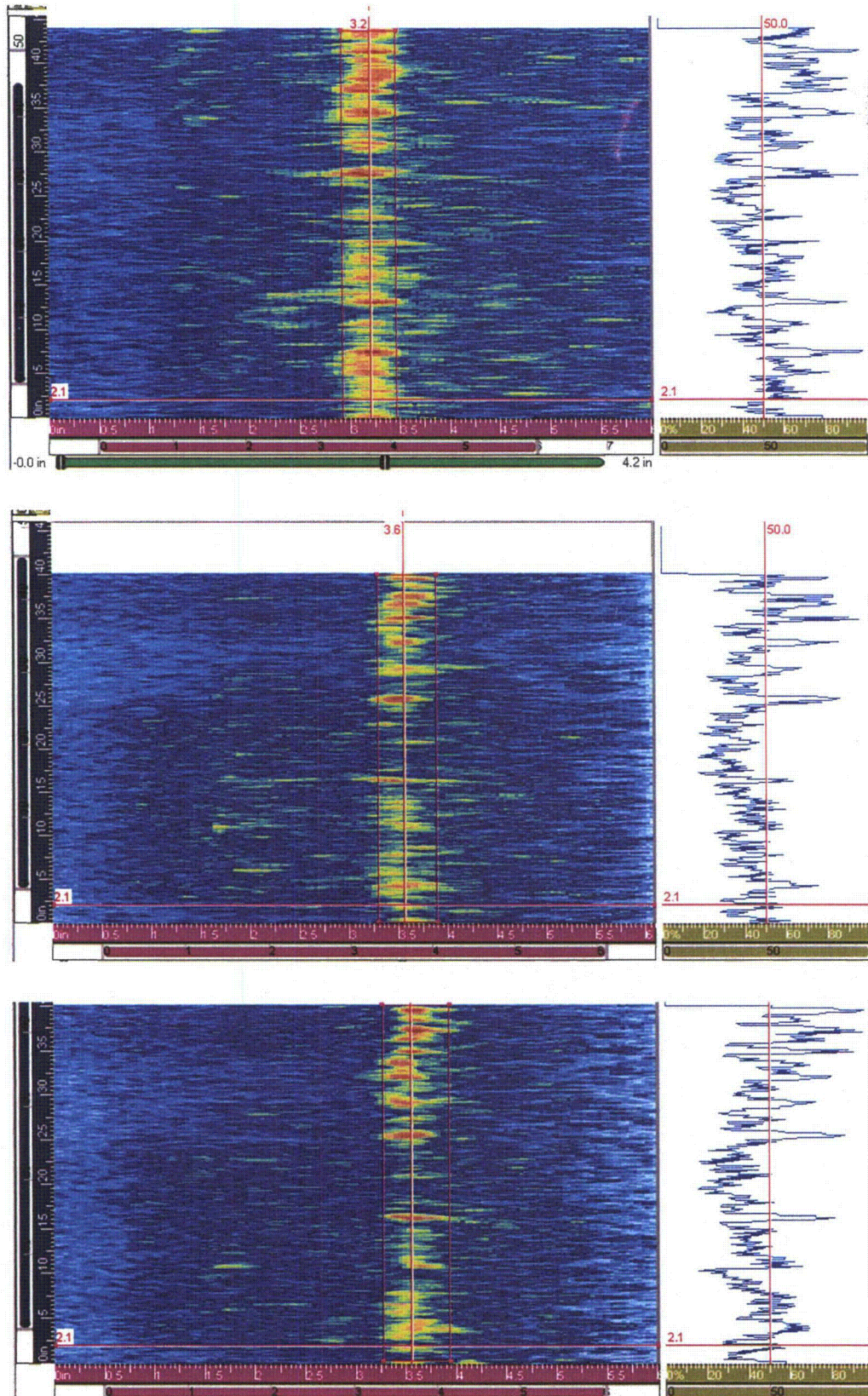


Figure B.1 IHI-SW Corner Response from Top to Bottom at 500, 750, and 1000 kHz

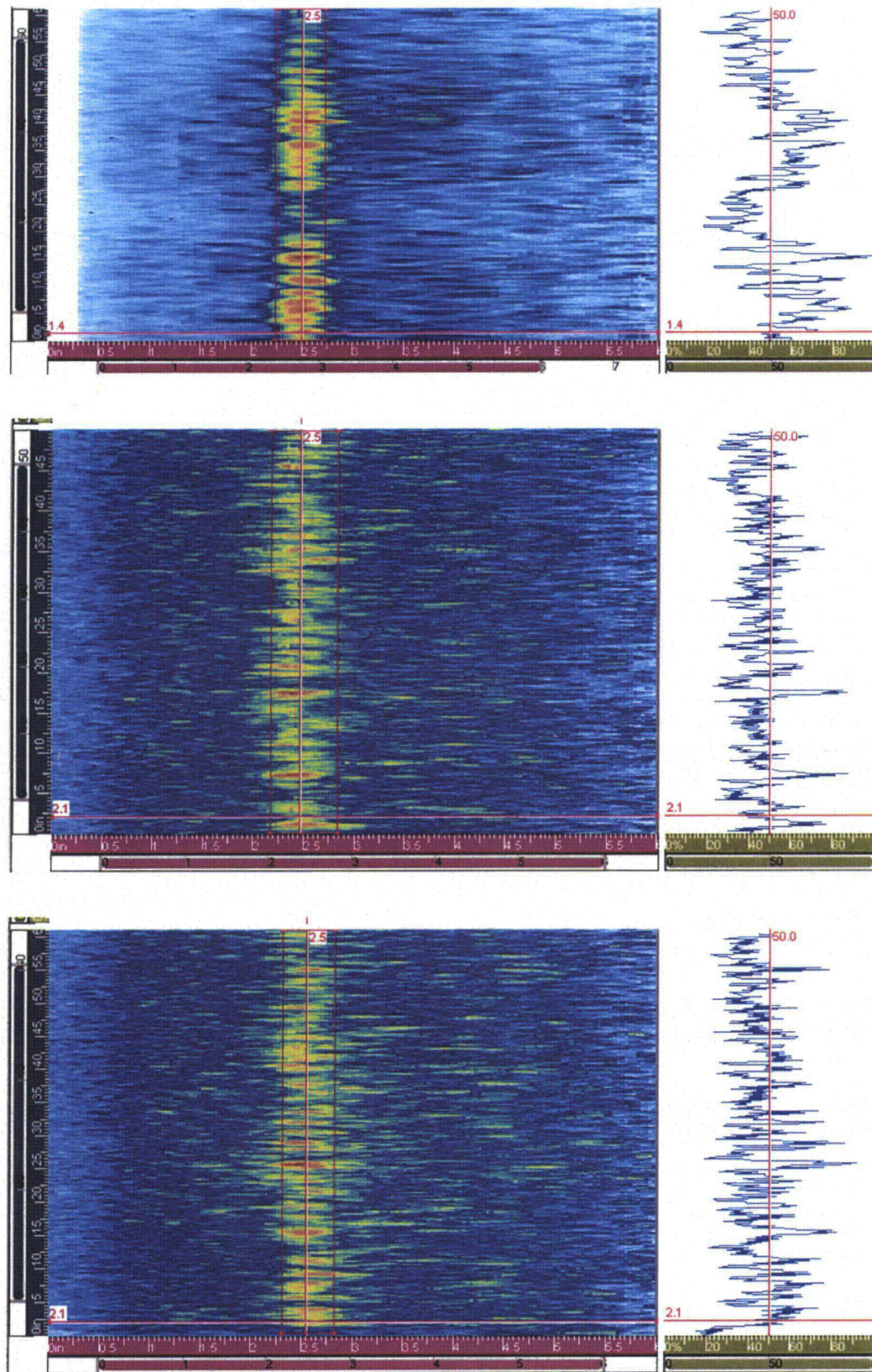


Figure B.2 EPR Corner Response from Top to Bottom at 500, 750, and 1000 kHz

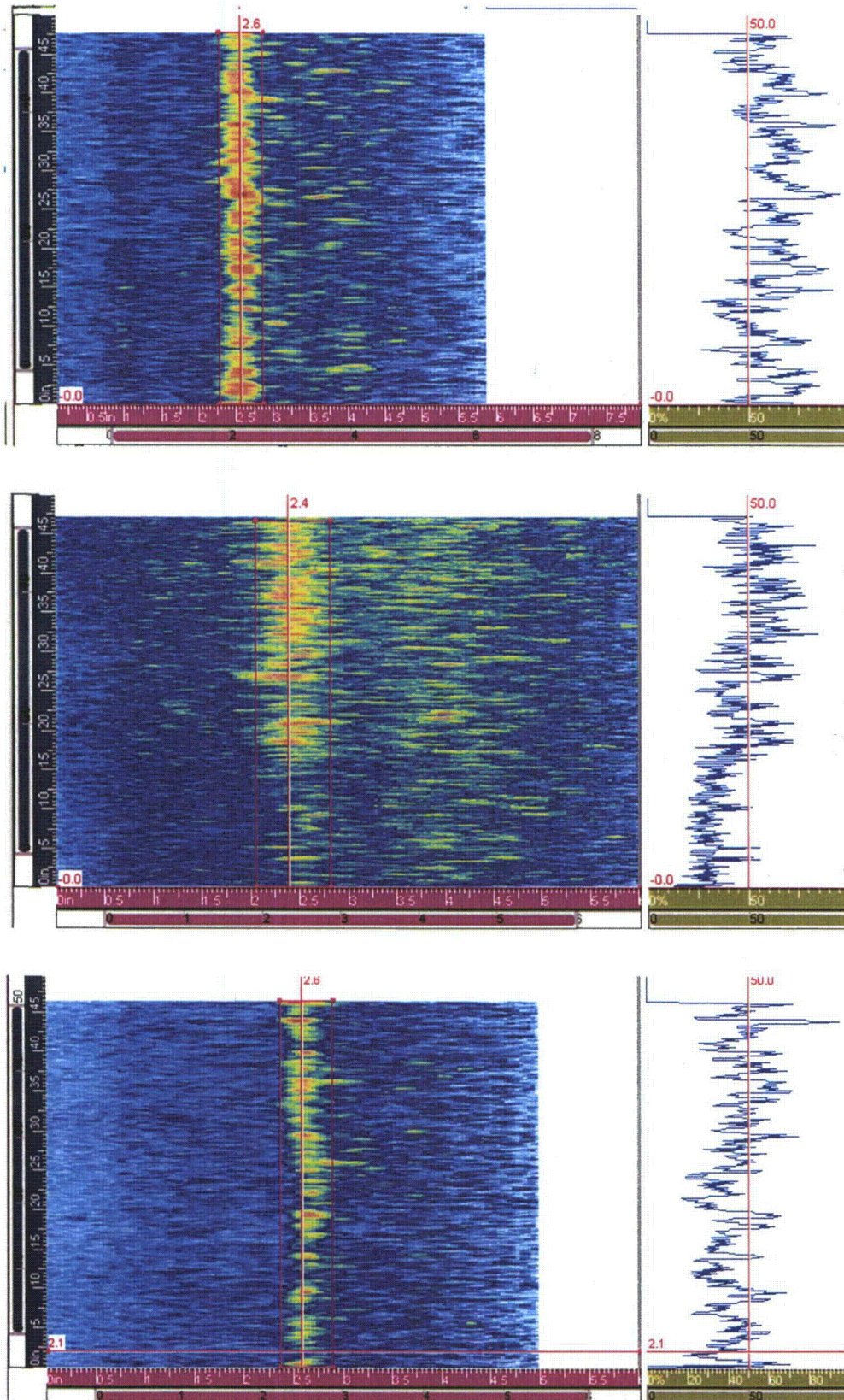


Figure B.3 Westinghouse Corner Response from Top to Bottom at 500, 750, and 1000 kHz

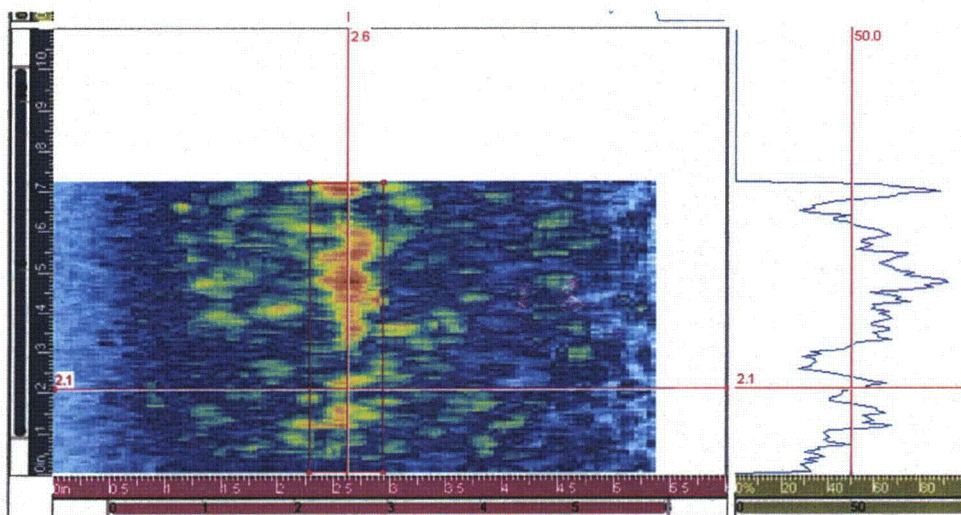
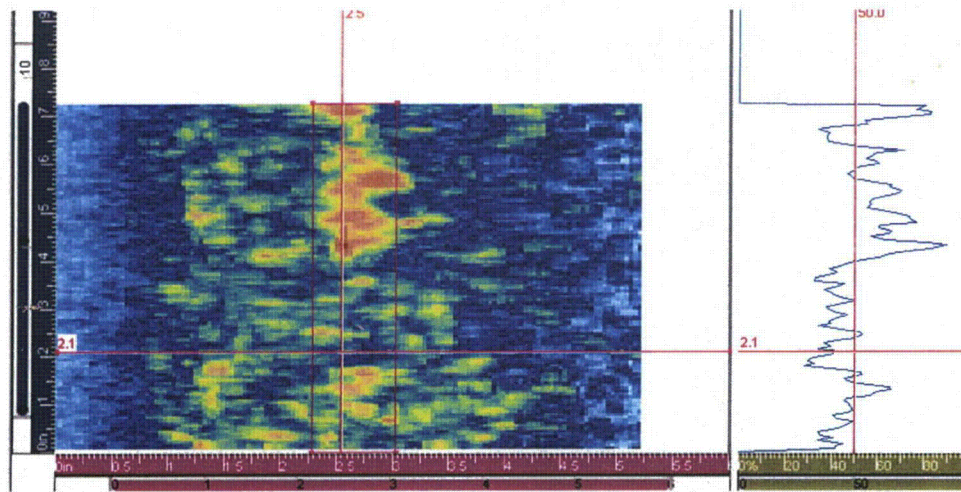
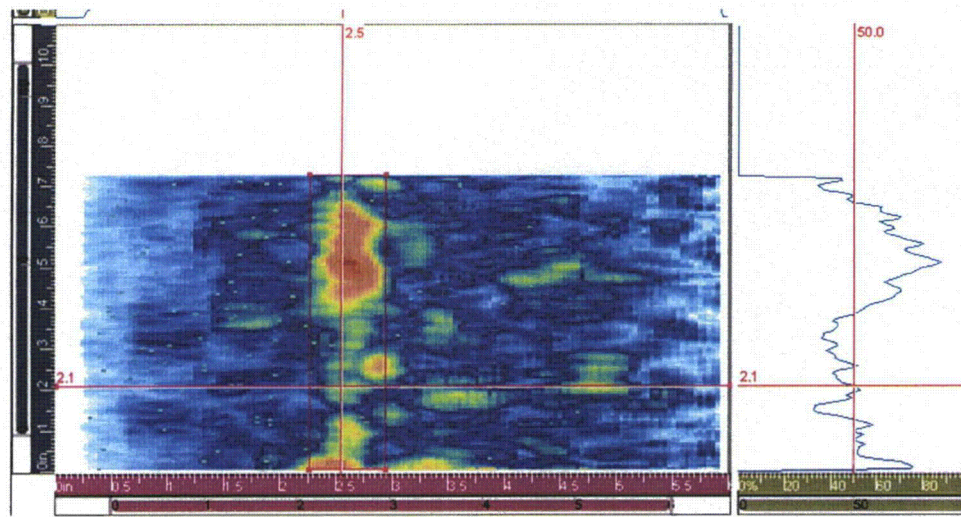


Figure B.4 APE-1 Corner Response from Top to Bottom at 500, 750, and 1000 kHz

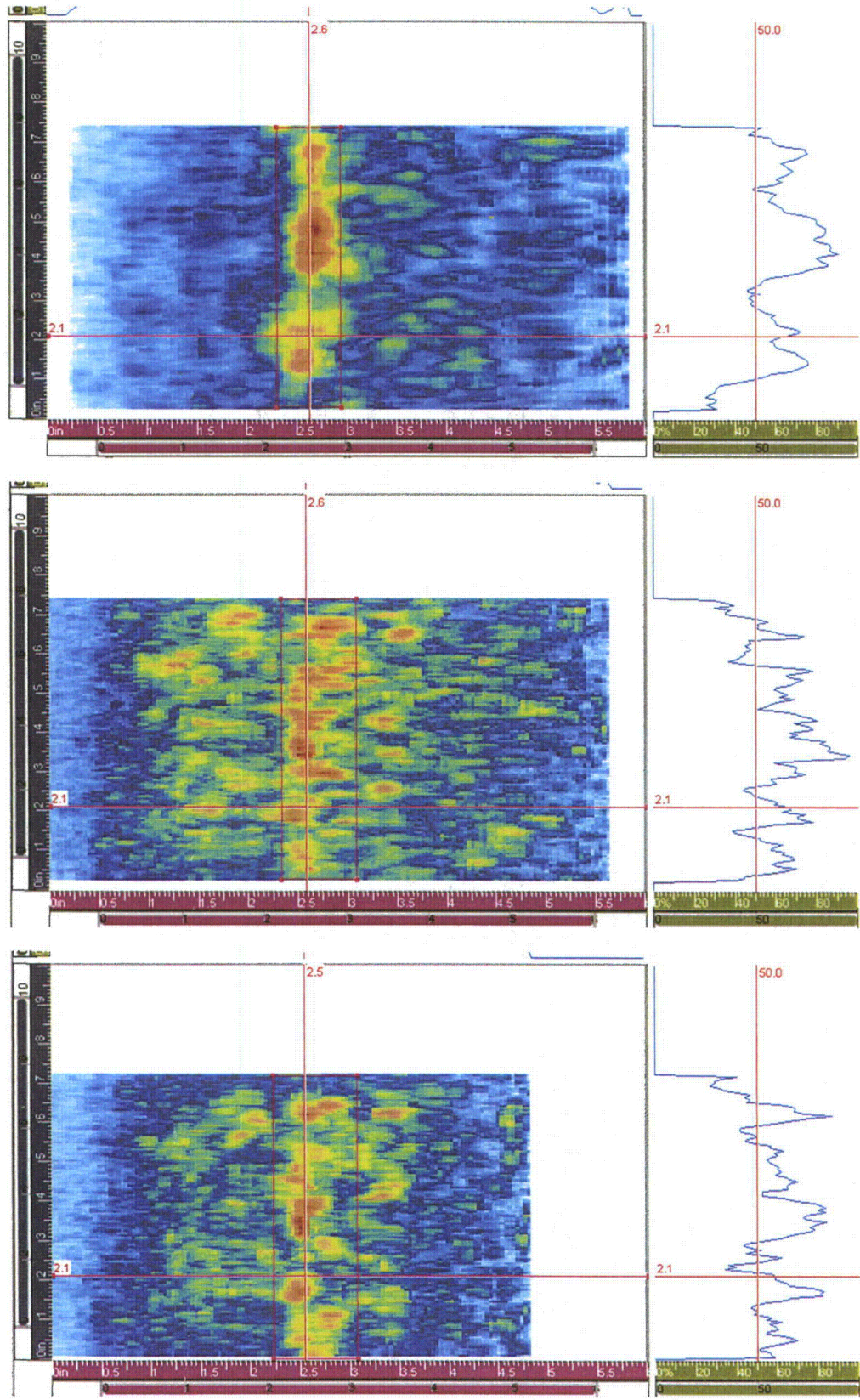


Figure B.5 MPE-3 Corner Response from Top to Bottom at 500, 750, and 1000 kHz

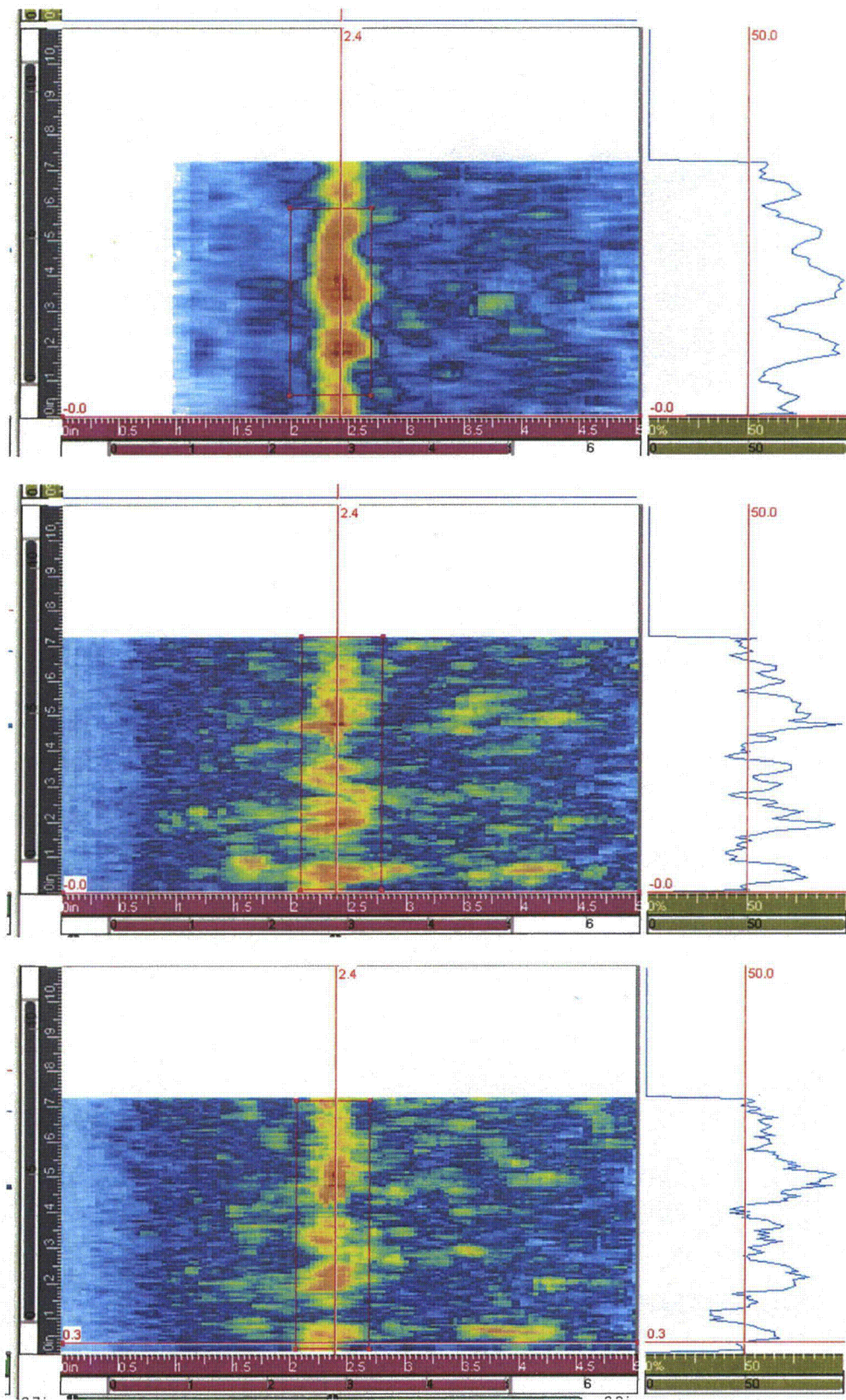


Figure B.6 OPE-5 Corner Response from Top to Bottom at 500, 750, and 1000 kHz

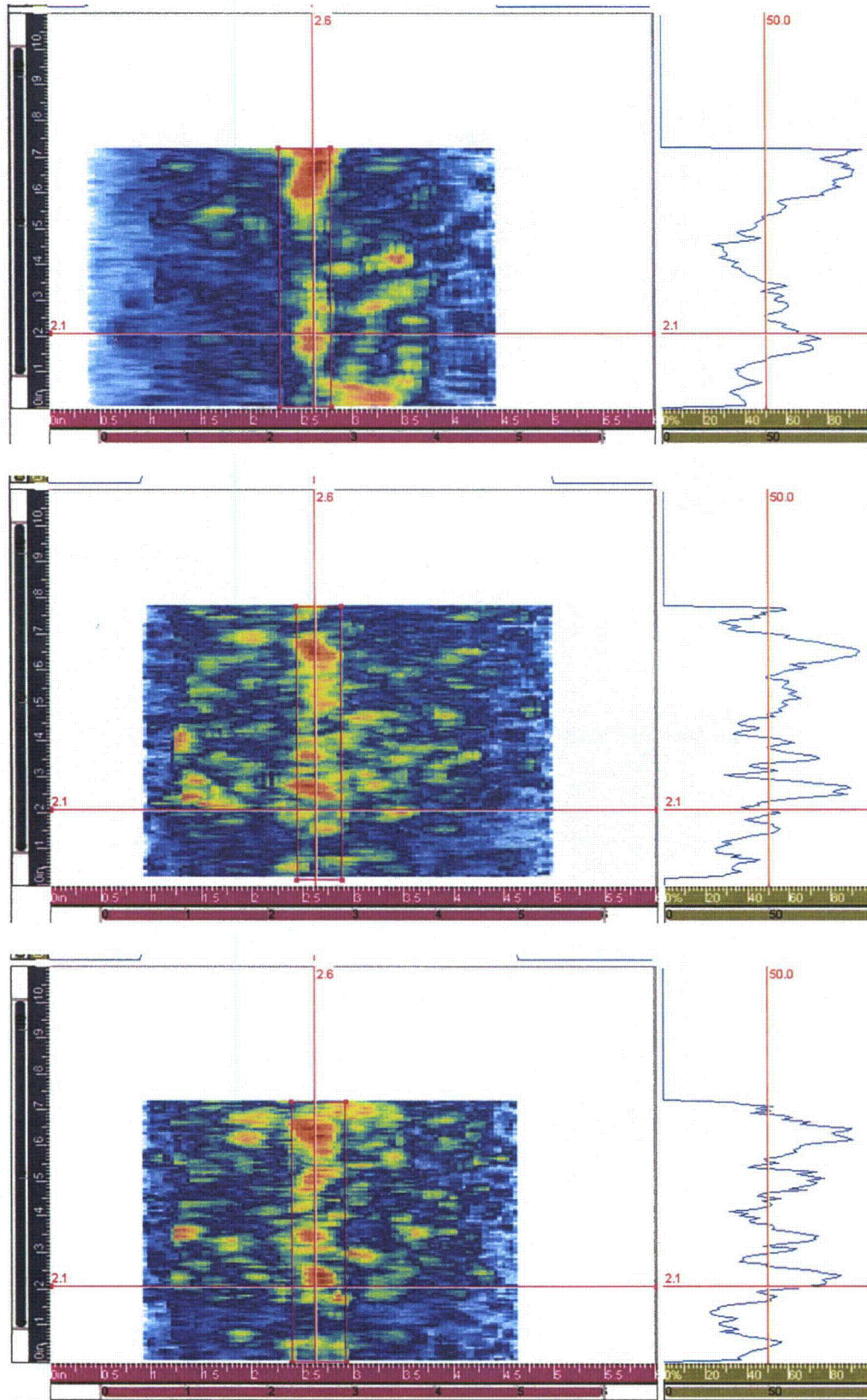


Figure B.7 POP-7 Corner Response from Top to Bottom at 500, 750, and 1000 kHz

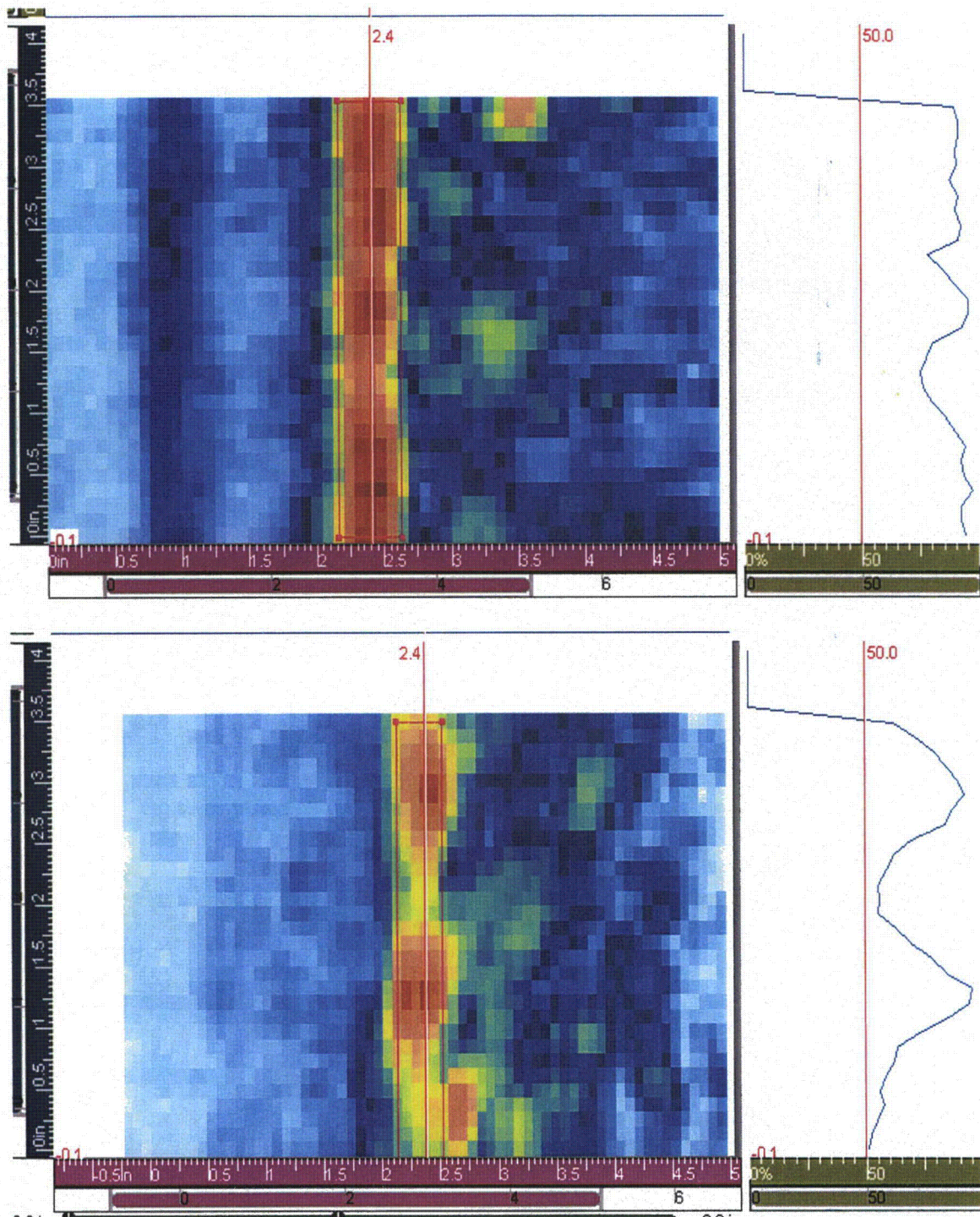


Figure B.8 PNNL Sample B508 Corner Response from the Columnar End (top) and Equiaxed End (bottom) at 500 kHz

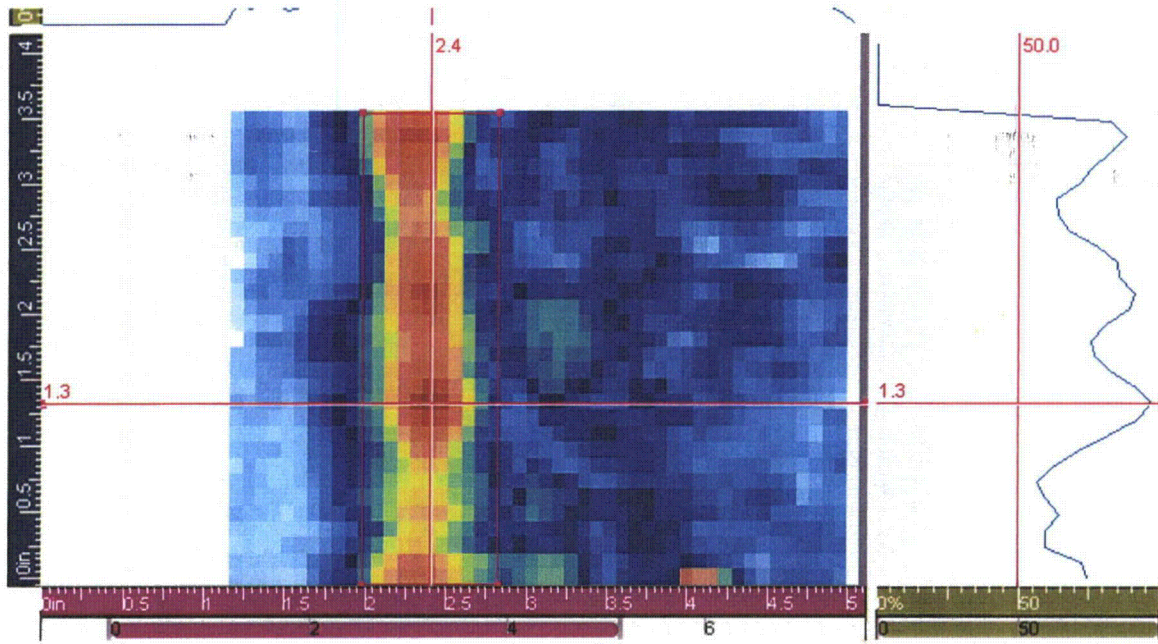
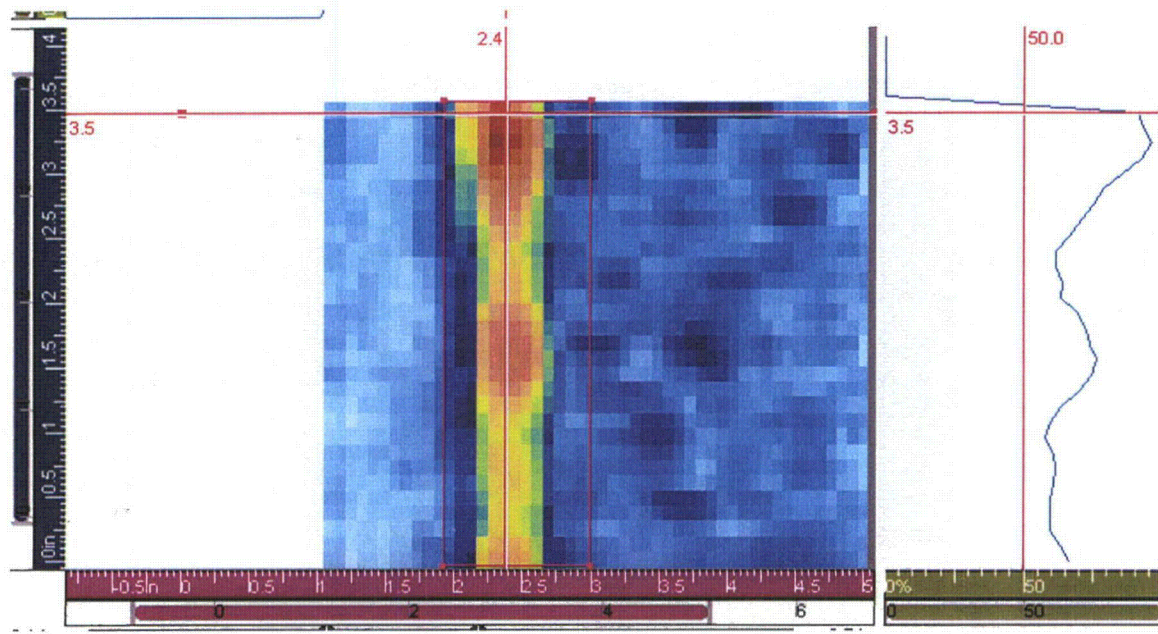


Figure B.9 PNNL Sample B511 Corner Response from the Columnar End (top) and Equiaxed End (bottom) at 500 kHz

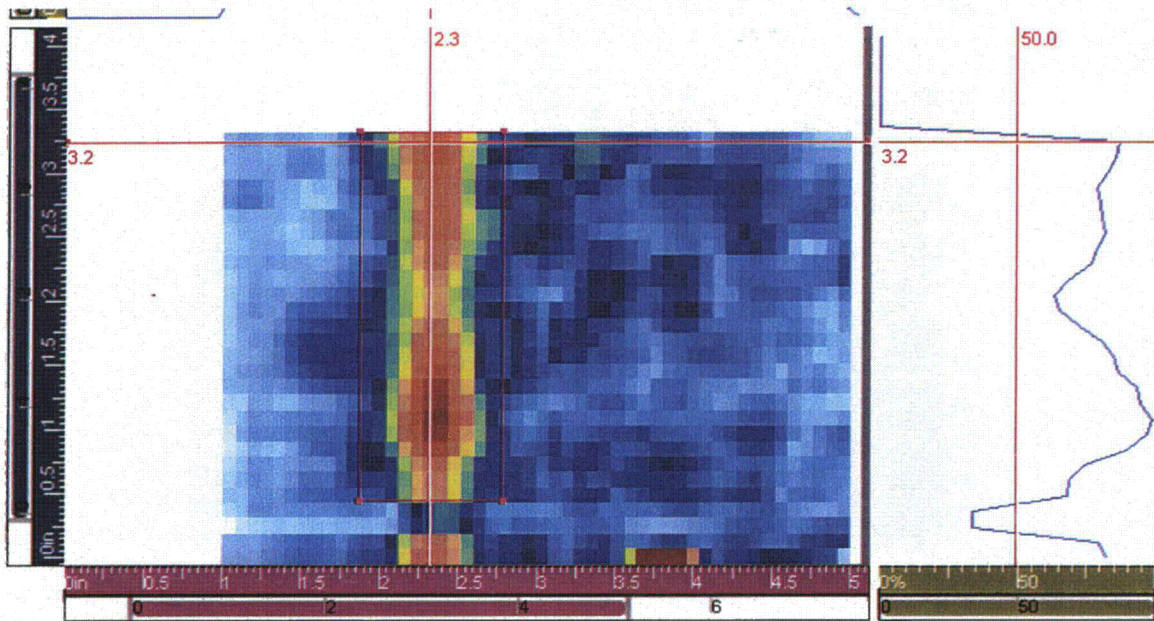
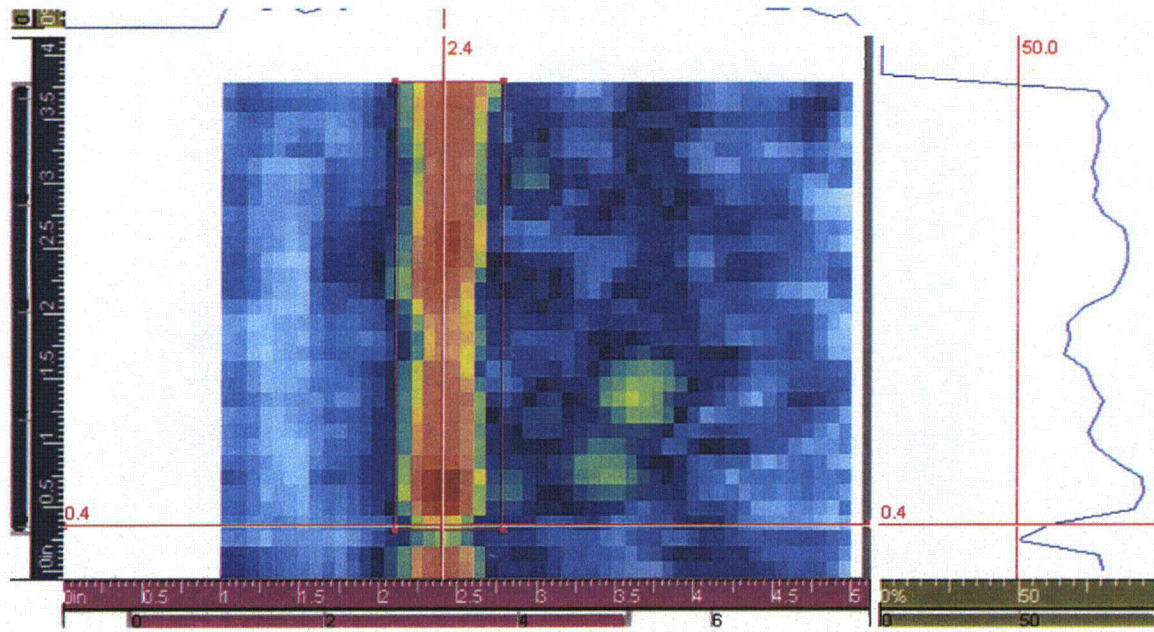


Figure B.10 PNNL Sample B520 Corner Response from the Columnar End (top) and Equiaxed End (bottom) at 500 kHz. Due to poor coupling on the rough surface the first approximately 0.5 inch (1.3 cm) of the scan should be ignored. The scan start is at the bottom.

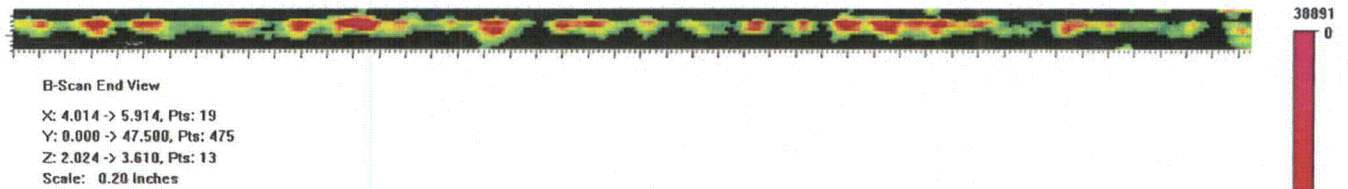
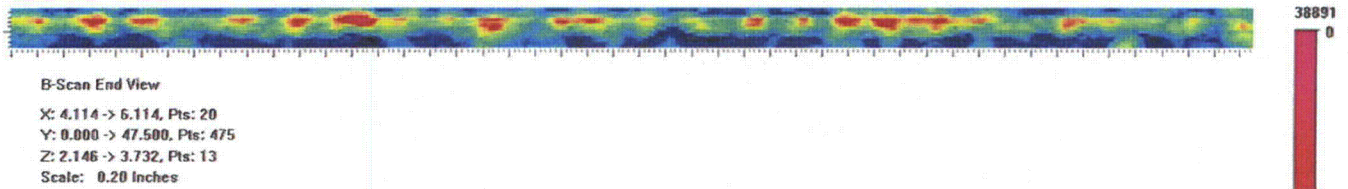
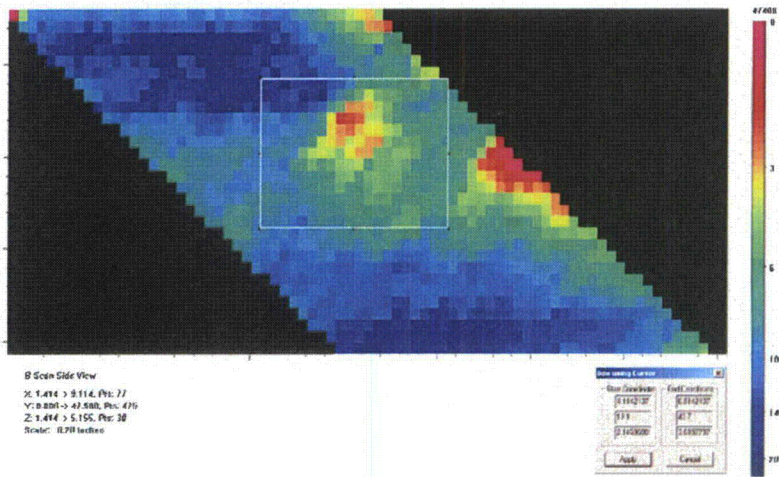
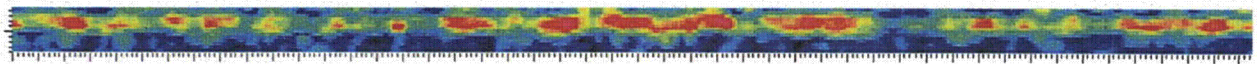
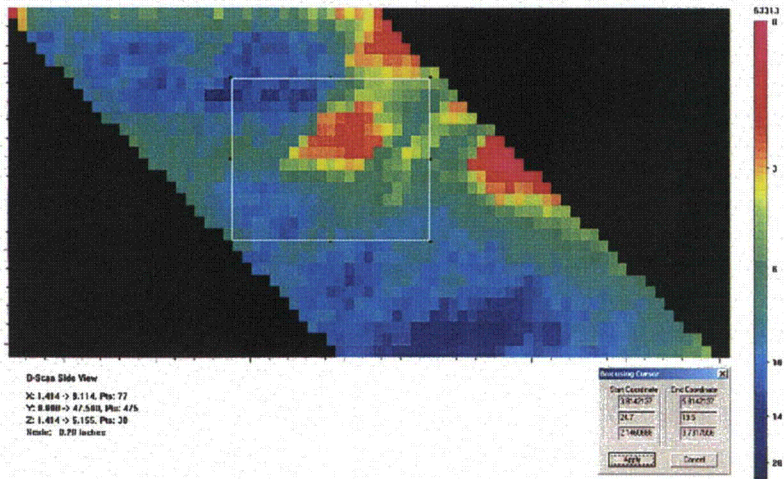


Figure B.11 Westinghouse Top Corner Response at 400 kHz



B-Scan End View
 X: 3.814 -> 5.914, Pts: 21
 Y: 0.000 -> 47.500, Pts: 475
 Z: 2.146 -> 3.054, Pts: 14
 Scale: 0.20 inches



B-Scan End View
 X: 4.214 -> 5.714, Pts: 15
 Y: 0.000 -> 47.500, Pts: 475
 Z: 2.146 -> 3.408, Pts: 11
 Scale: 0.20 inches

Figure B.12 Westinghouse Bottom Corner Response at 400 kHz

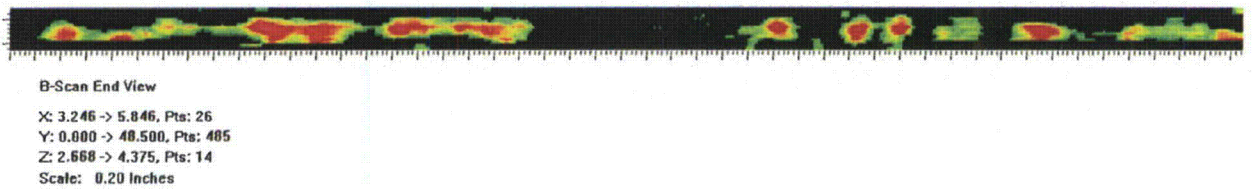
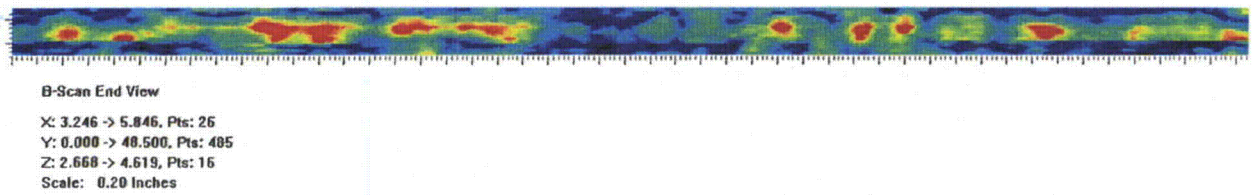
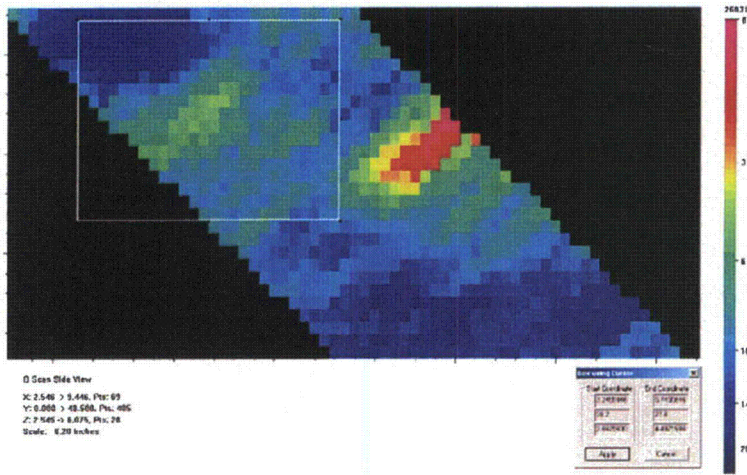
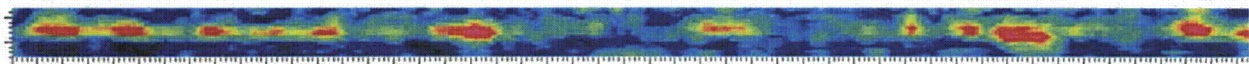
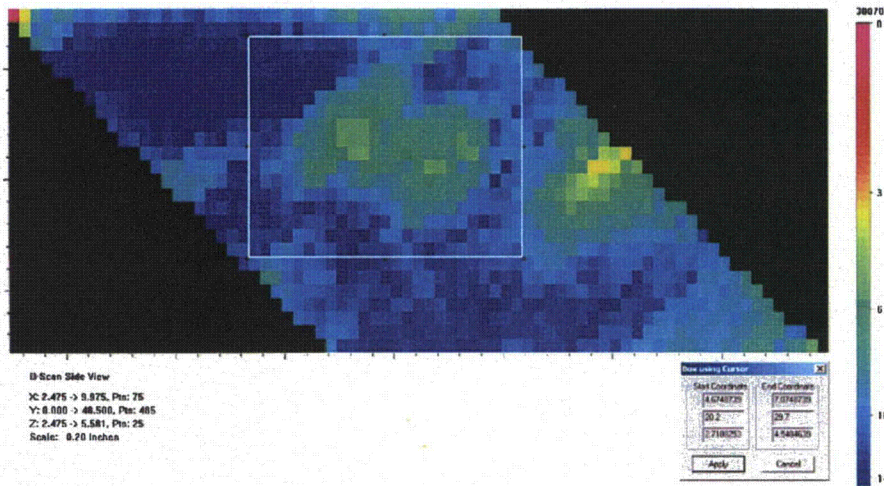
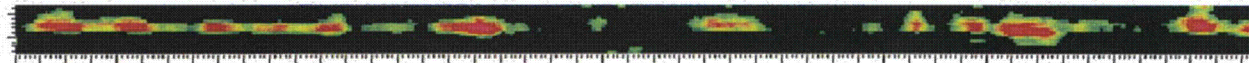


Figure B.13 IHI-Southwest Top Corner Response at 400 kHz



B-Scan End View
 X: 4.675 -> 7.175, Pts: 25
 Y: 0.000 -> 48.500, Pts: 485
 Z: 2.719 -> 4.670, Pts: 16
 Scale: 0.20 Inches



B-Scan End View
 X: 4.775 -> 7.275, Pts: 25
 Y: 0.000 -> 48.500, Pts: 485
 Z: 2.719 -> 4.792, Pts: 17
 Scale: 0.20 Inches

Figure B.14 IHI-Southwest Bottom Corner Response at 400 kHz

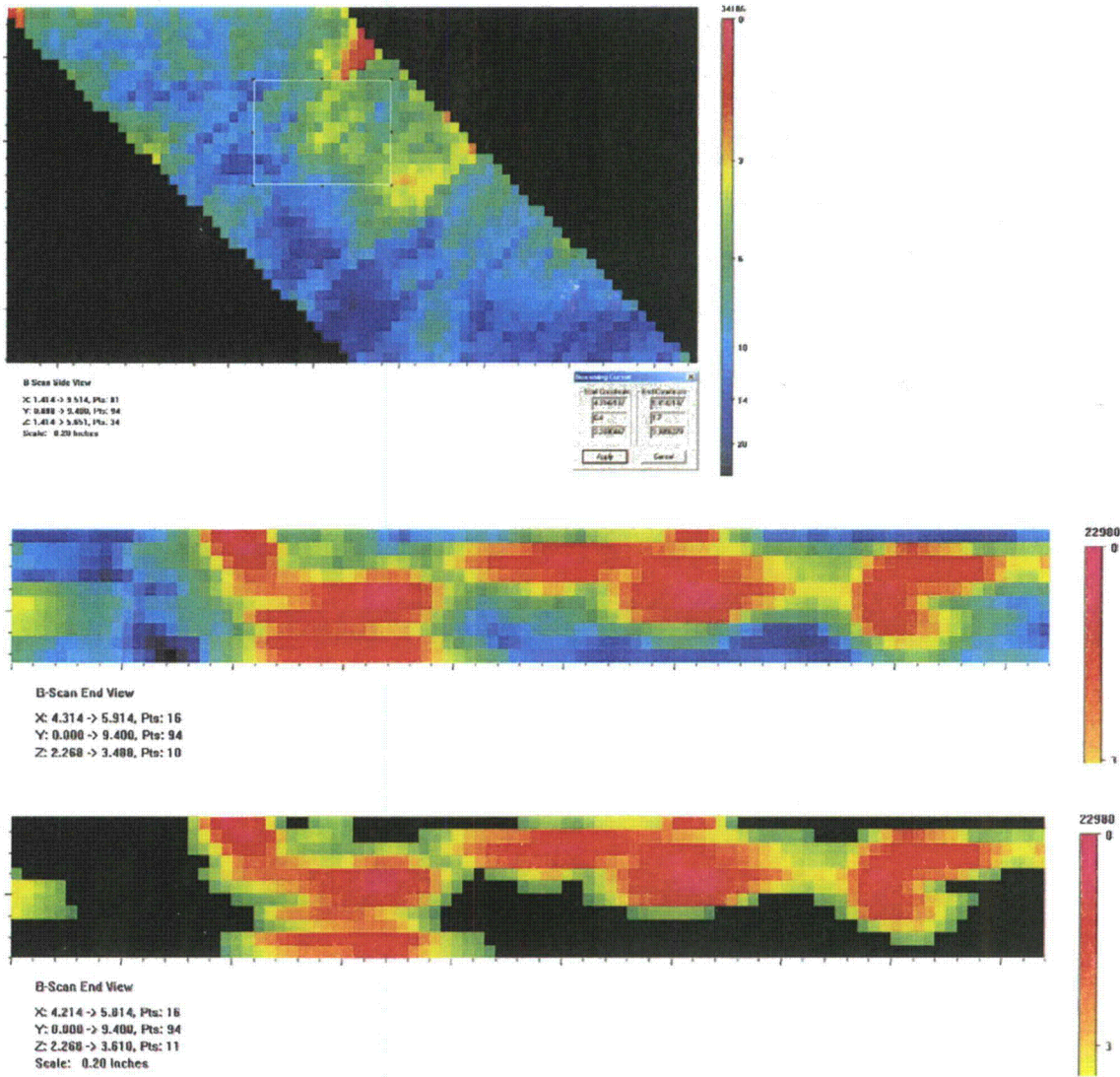


Figure B.15 APE-1 Corner Response at 400 kHz

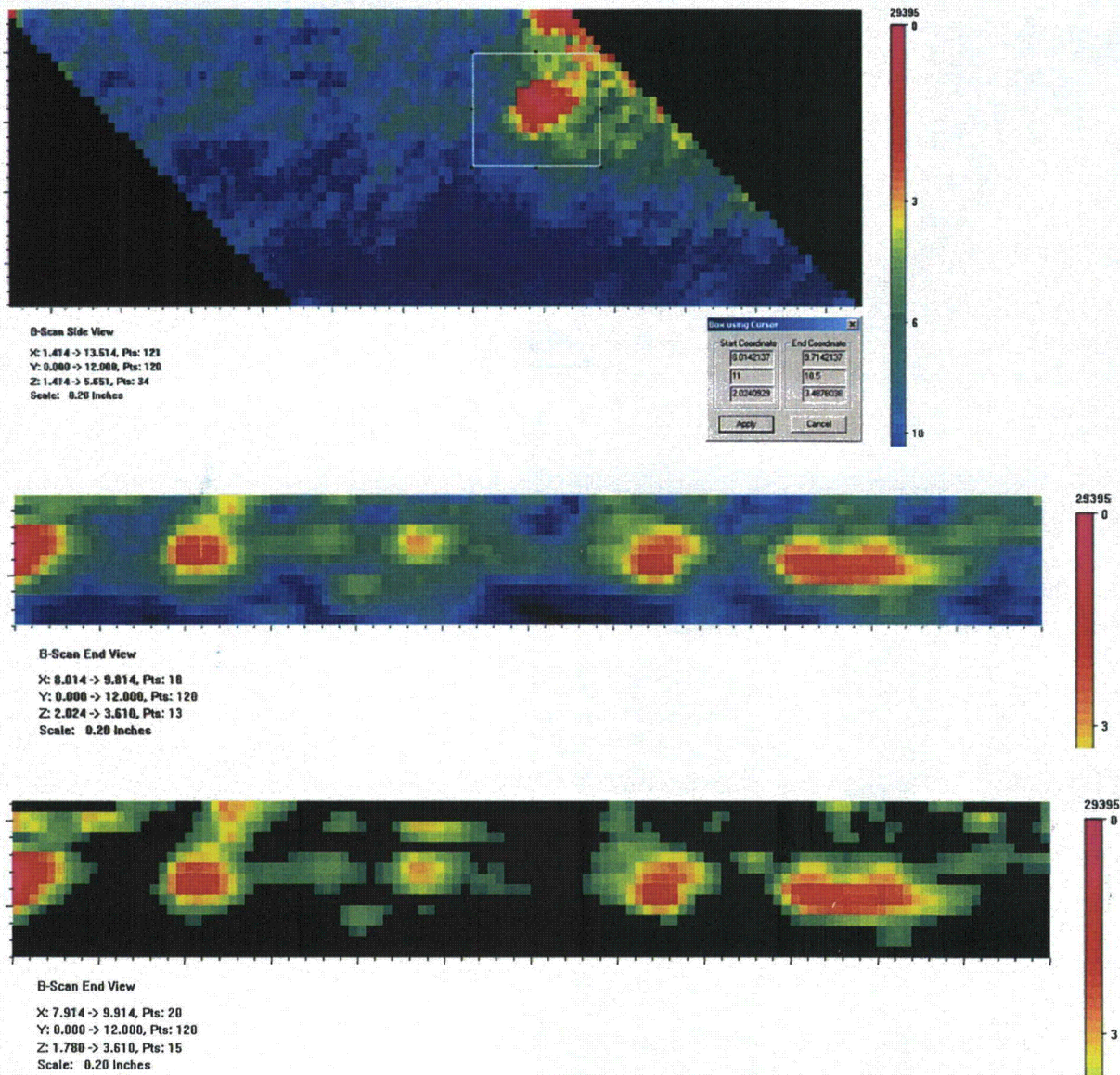


Figure B.16 MPE-6 Corner Response at 400 kHz

Appendix C

Phased Array Detection Data from WOG and PNNL Flaws

(All scales are in inches.)

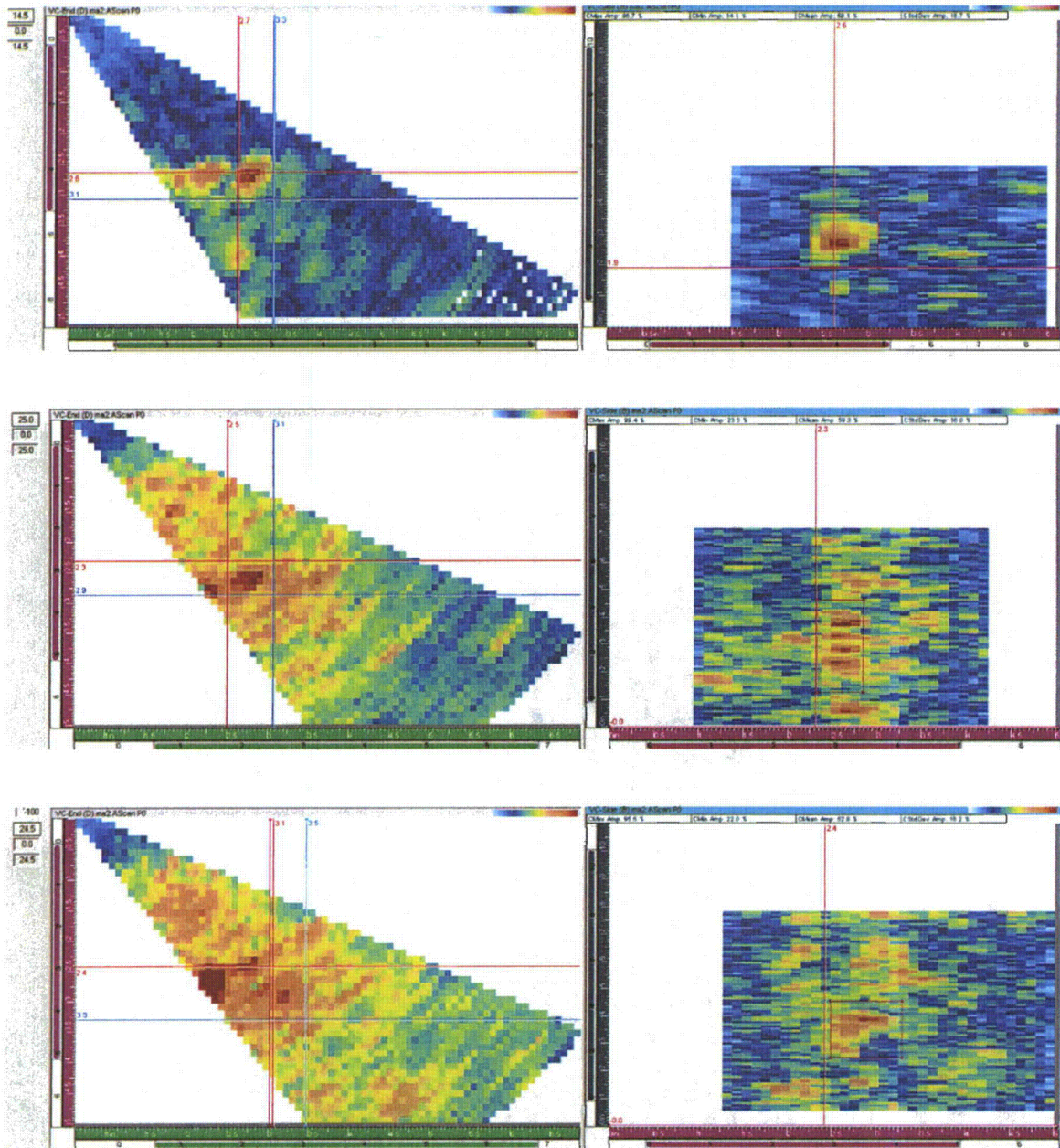


Figure C.1 WOG Sample APE-1 CCSS from Top to Bottom 500, 750 and 1000 kHz Showing Detection as: Yes, No, and Marginal

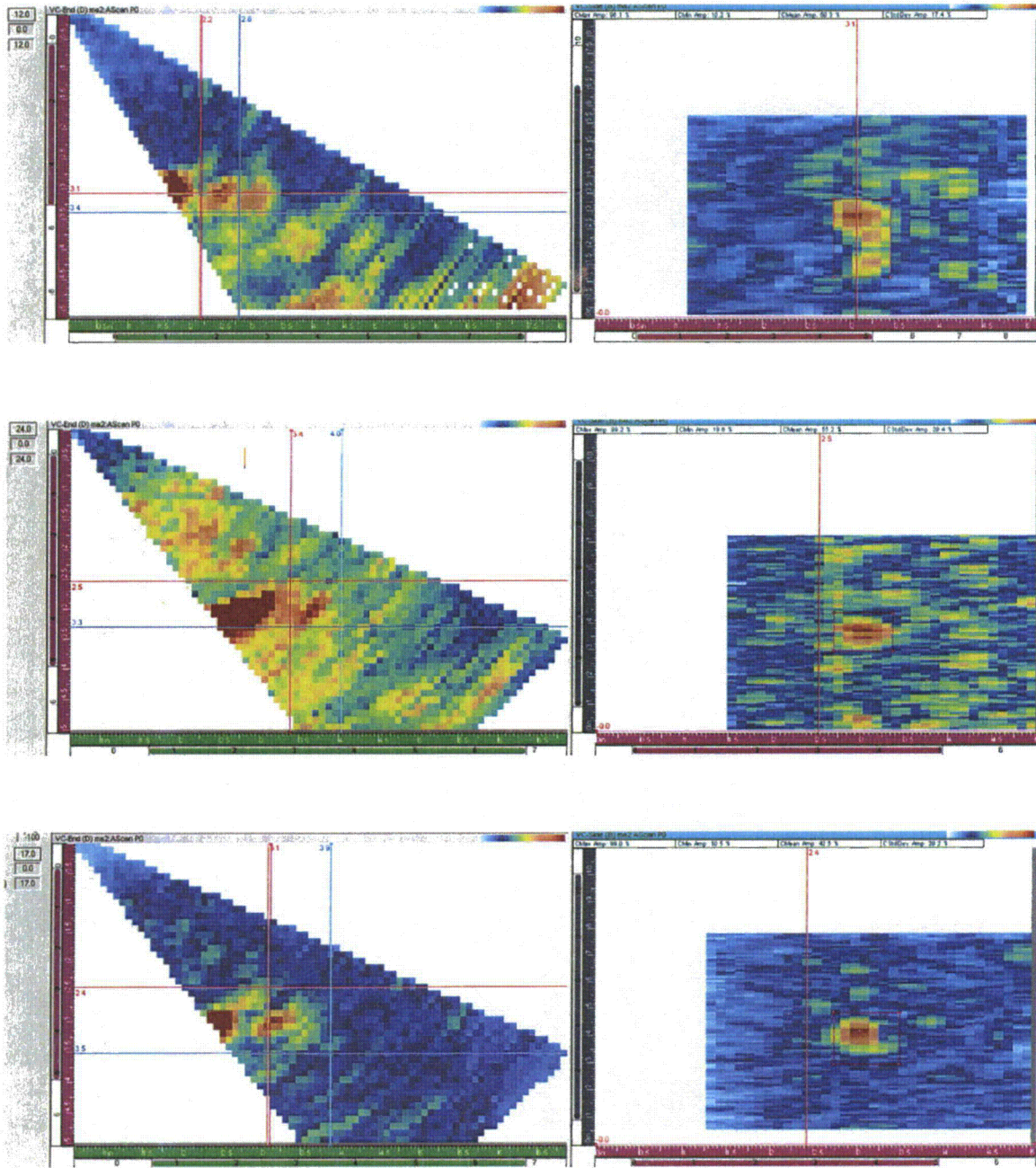


Figure C.2 WOG Sample APE-1 SCSS from Top to Bottom 500, 750 and 1000 kHz Showing Detection as: Yes, Yes and Yes

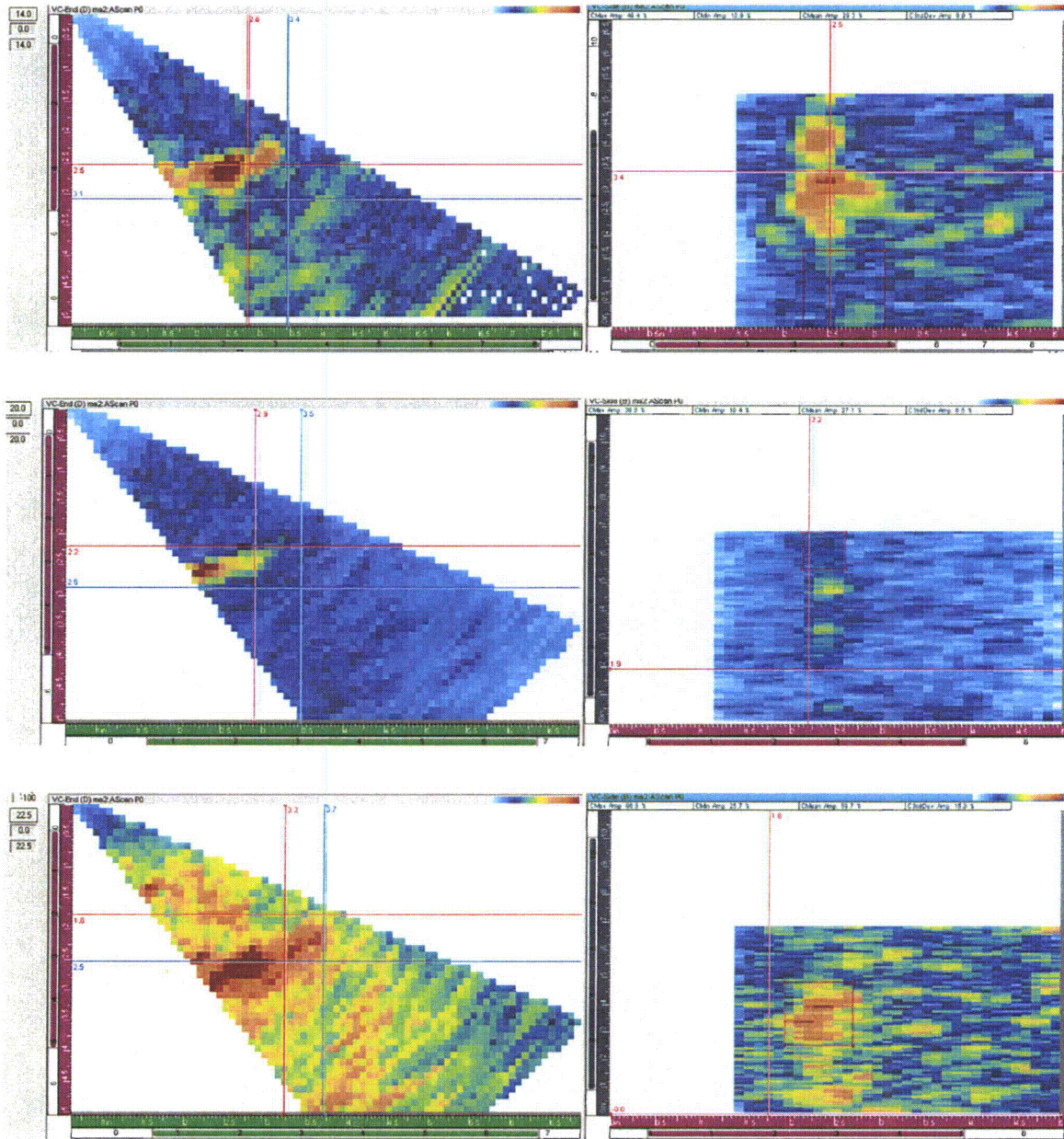


Figure C.3 WOG Sample APE-4 CCSS from Top to Bottom 500, 750 and 1000 kHz Showing Detection as: Yes, Yes and Yes

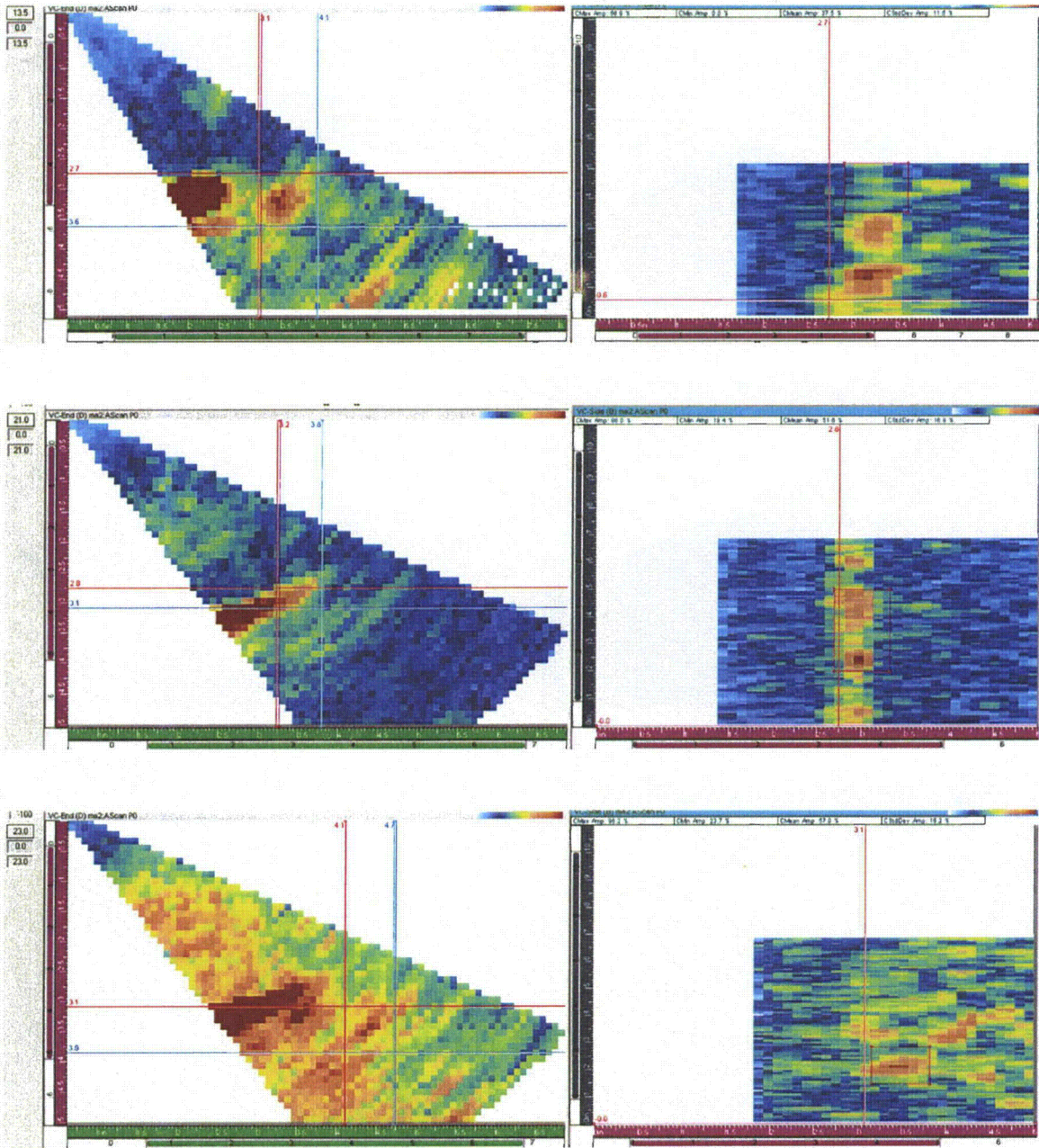


Figure C.4 WOG Sample APE-4 SCSS from Top to Bottom 500, 750 and 1000 kHz Showing Detection as: Yes, No, and No

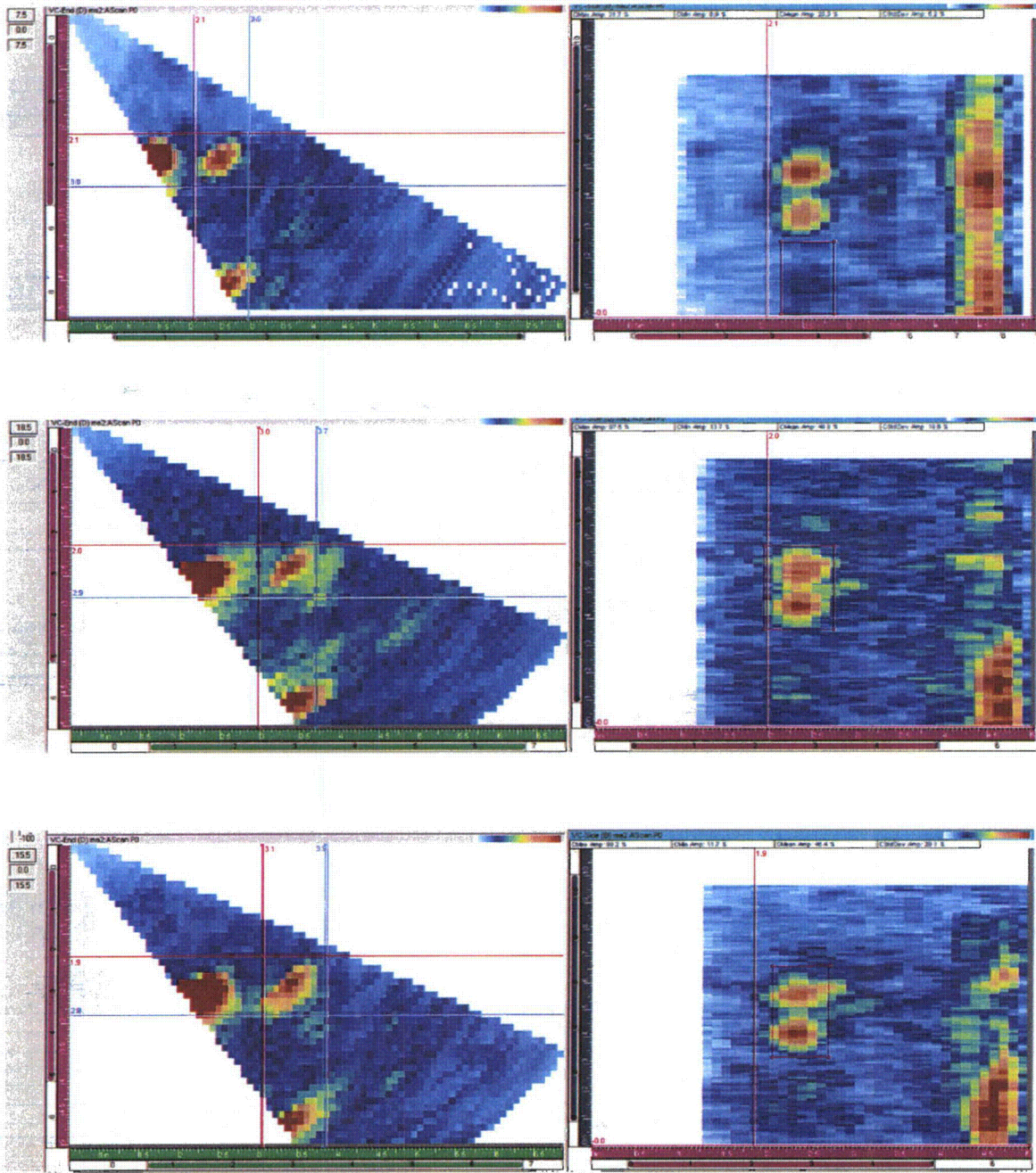


Figure C.5 WOG Sample INE-A-1 SCSS from Top to Bottom 500, 750 and 1000 kHz Showing Detection as: Yes, Yes and Yes

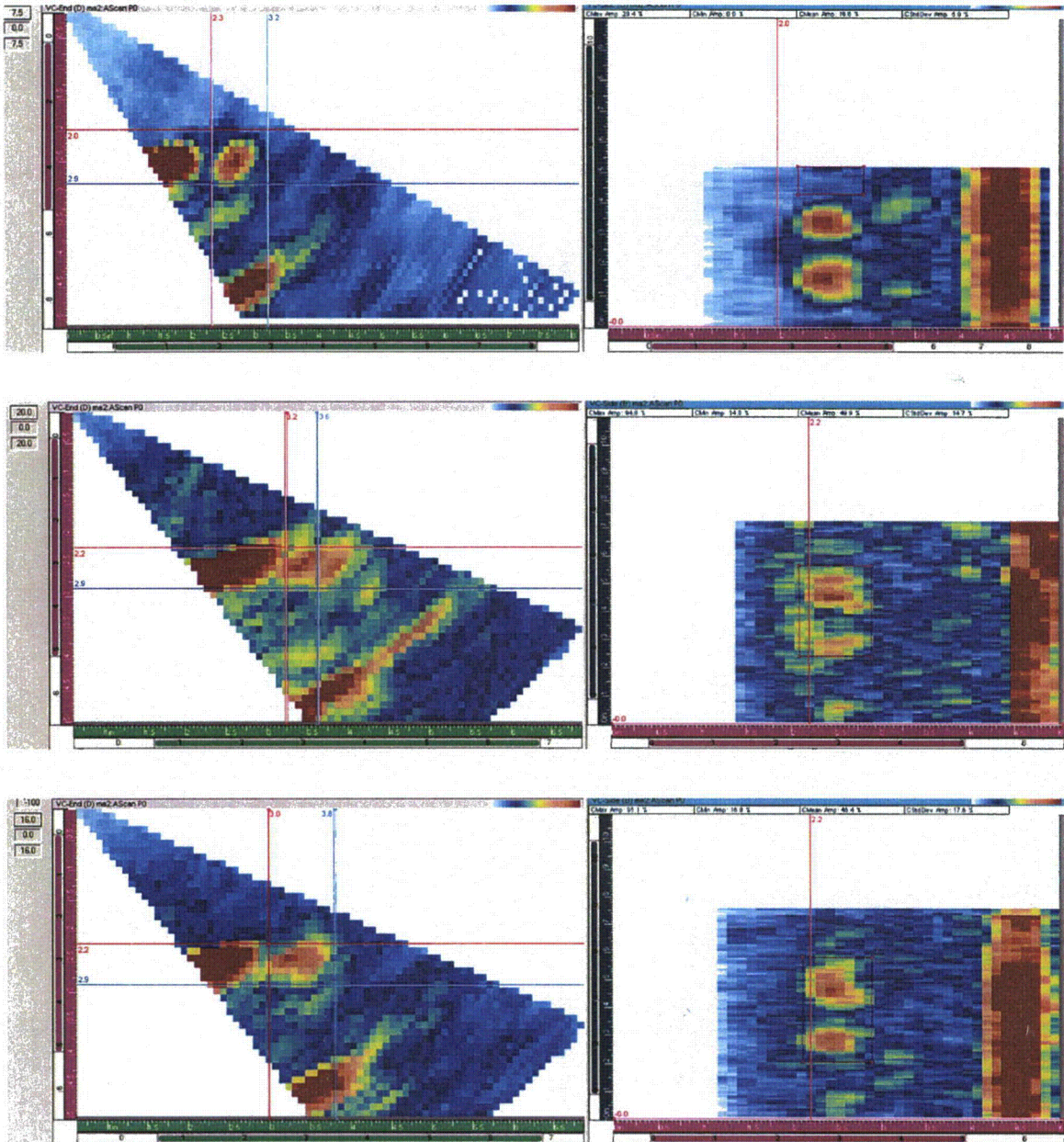


Figure C.6 WOG Sample INE-A-4 SCSS from Top to Bottom 500, 750 and 1000 kHz Showing Detection as: Yes, Yes and Yes

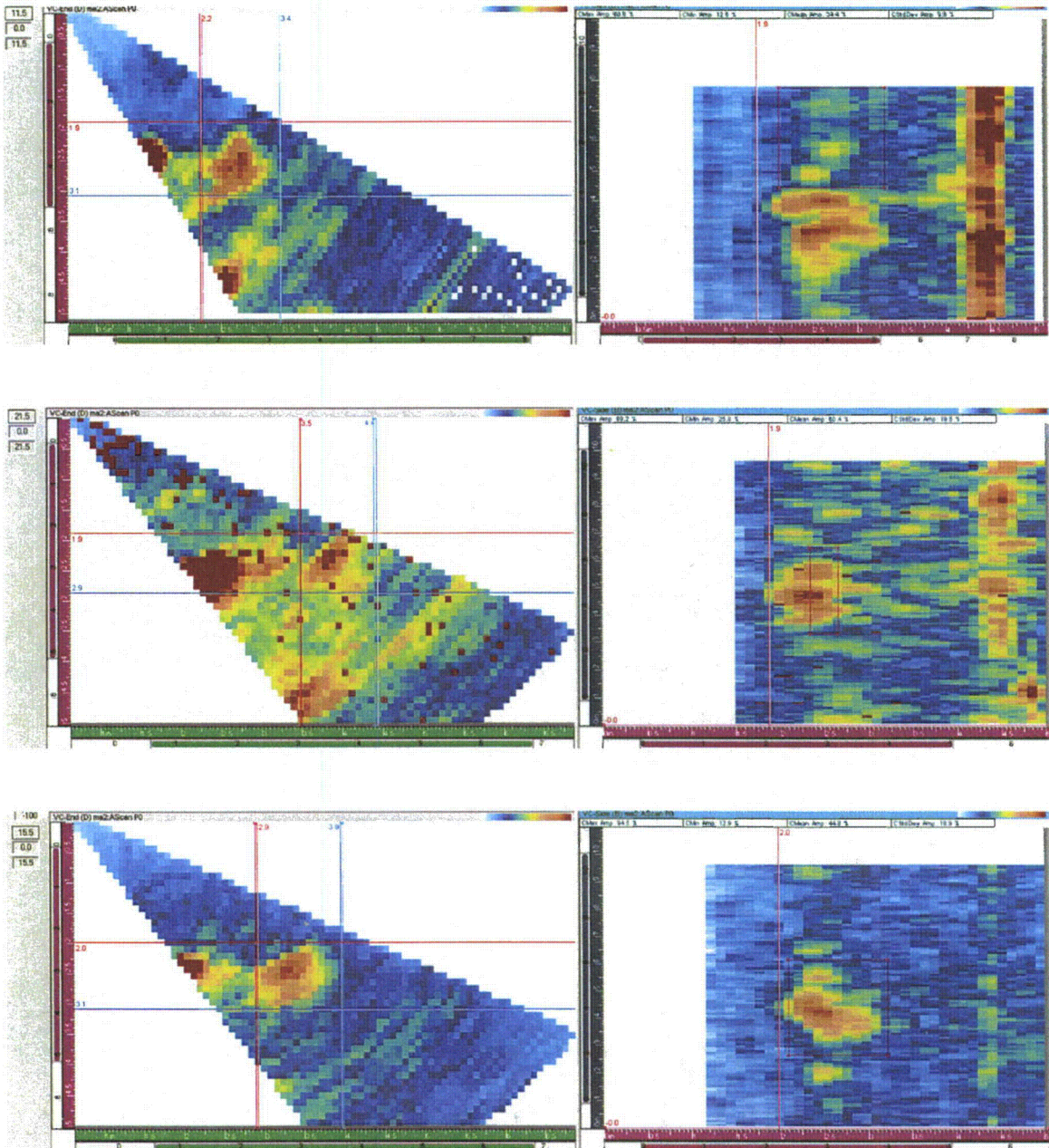


Figure C.7 WOG Sample INE-A-5 SCSS from Top to Bottom 500, 750 and 1000 kHz Showing Detection as: Yes, Yes and Yes

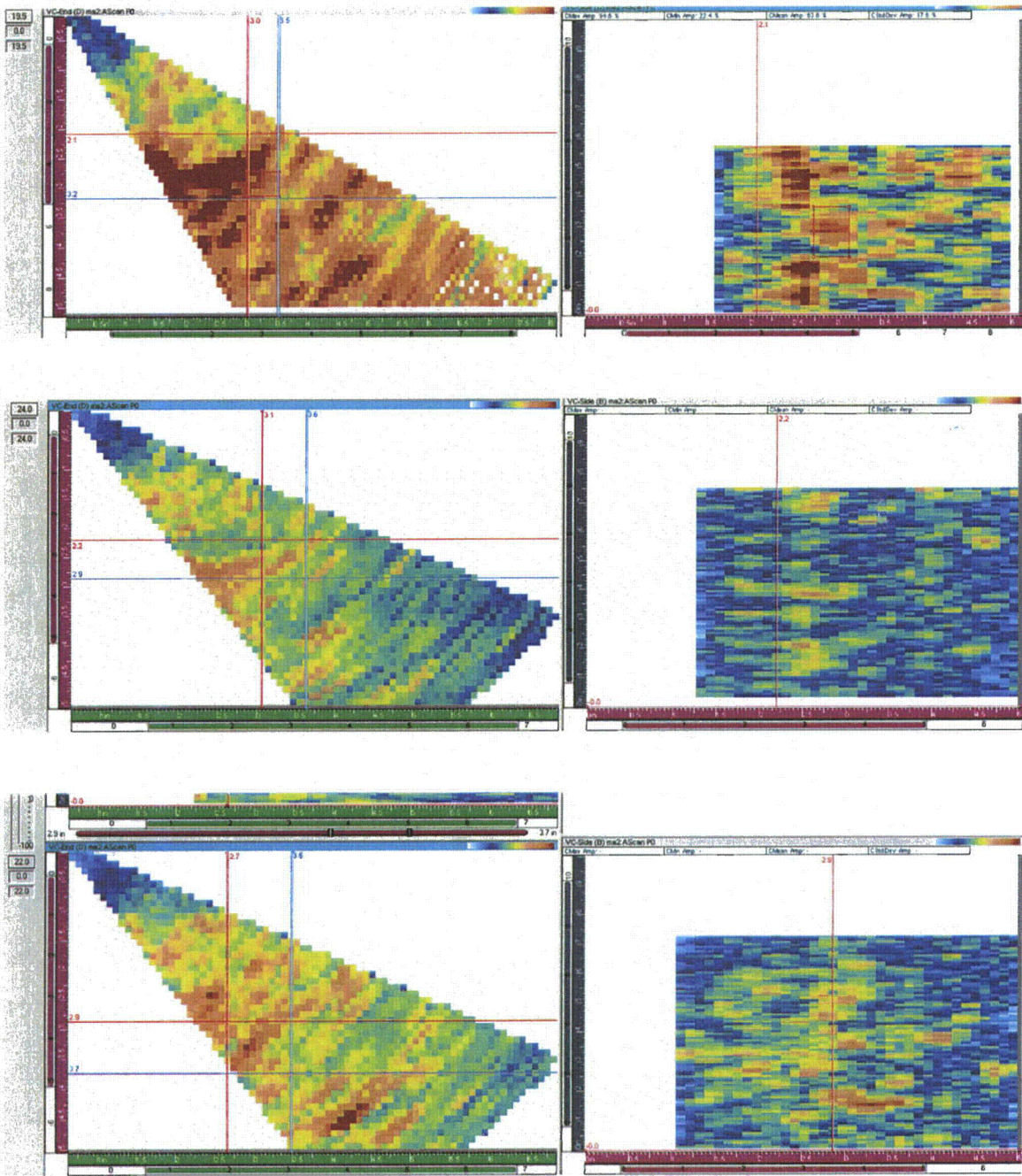


Figure C.8 WOG Sample MPE-3 CCSS from Top to Bottom 500, 750 and 1000 kHz Showing Detection as: Yes, No, and No

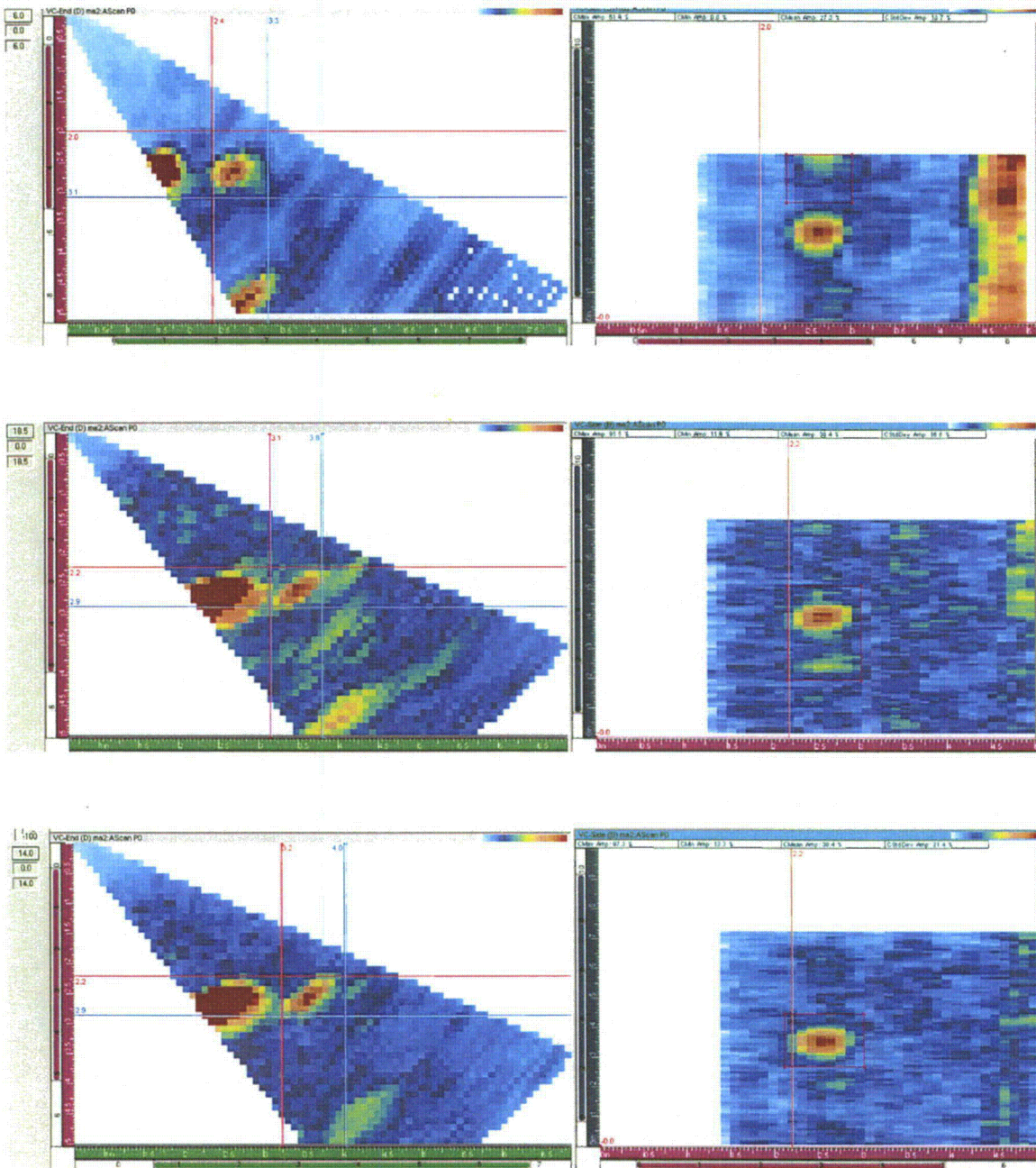


Figure C.9 WOG Sample MPE-3 SCSS from Top to Bottom 500, 750 and 1000 kHz Showing Detection as: Yes, Yes, and Yes

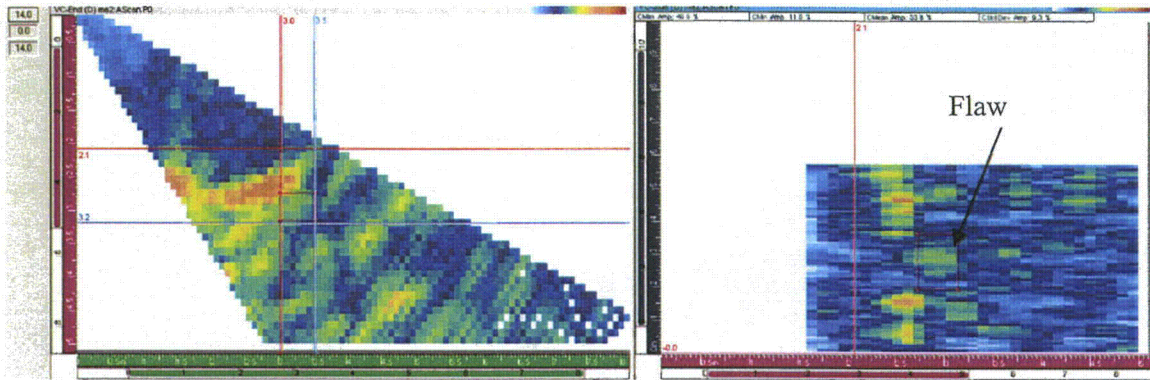
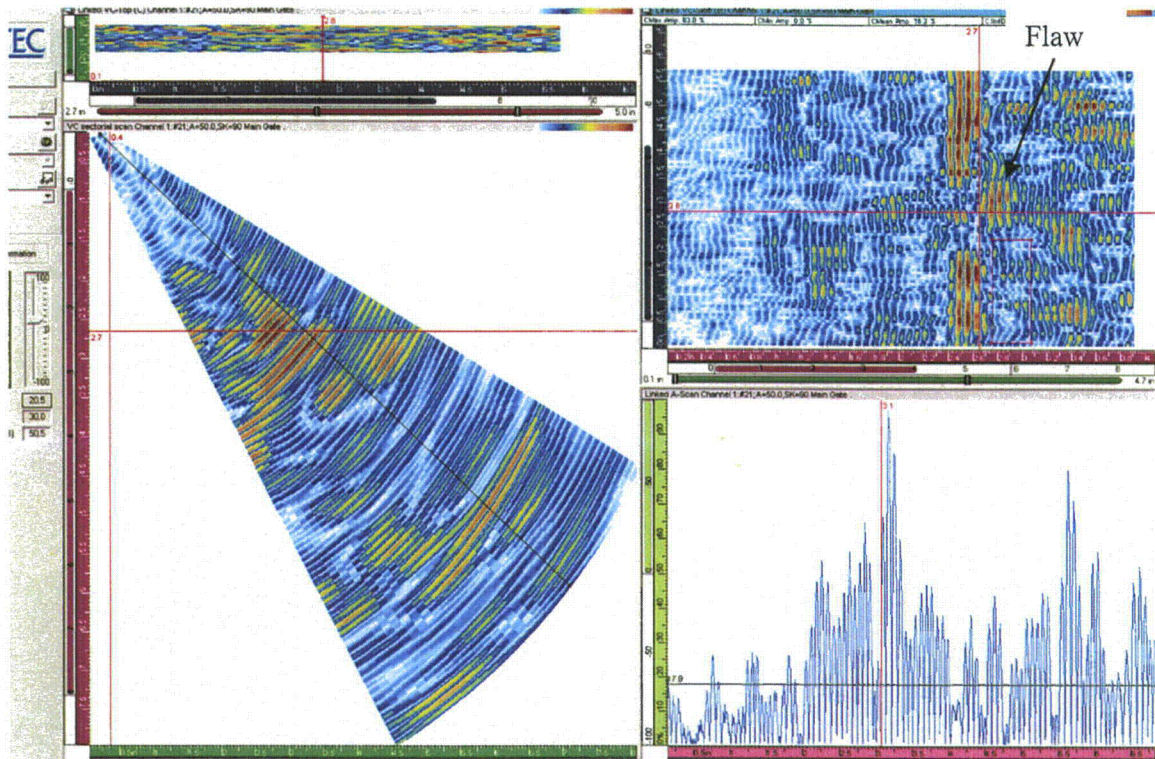


Figure C.10 WOG Sample MPE-3 CCSS at 500 kHz

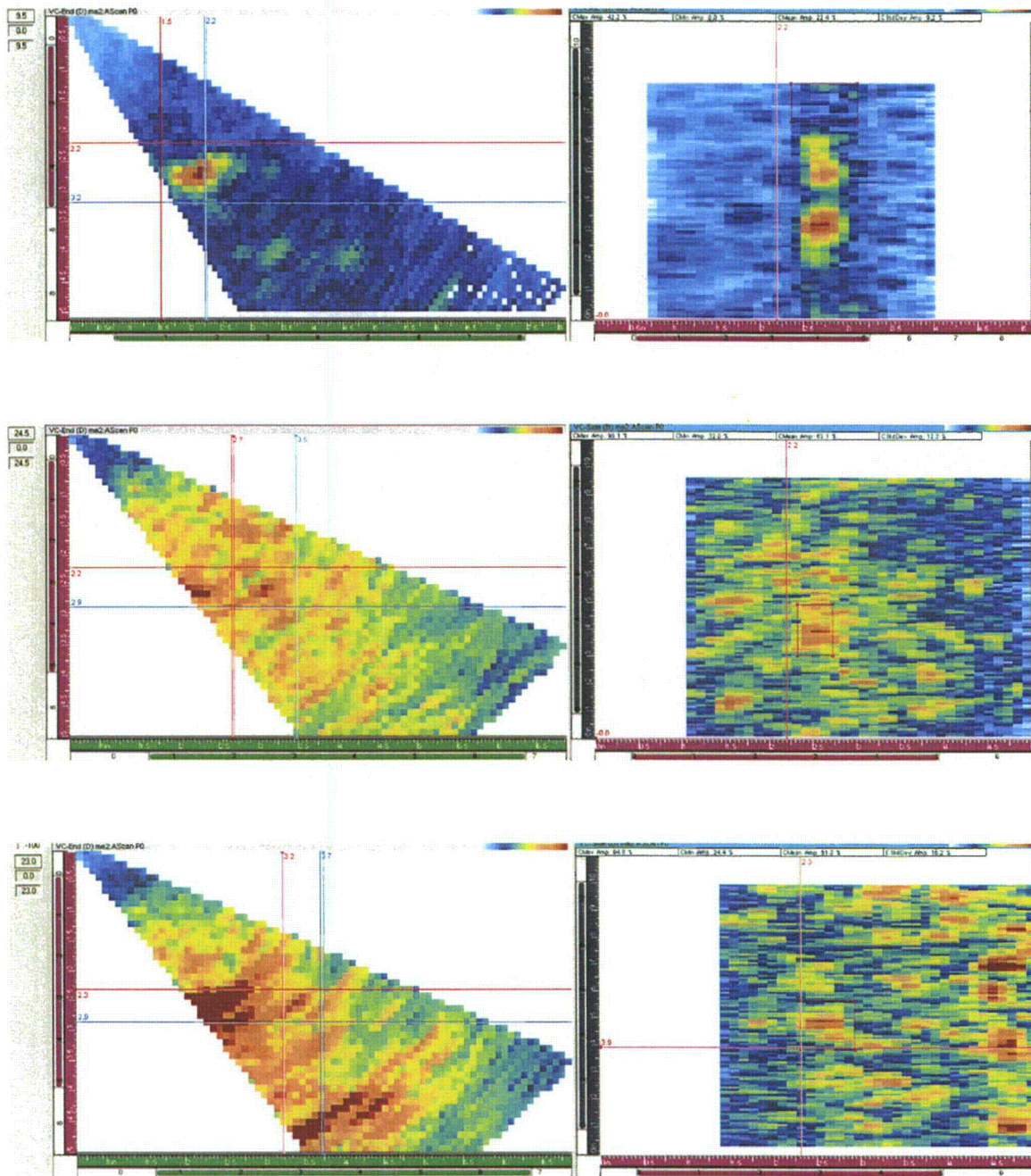


Figure C.11 WOG Sample MPE-6 CCSS from Top to Bottom 500, 750 and 1000 kHz Showing Detection as: Yes, Yes, and Marginal

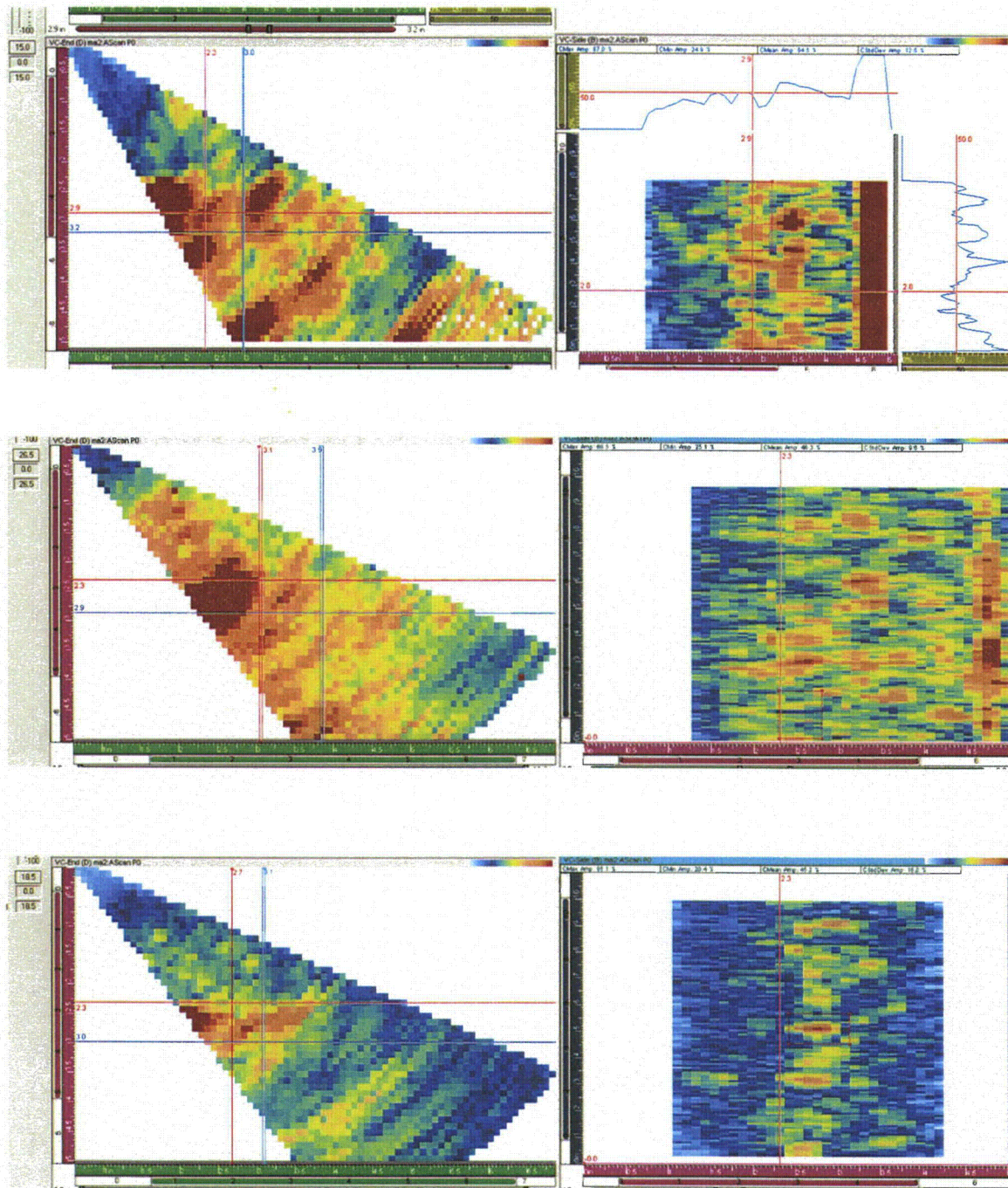


Figure C.12 WOG Sample MPE-6 SCSS from Top to Bottom 500, 750 and 1000 kHz Showing Detection as: Marginal, No, and No

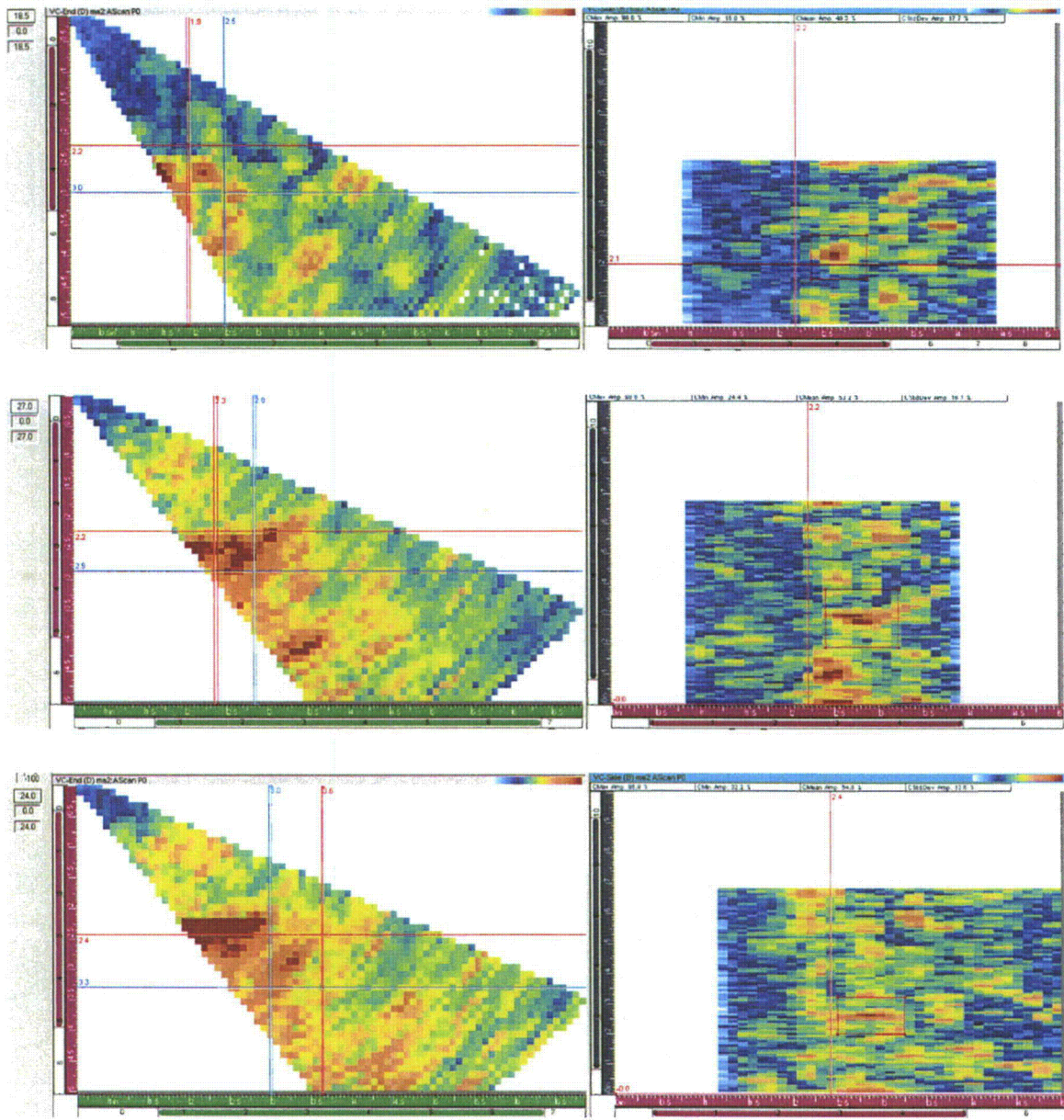


Figure C.13 WOG Sample ONP-3-5 CCSS from Top to Bottom 500, 750 and 1000 kHz Showing Detection as: Marginal, No, and No

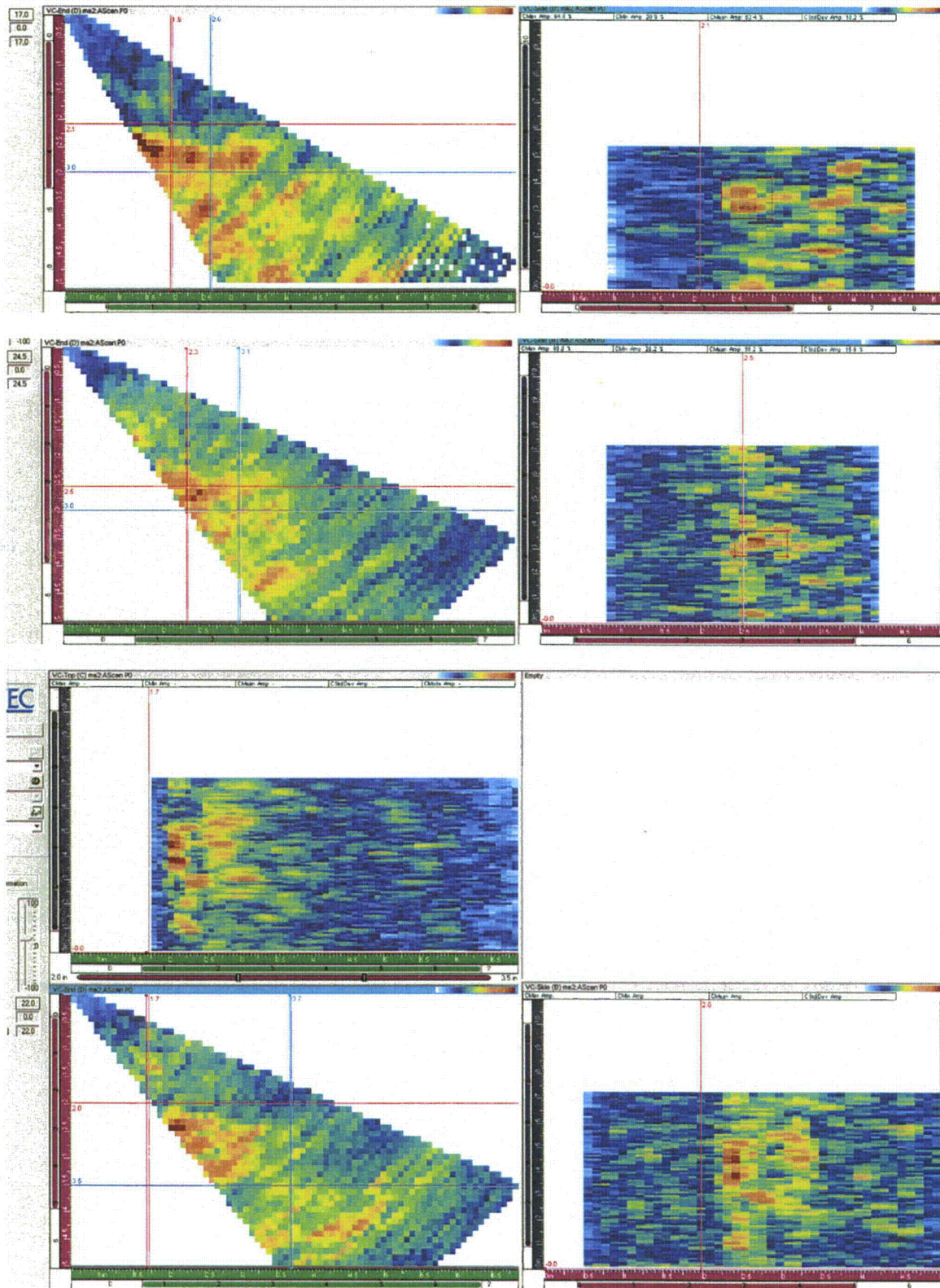


Figure C.14 WOG Sample ONP-3-8 CCSS from Top to Bottom 500, 750 and 1000 kHz Showing Detection as: Marginal, Yes, and Marginal

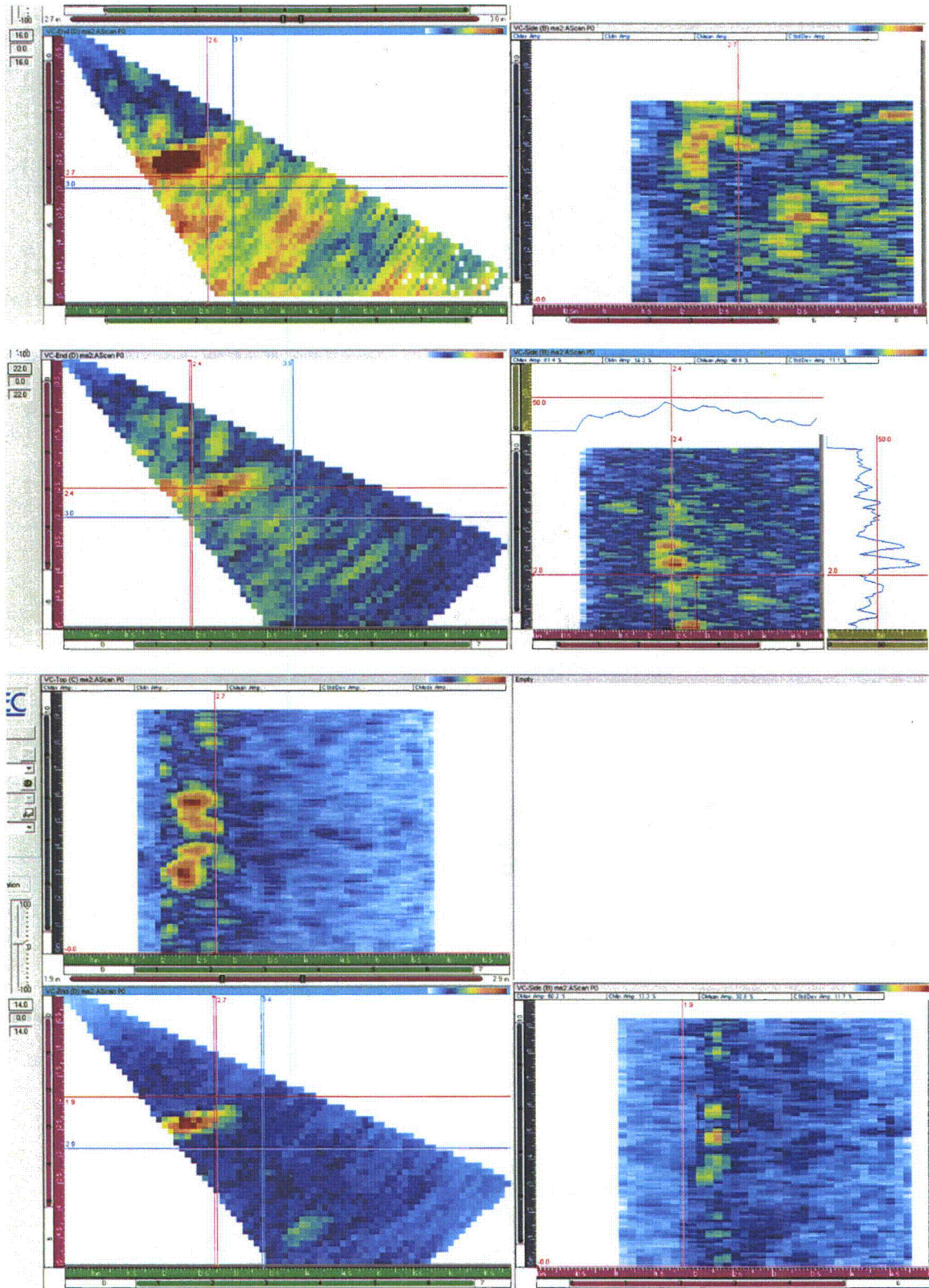


Figure C.15 WOG Sample ONP-D-2 CCSS from Top to Bottom 500, 750 and 1000 kHz Showing Detection as: Marginal, Yes, and Marginal

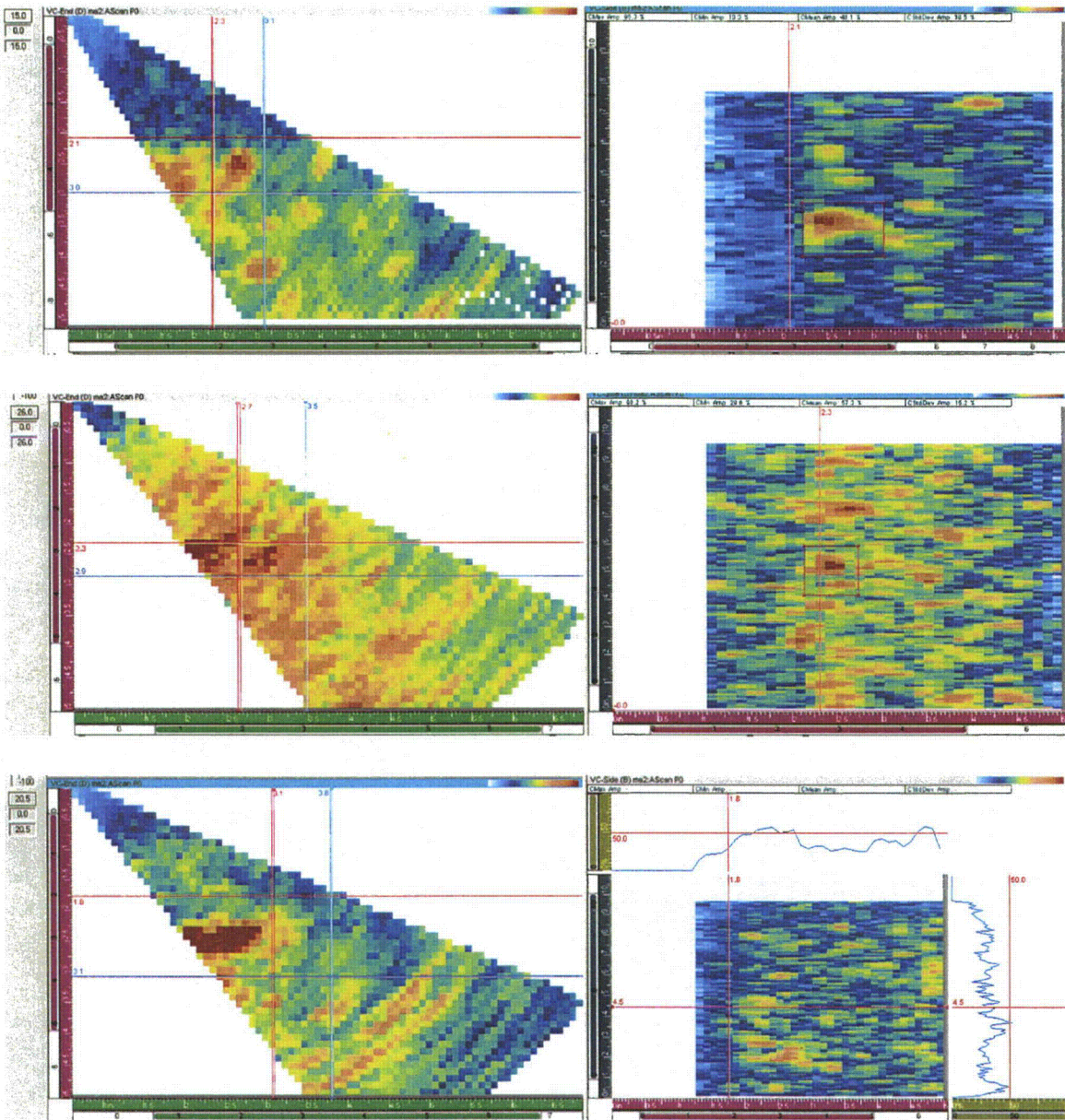


Figure C.16 WOG Sample ONP-D-5 CCSS from Top to Bottom 500, 750 and 1000 kHz Showing Detection as: Yes, Marginal, and Marginal

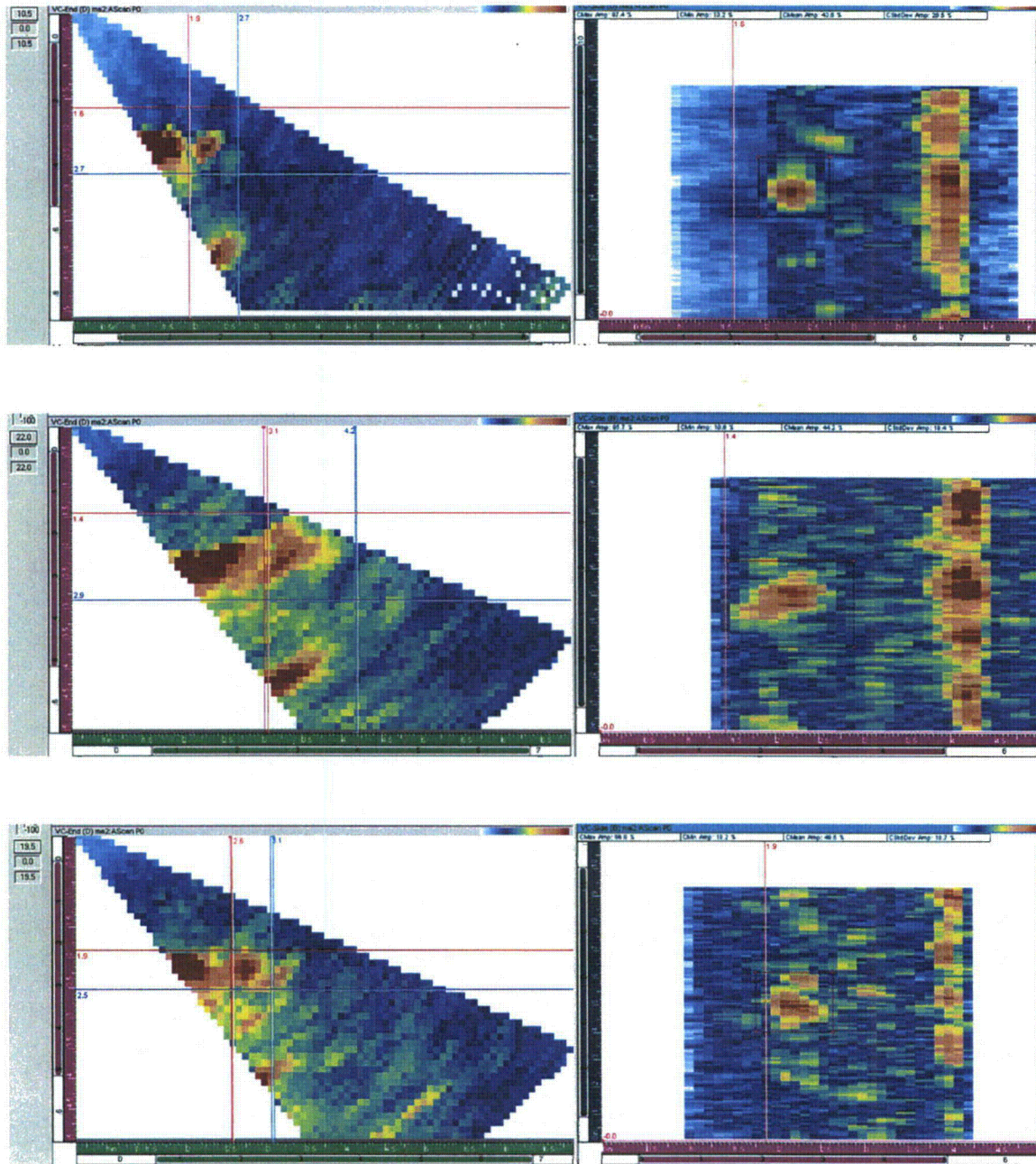


Figure C.17 WOG Sample OPE-2 CCSS from Top to Bottom 500, 750 and 1000 kHz Showing Detection as: Yes, Yes, and Yes

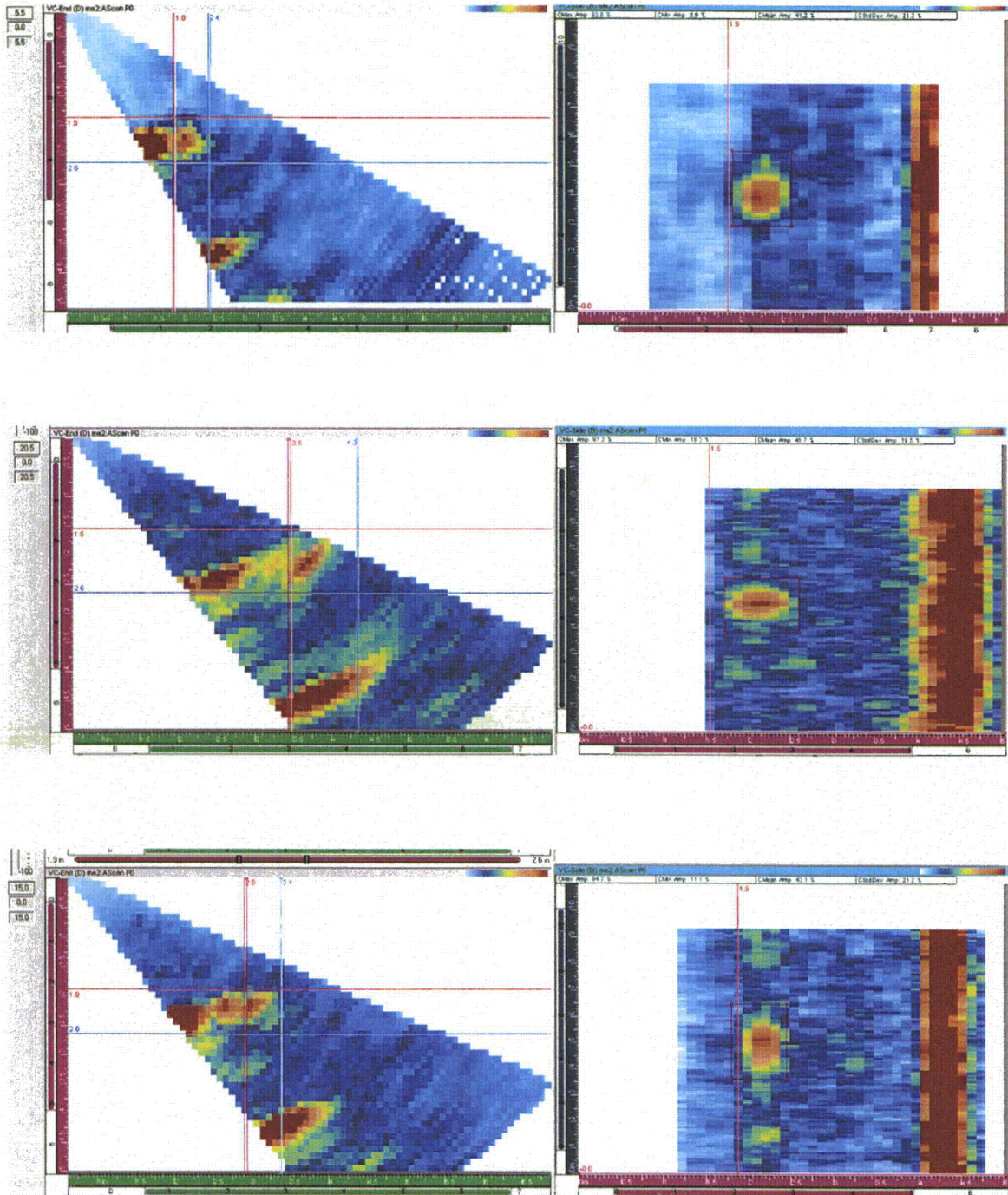


Figure C.18 WOG Sample OPE-2 SCSS from Top to Bottom 500, 750 and 1000 kHz Showing Detection as: Yes, Yes, and Yes

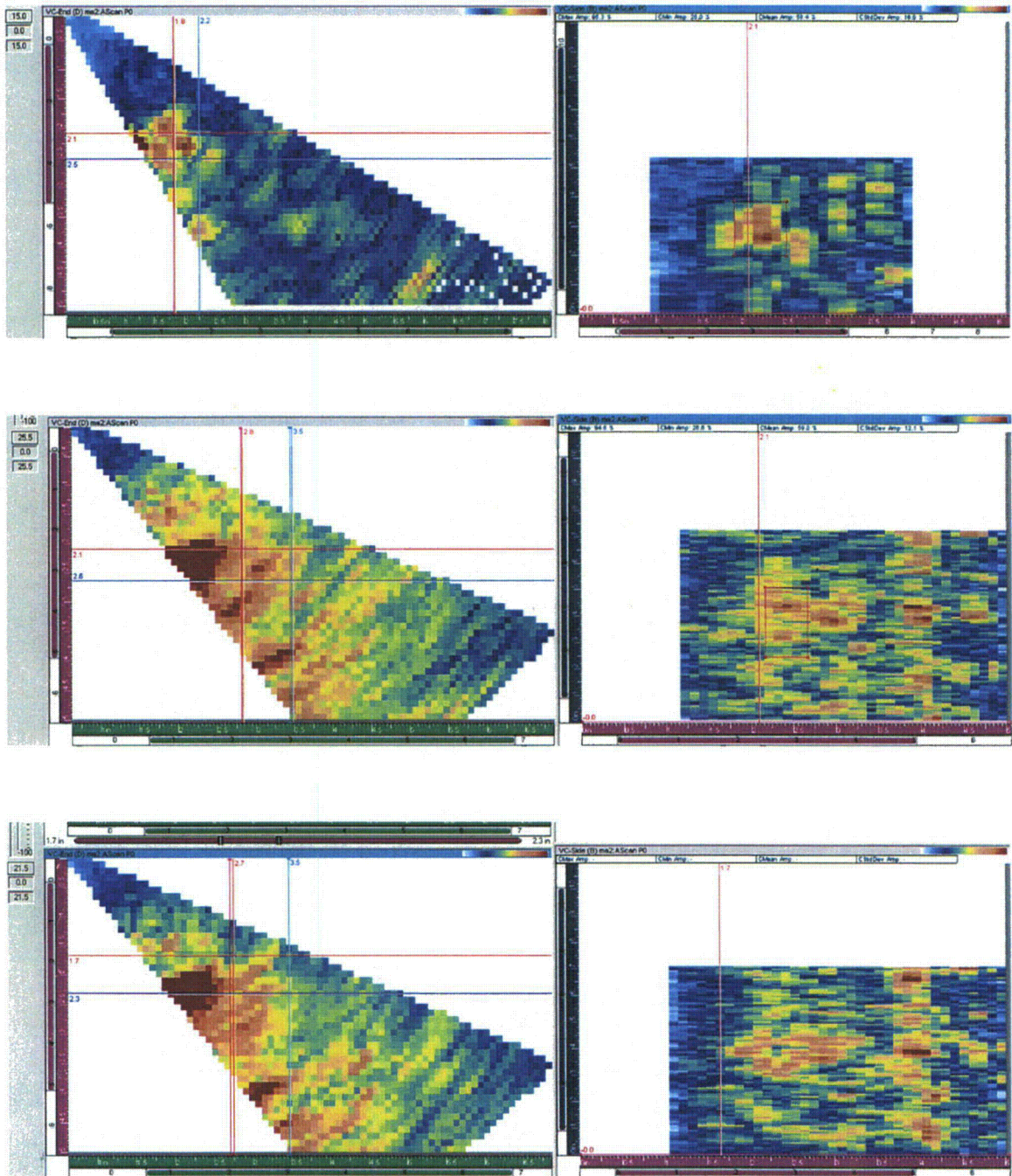


Figure C.19 WOG Sample OPE-5 CCSS from Top to Bottom 500, 750 and 1000 kHz Showing Detection as: Yes, Marginal, and Marginal

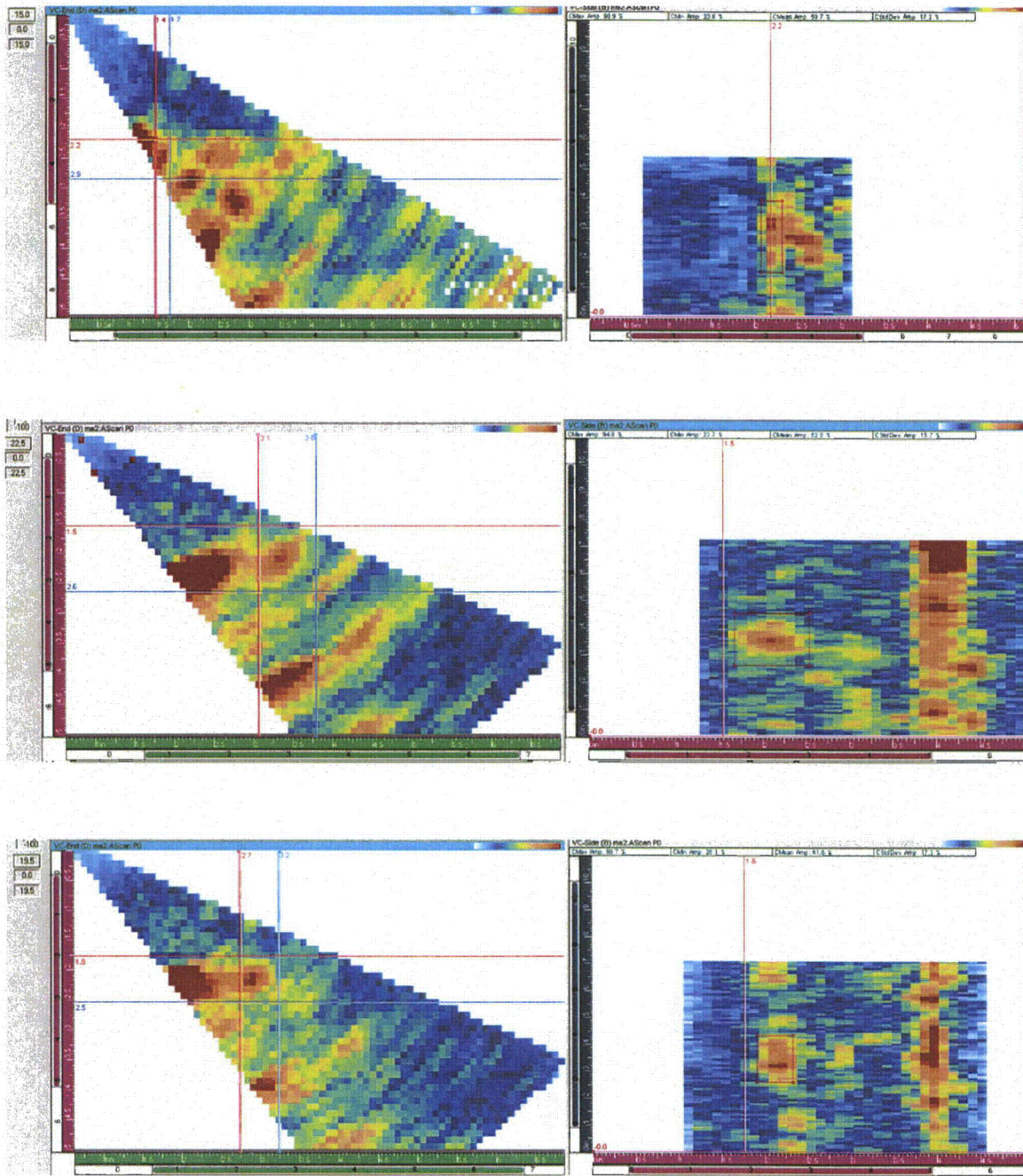


Figure C.20 WOG Sample OPE-5 SCSS from Top to Bottom 500, 750 and 1000 kHz Showing Detection as: Yes, Yes, and Yes

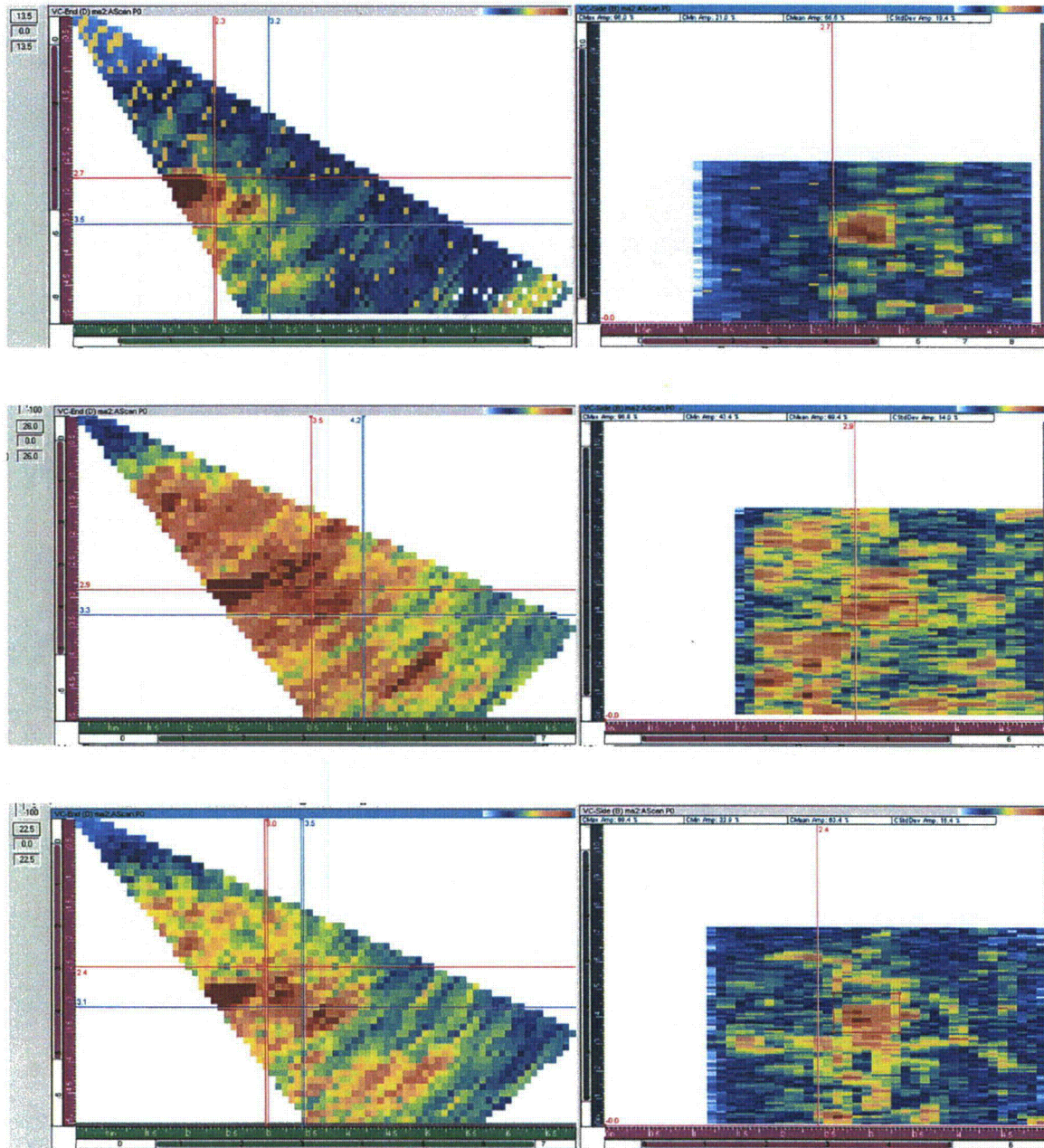


Figure C.21 WOG Sample POP-7 CCSS from Top to Bottom 500, 750 and 1000 kHz Showing Detection as: Yes, No, and Yes

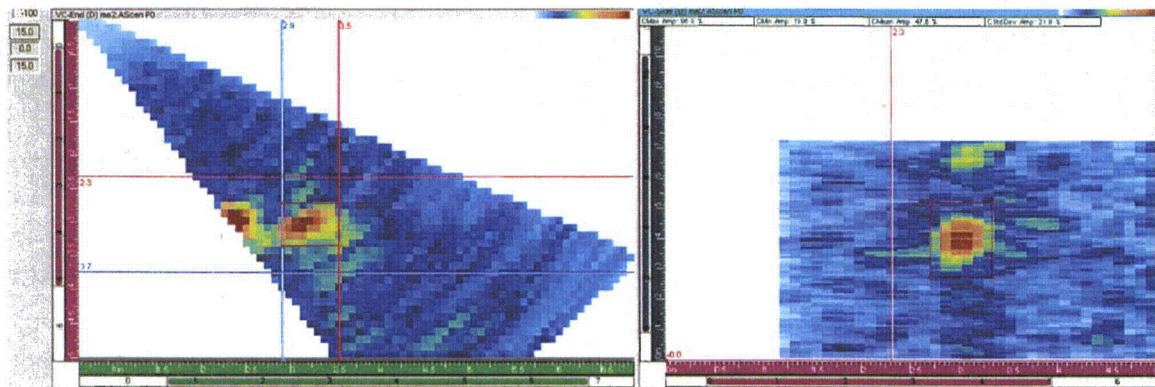
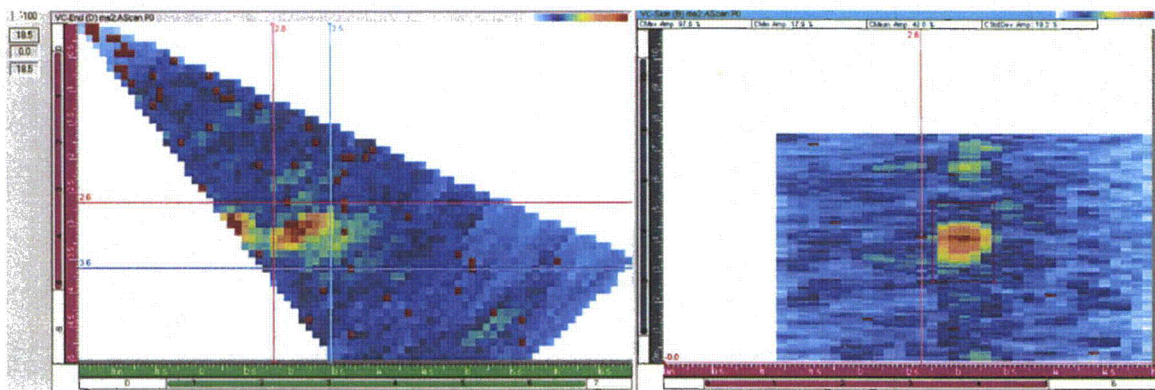
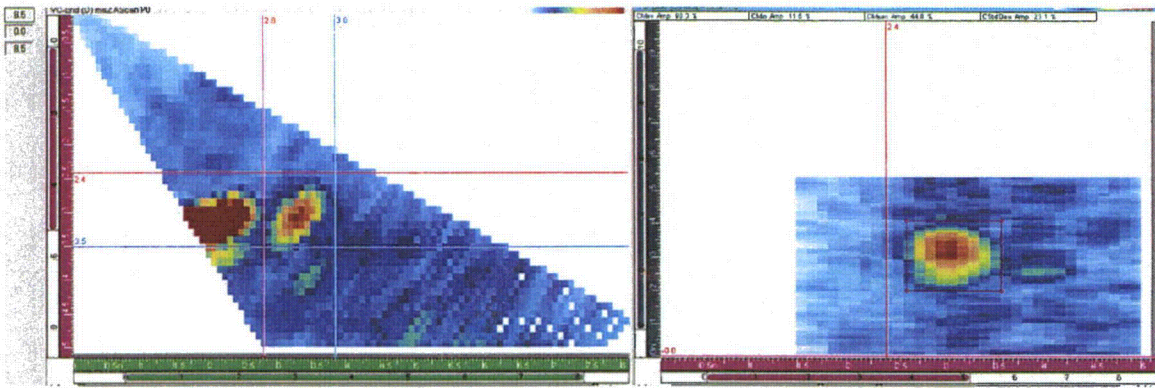


Figure C.22 WOG Sample POP-7 SCSS from Top to Bottom 500, 750 and 1000 kHz Showing Detection as: Yes, Yes, and Yes

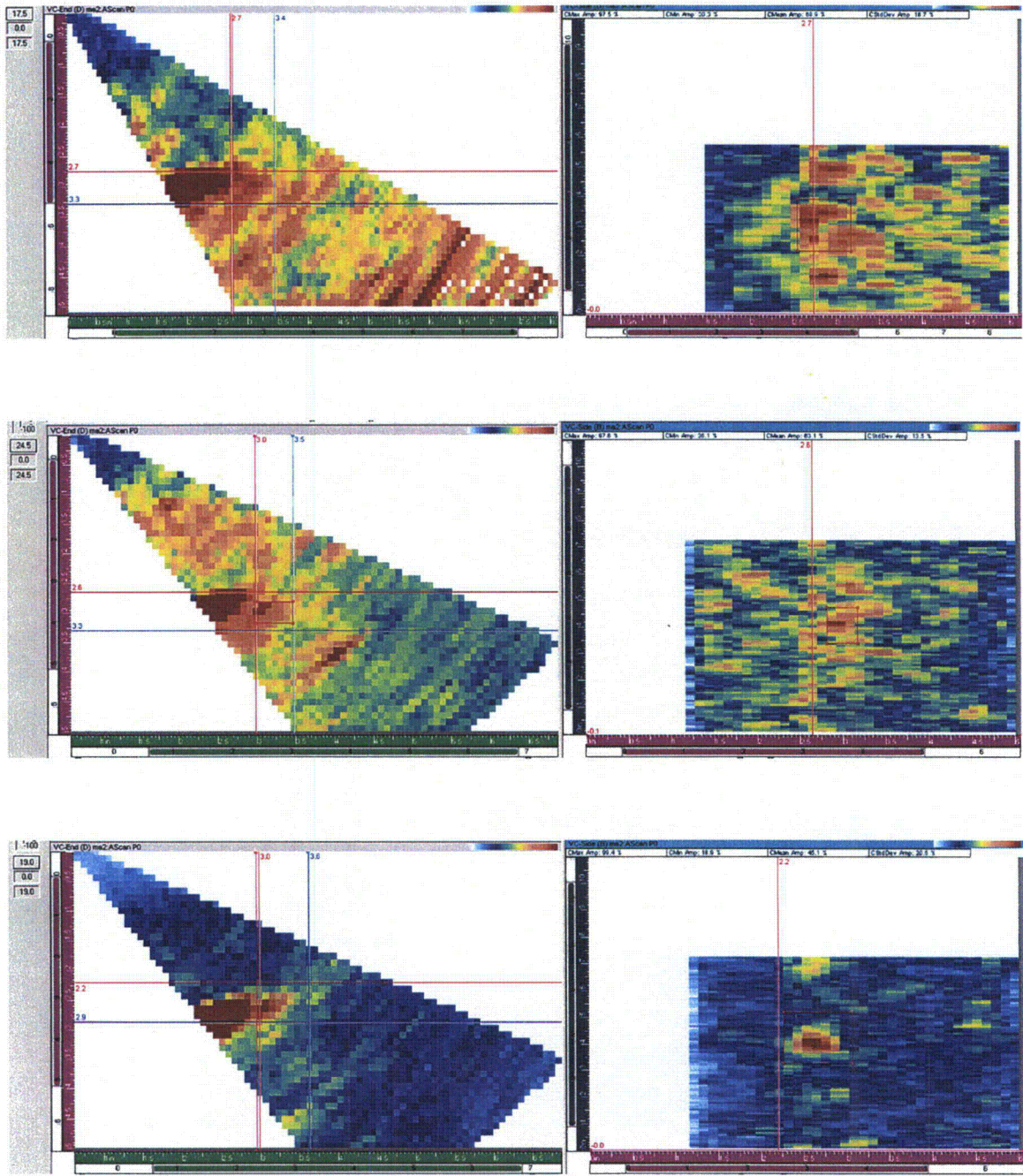


Figure C.23 WOG Sample POP-8 CCSS from Top to Bottom 500, 750 and 1000 kHz Showing Detection as: Marginal, Marginal, and Yes

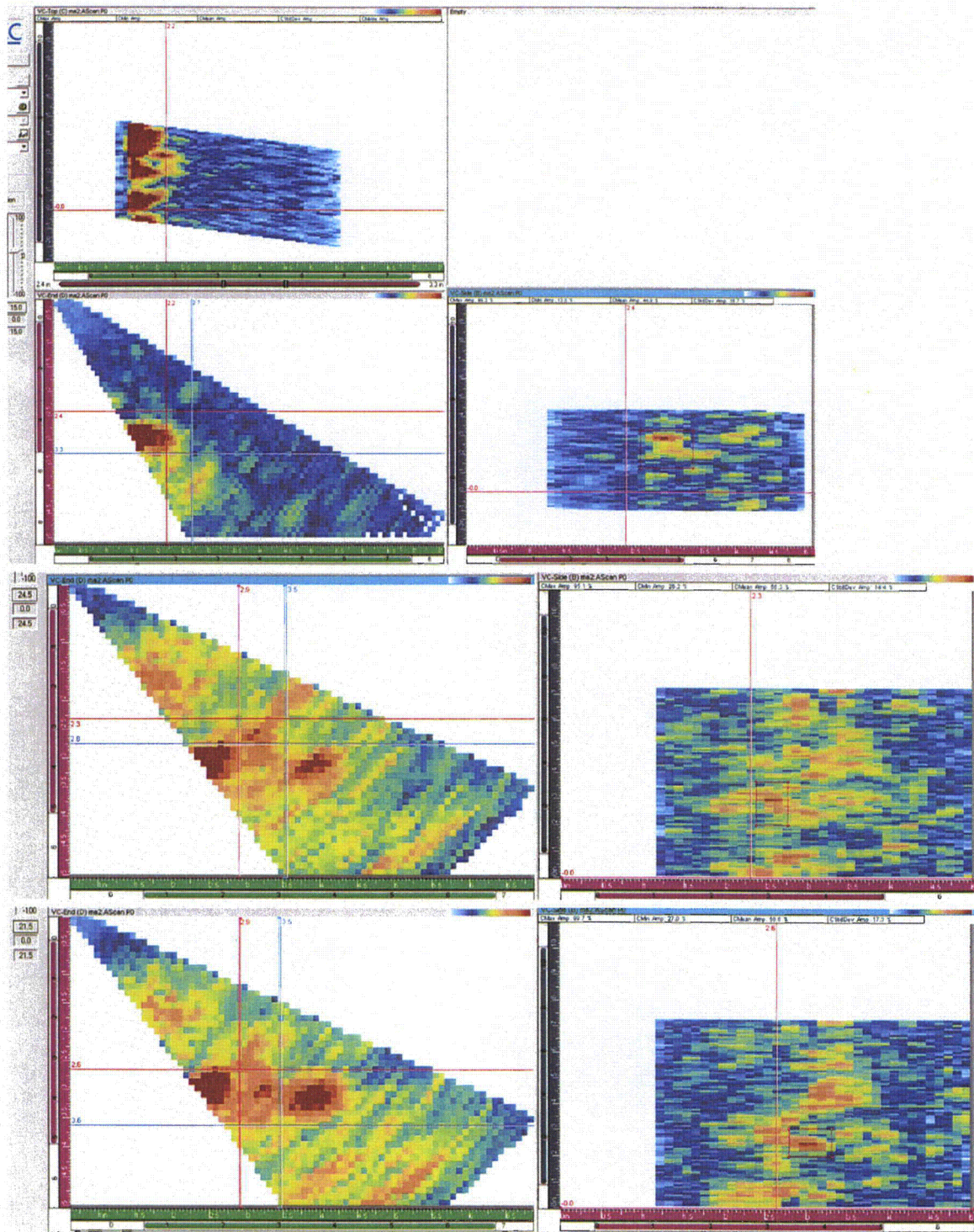


Figure C.24 WOG Sample POP-8 SCSS from Top to Bottom 500, 750 and 1000 kHz Showing Detection as: Yes, Marginal, and Marginal. The 500 kHz data is skewed by 20 degrees.

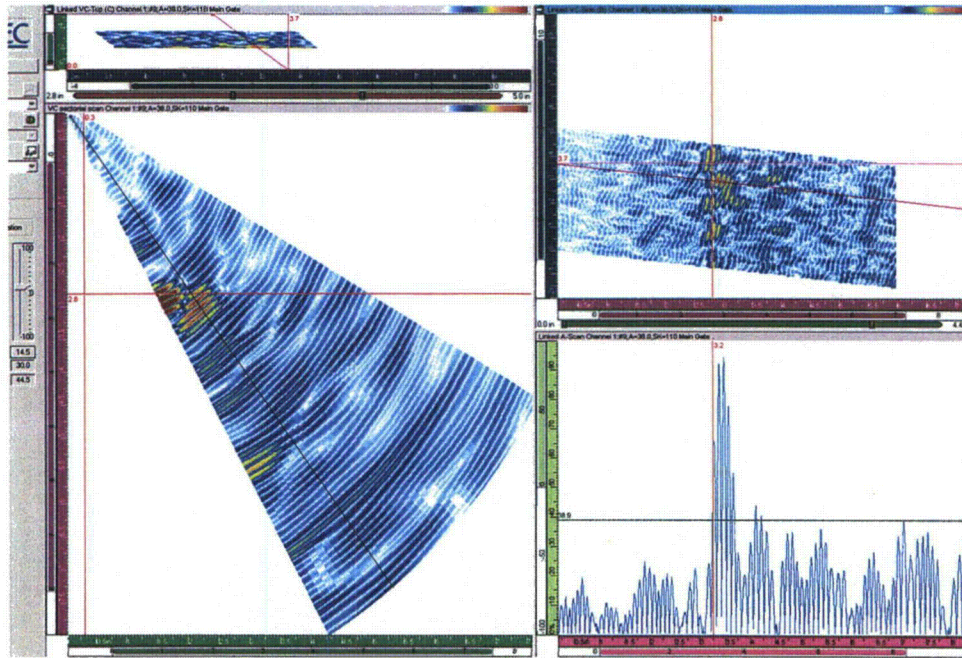


Figure C.25 WOG Sample POP-8 SCSS at 500 kHz with a 20 Degree Skew Showing a Detection

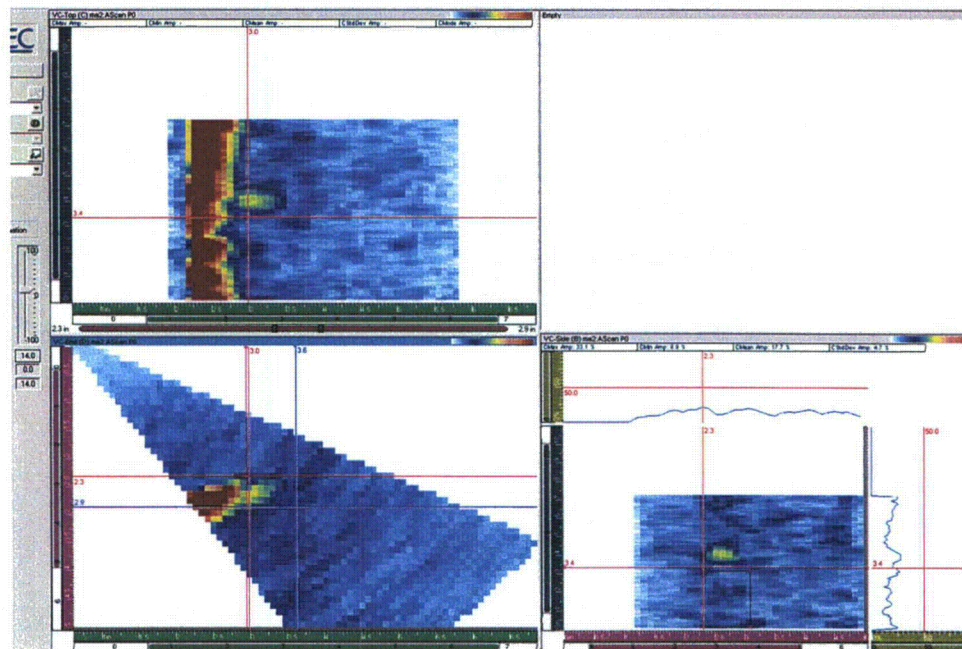


Figure C.26 WOG Sample POP-8 CCSS at 1 MHz Showing a Detection

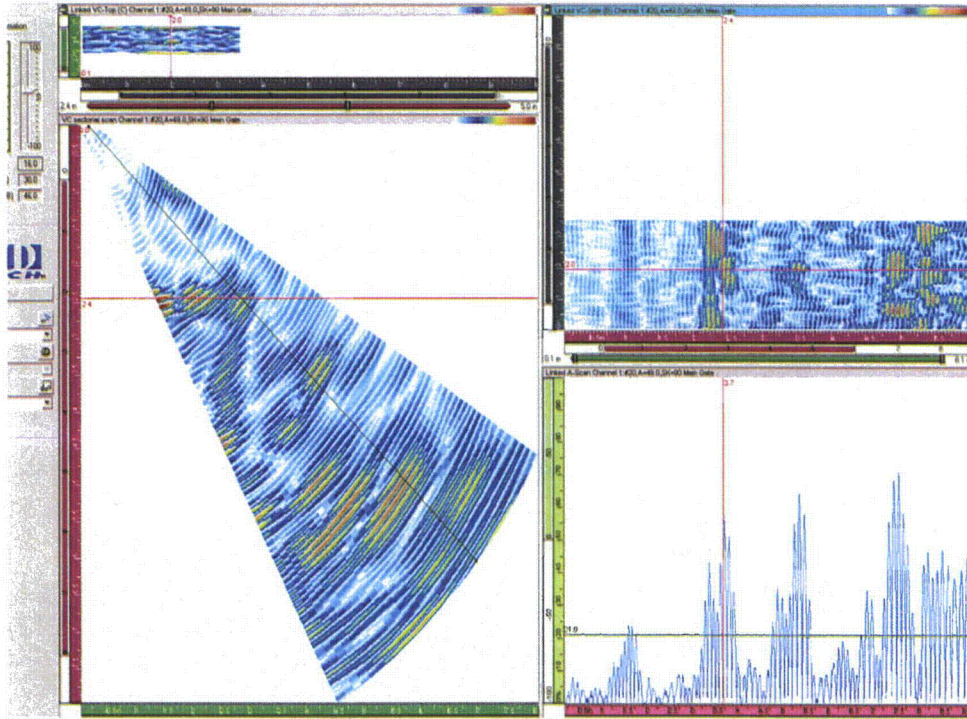


Figure C.27 B501 Sample as Inspected From the Columnar Side of the Weld, Showing a Marginal Detection

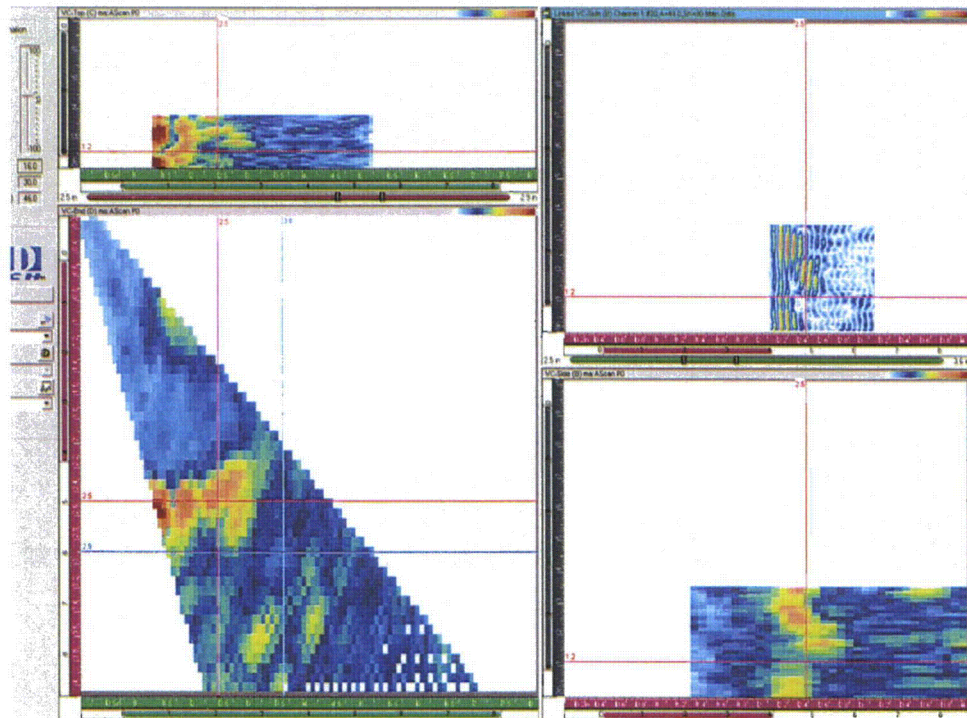


Figure C.28 B501 Sample as Inspected From the Columnar Side of the Weld with Merged Data, Showing a Marginal Detection

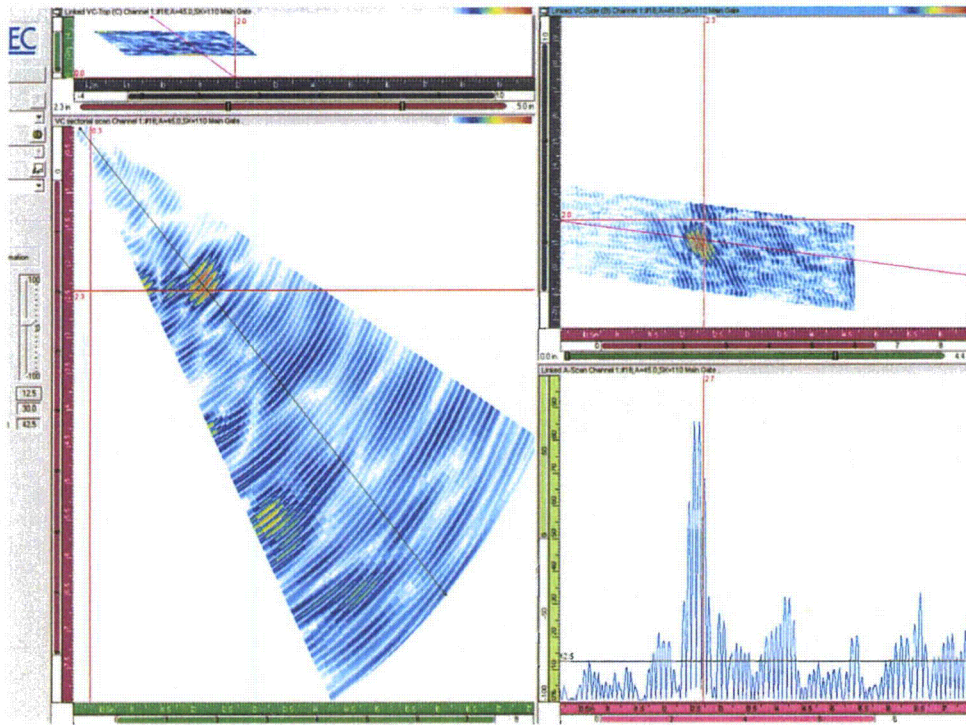


Figure C.29 B501 as Inspected from the Equiaxed Side of the Weld, Showing a Yes Detected

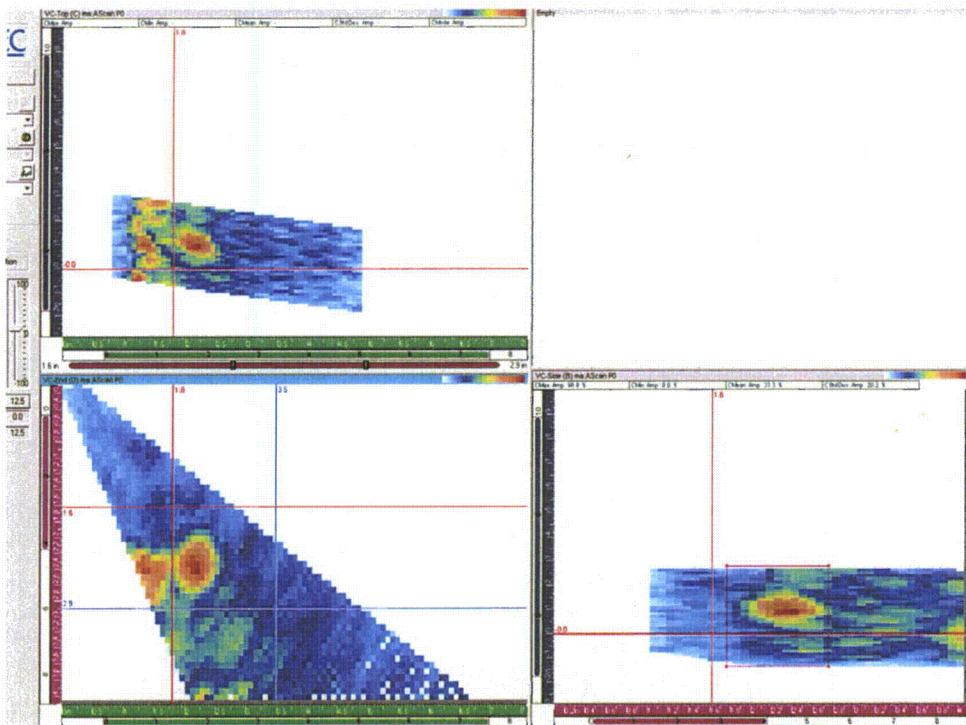


Figure C.30 B501 as Inspected from the Equiaxed Side of the Weld with Merged Data, Showing a Yes Detected

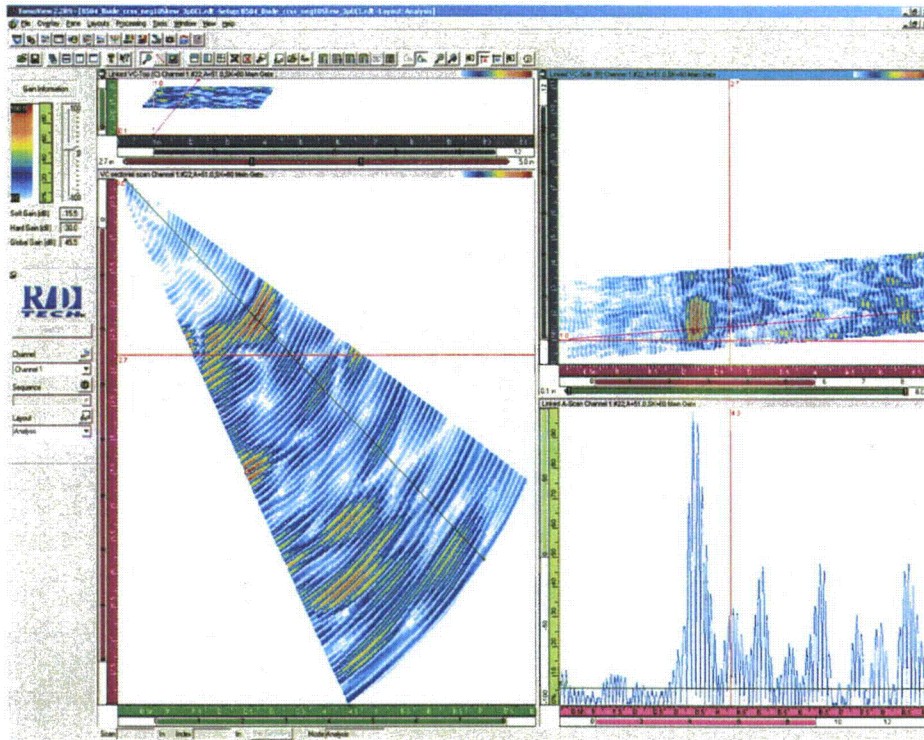


Figure C.31 B504 as Inspected from the Columnar Side of the Weld, Showing a Yes Detected

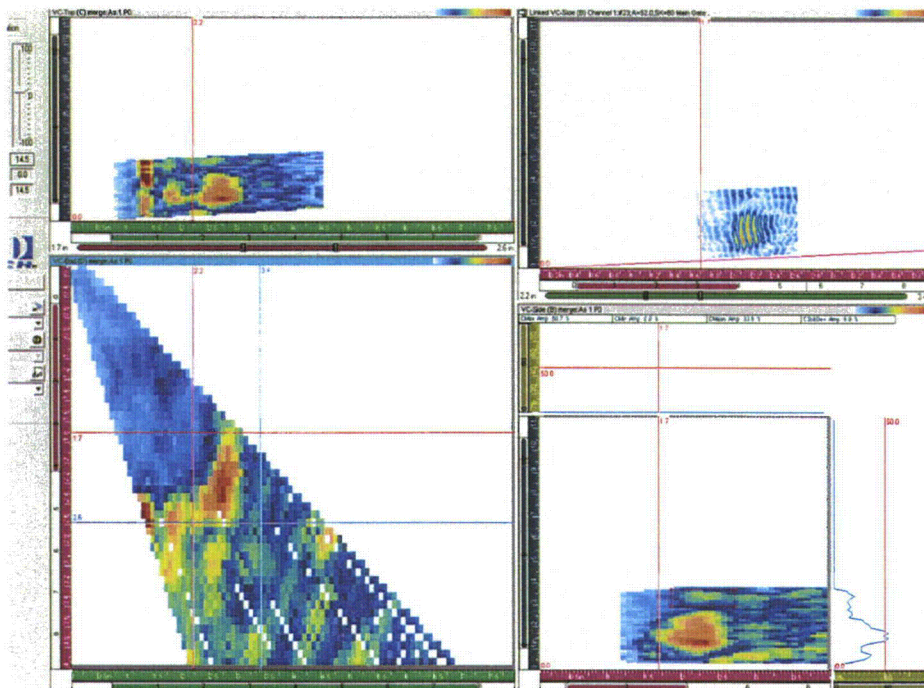


Figure C.32 B504 as Inspected from the Columnar Side of the Weld with Merged Data, Showing a Yes Detected

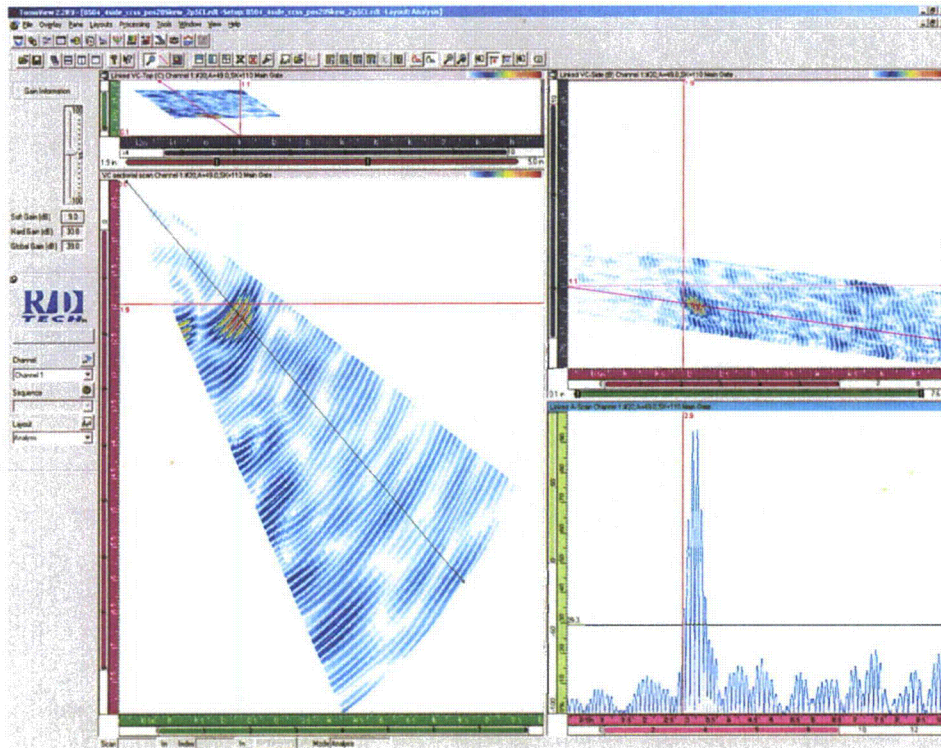


Figure C.33 B504 as Inspected from the Equiaxed Side of the Weld, Showing a Yes Detected

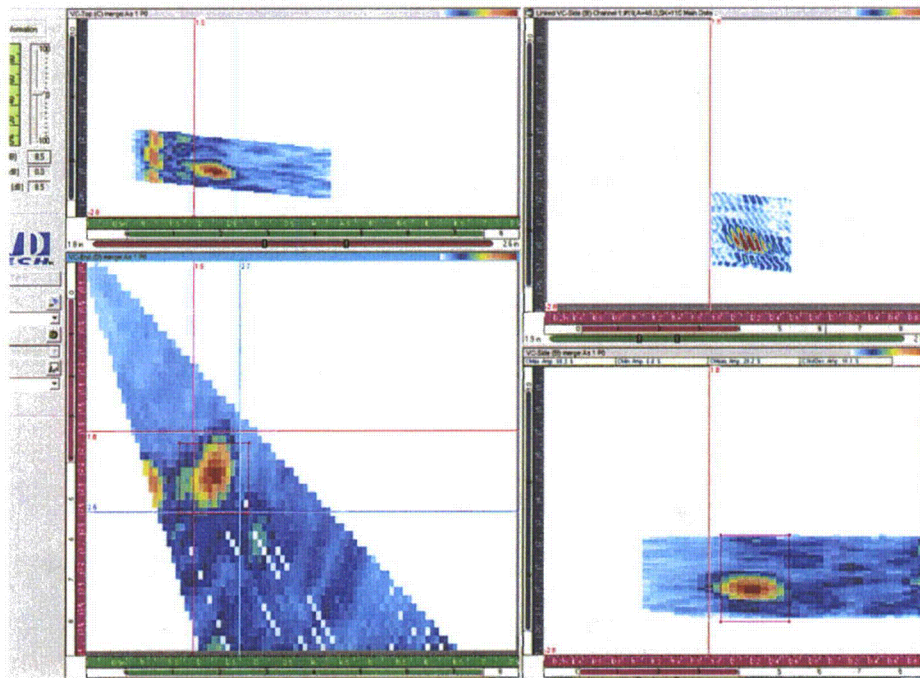


Figure C.34 B504 as Inspected from the Equiaxed Side of the Weld with Merged Data, Showing a Yes Detected

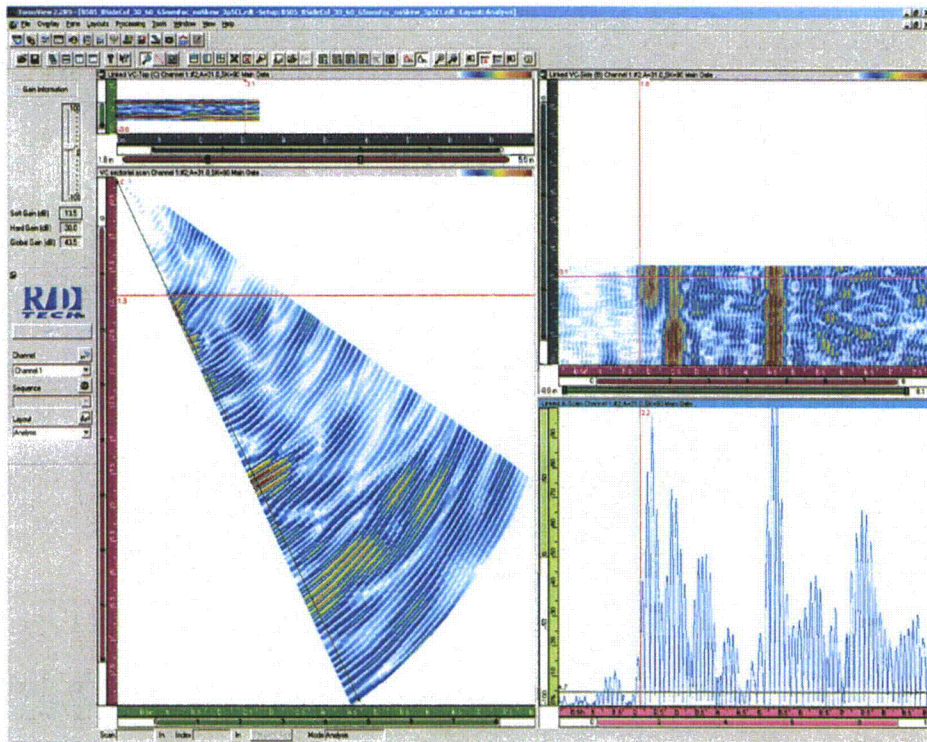


Figure C.35 B505 Inspected from the Columnar Side of the Weld, Showing a Yes Detected

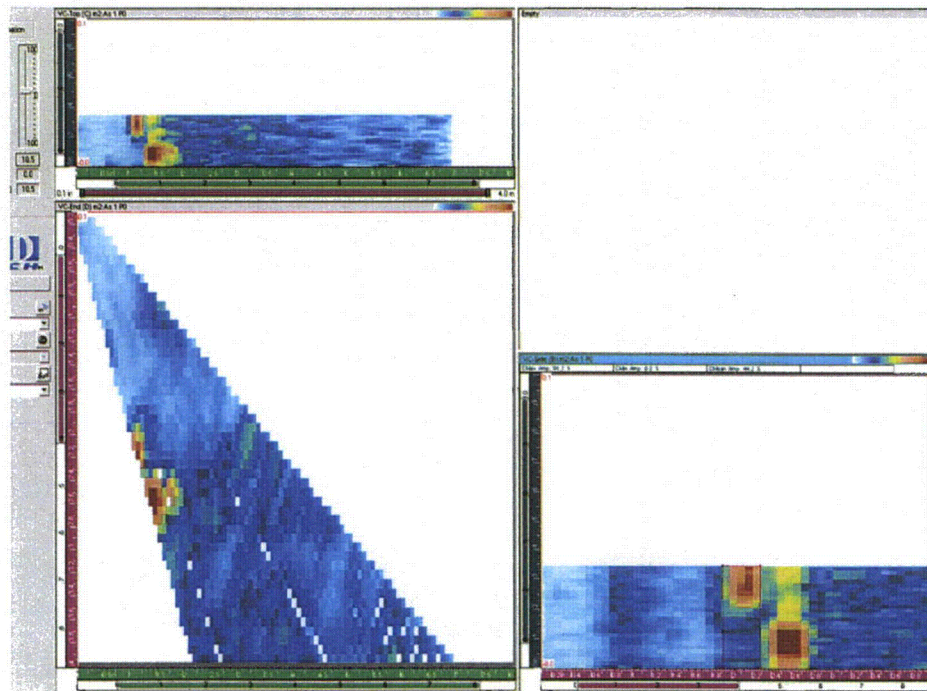


Figure C.36 B505 Inspected from the Columnar Side of the Weld with Merged Data, Showing a Yes Detected

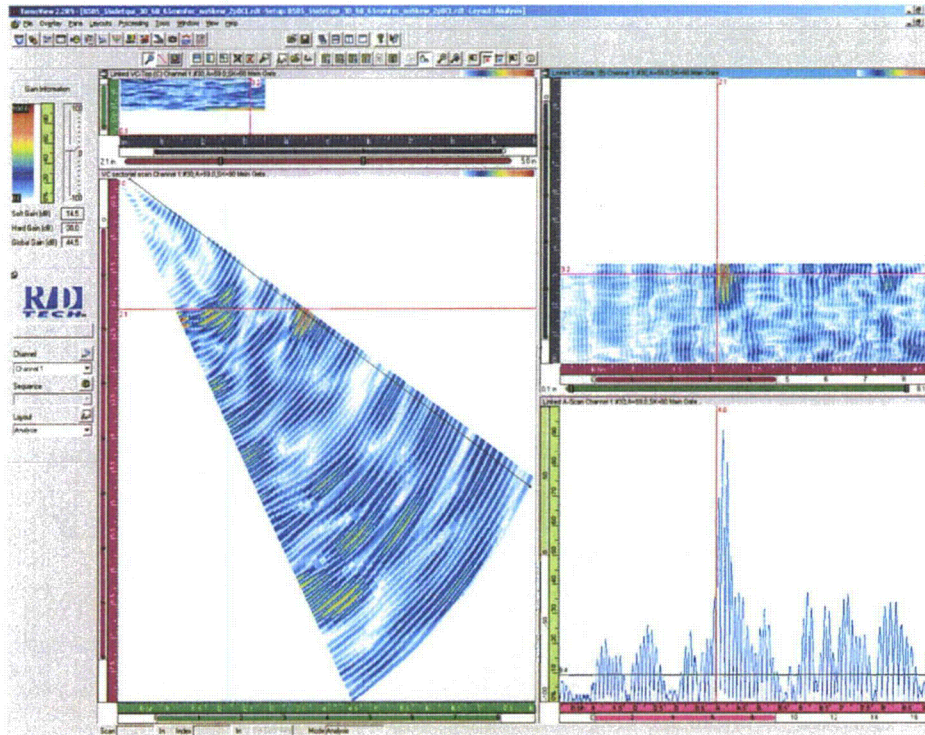


Figure C.37 B505 Inspected from the Equiaxed Side of the Weld, Showing a Yes Detected

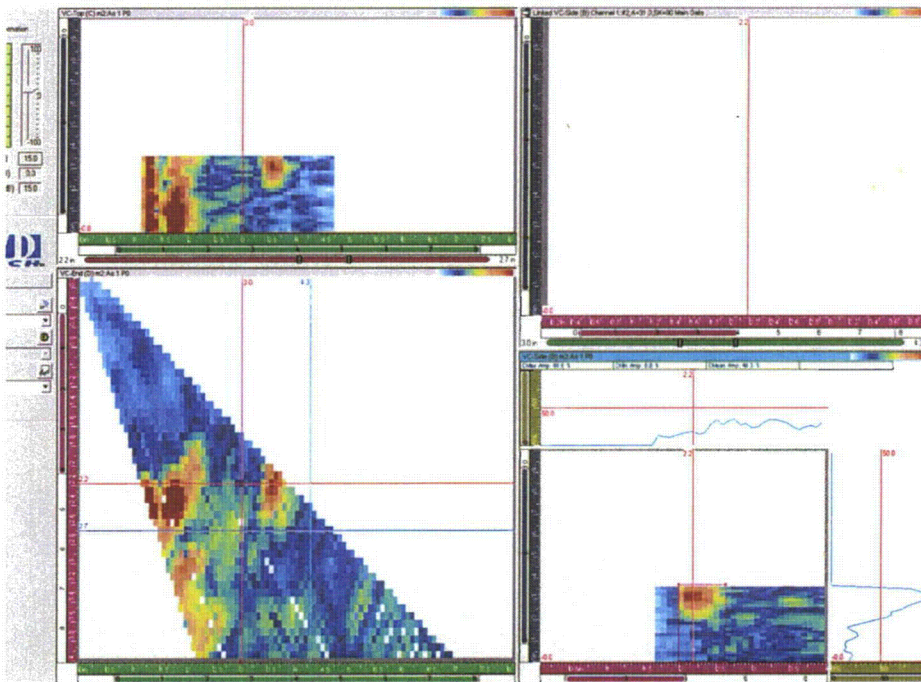


Figure C.38 B505 Inspected from the Equiaxed Side of the Weld with Merged Data, Showing a Yes Detected

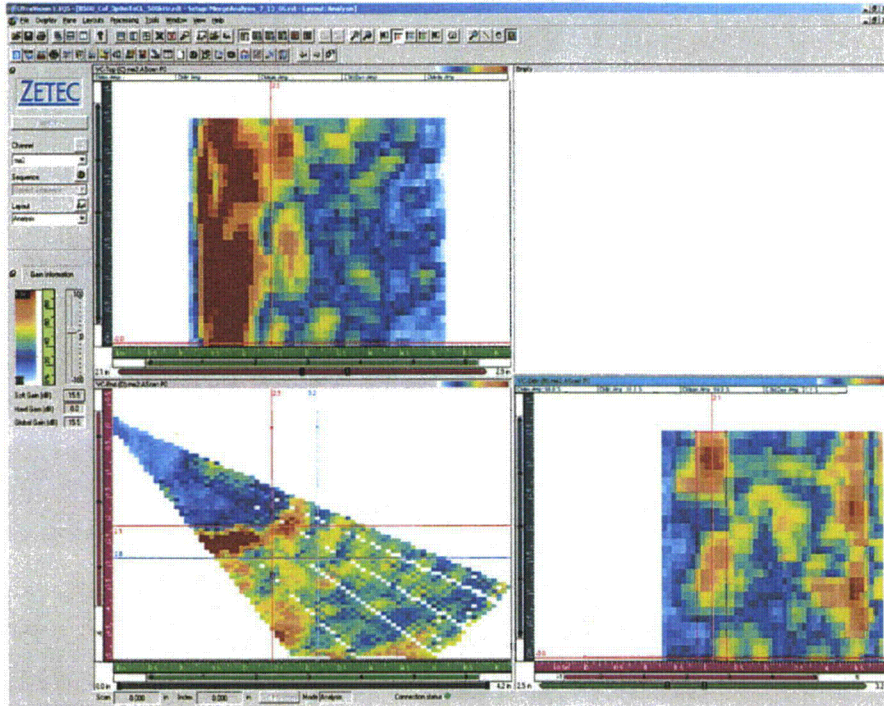


Figure C.39 B508 as Inspected from the Columnar Side of the Weld with Merged Data, Showing a No Detection

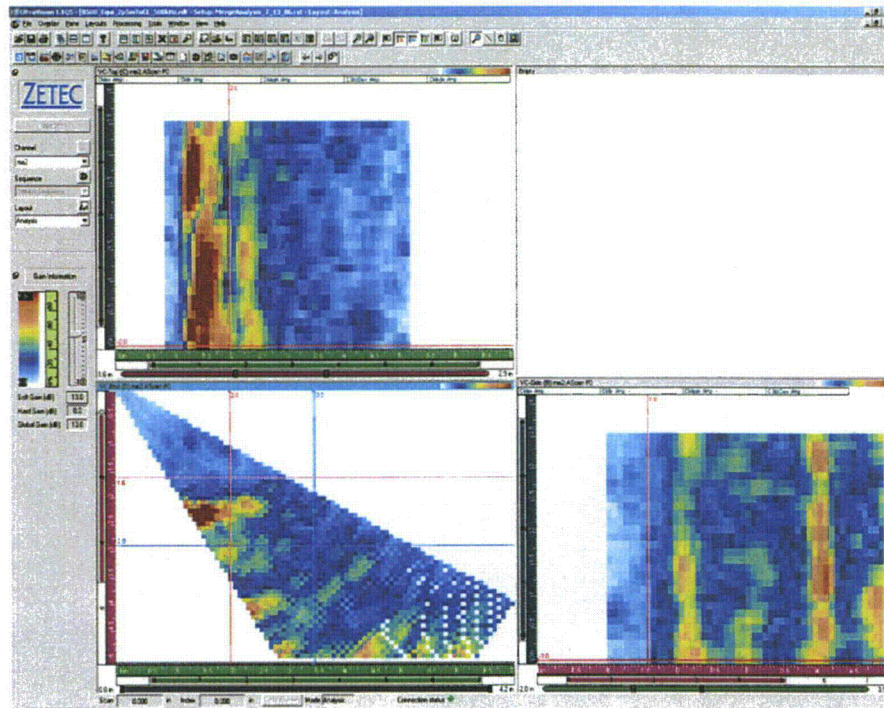


Figure C.40 B508 as Inspected from the Equiaxed Side of the Weld with Merged Data, Showing a No Detection

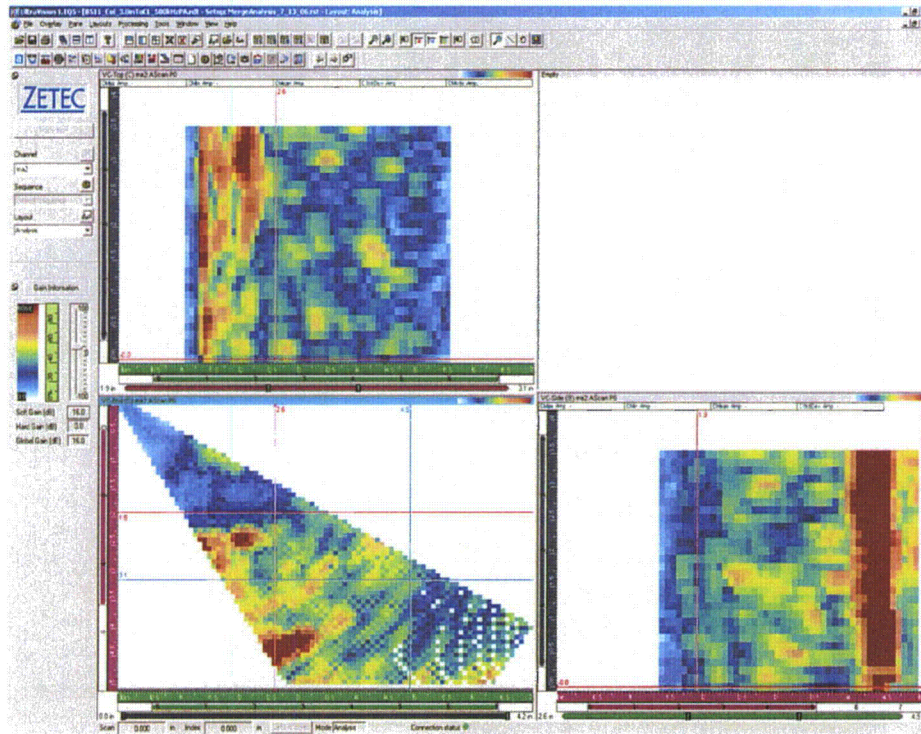


Figure C.41 B511 as Inspected from the Columnar Side. This is blank material, i.e., no crack.

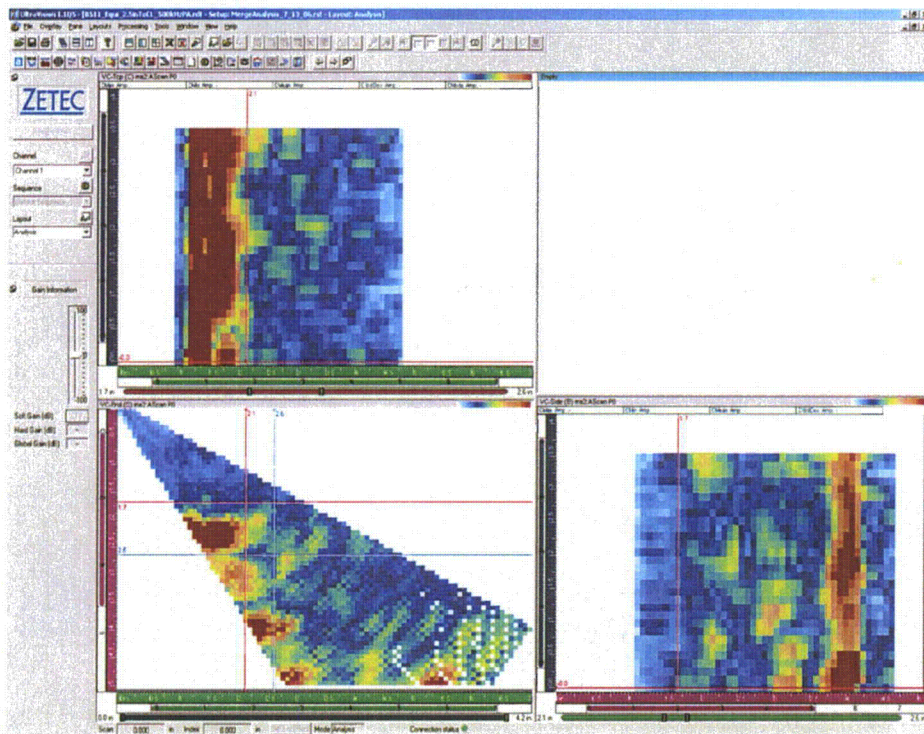


Figure C.42 B511 as Inspected from the Equiaxed Side. This is blank material, i.e., no crack.

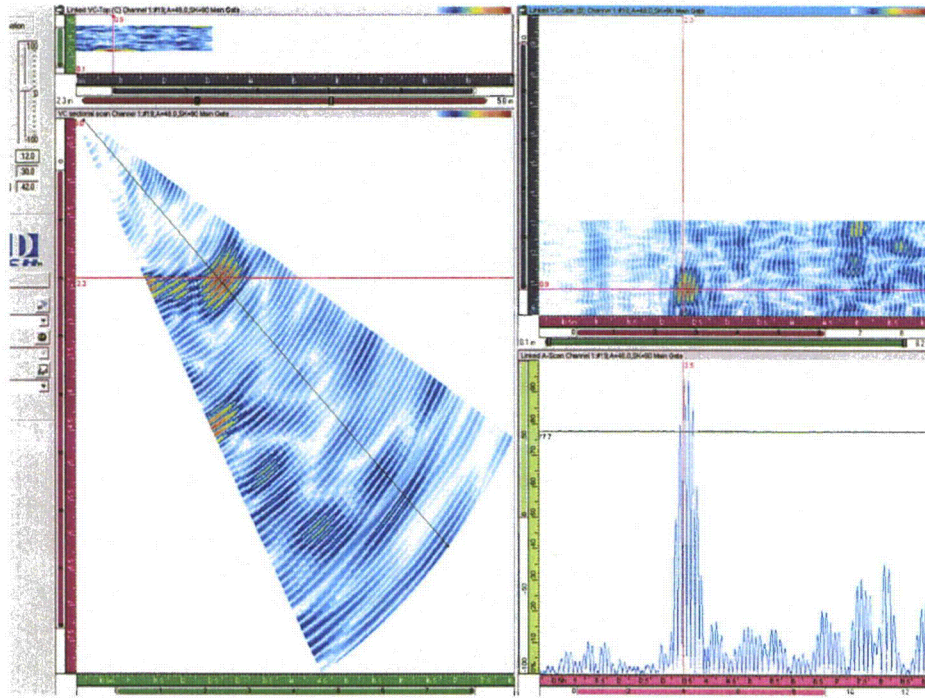


Figure C.43 B515 as Inspected from the Columnar Side of the Weld, Showing a Yes Detected

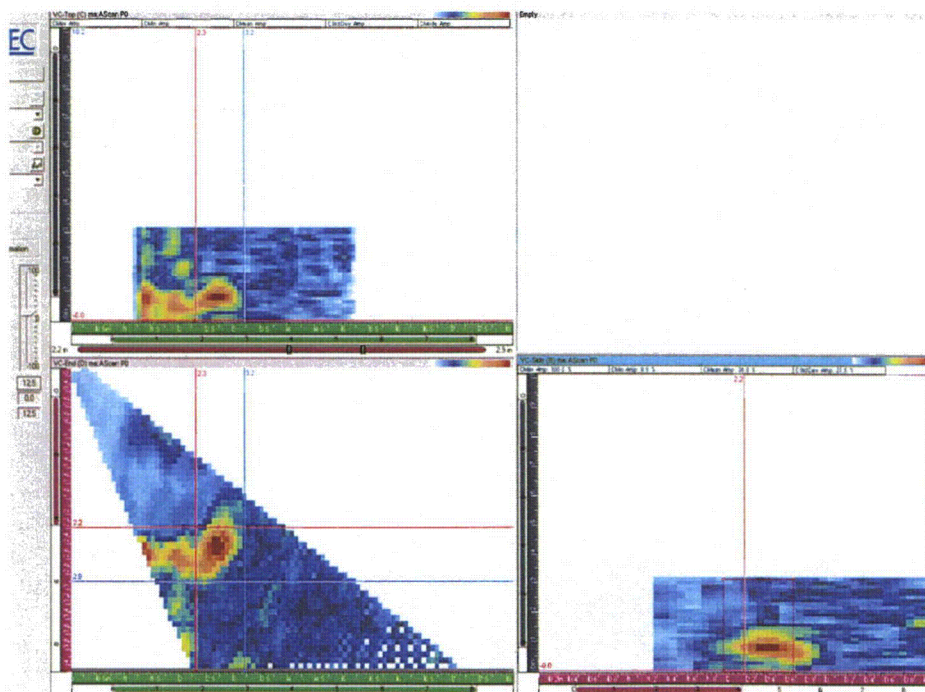


Figure C.44 B515 as Inspected from the Columnar Side of the Weld with Merged Data, Showing a Yes Detected

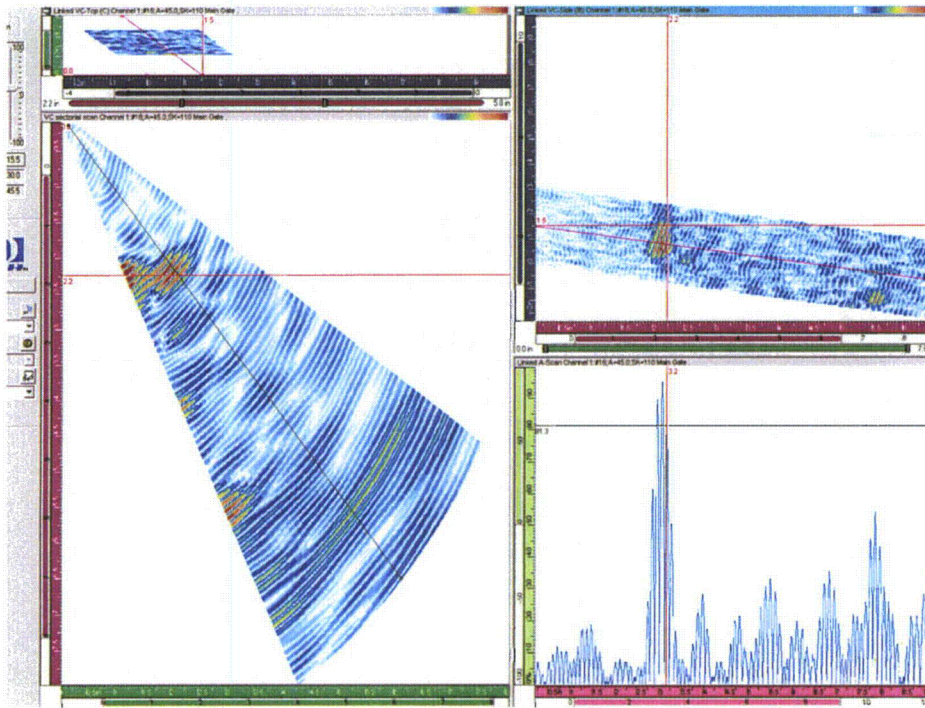


Figure C.45 B515 as Inspected from the Equiaxed Side of the Weld, Showing a Yes Detected

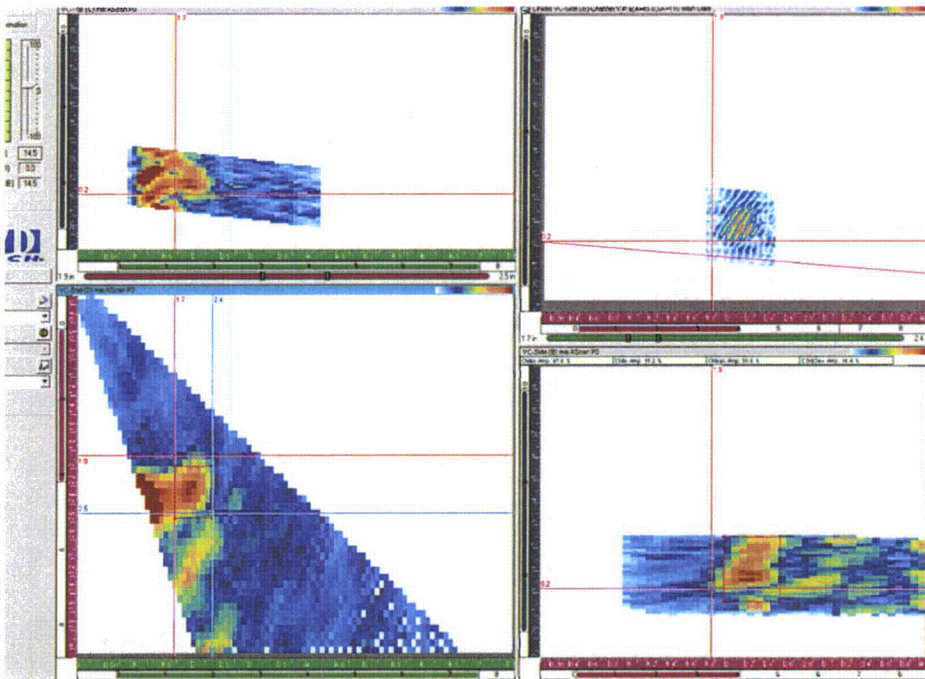


Figure C.46 B515 as Inspected from the Equiaxed Side of the Weld with Merged Data, Showing a Yes Detected

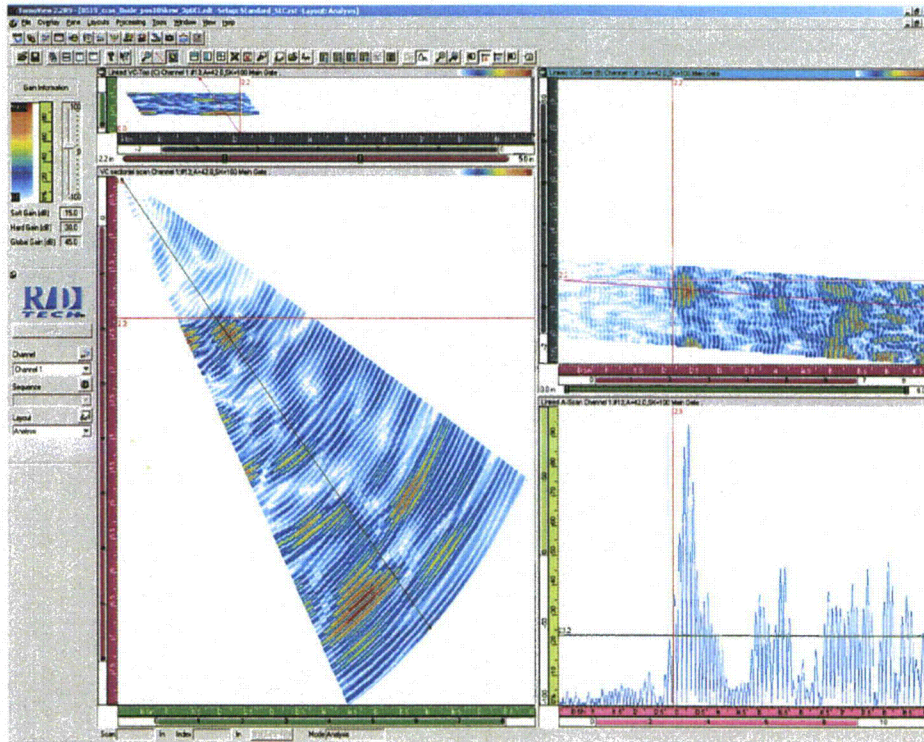


Figure C.47 B519 as Inspected from the Columnar Side of the Weld, Showing a Marginal Detection

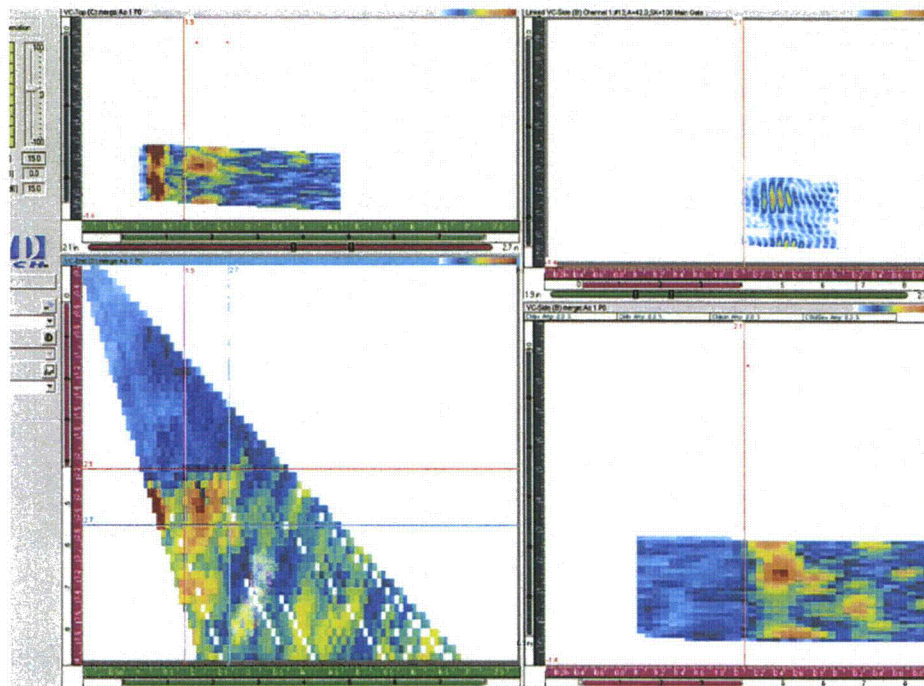


Figure C.48 B519 as Inspected From the Columnar Side of the Weld with Merged Data, Showing a Marginal Detection

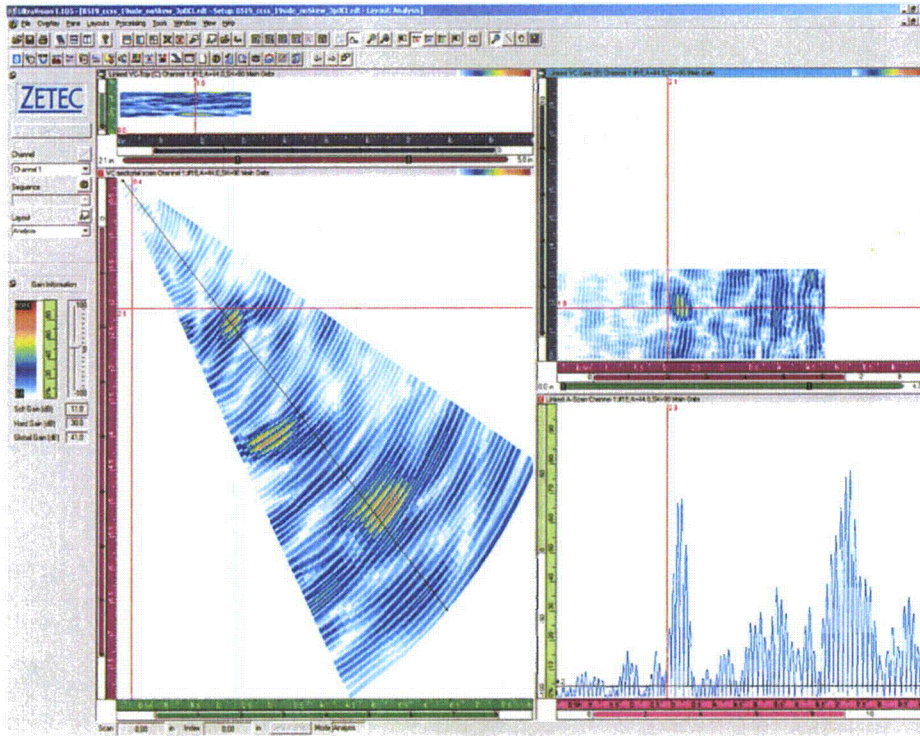


Figure C.49 B519 Inspected from the Equiaxed Side of the Weld, Showing a Yes Detected

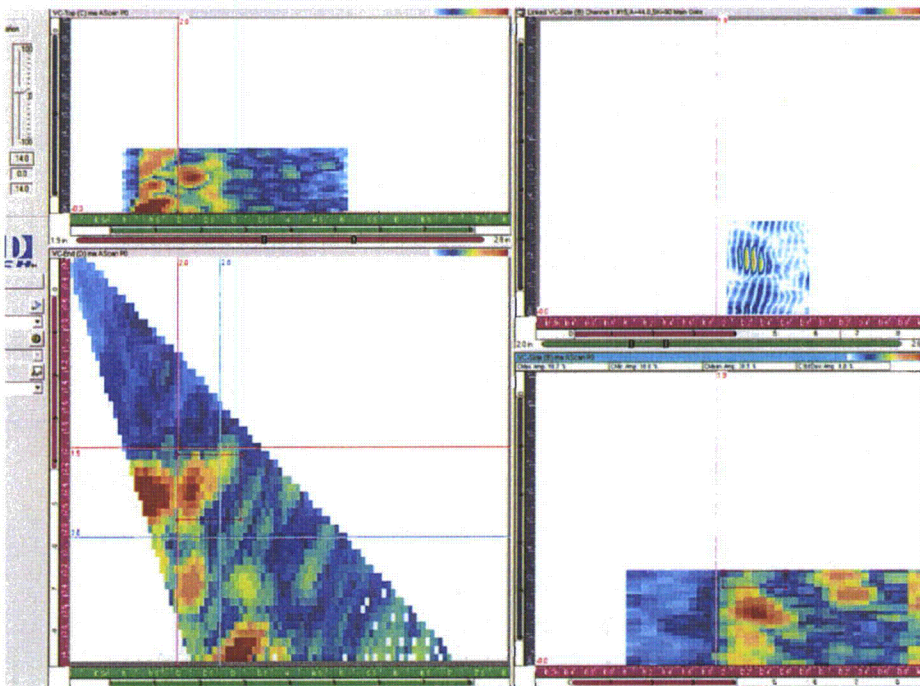


Figure C.50 B519 as Inspected From the Equiaxed Side of the Weld with Merged Data, Showing a Yes Detected

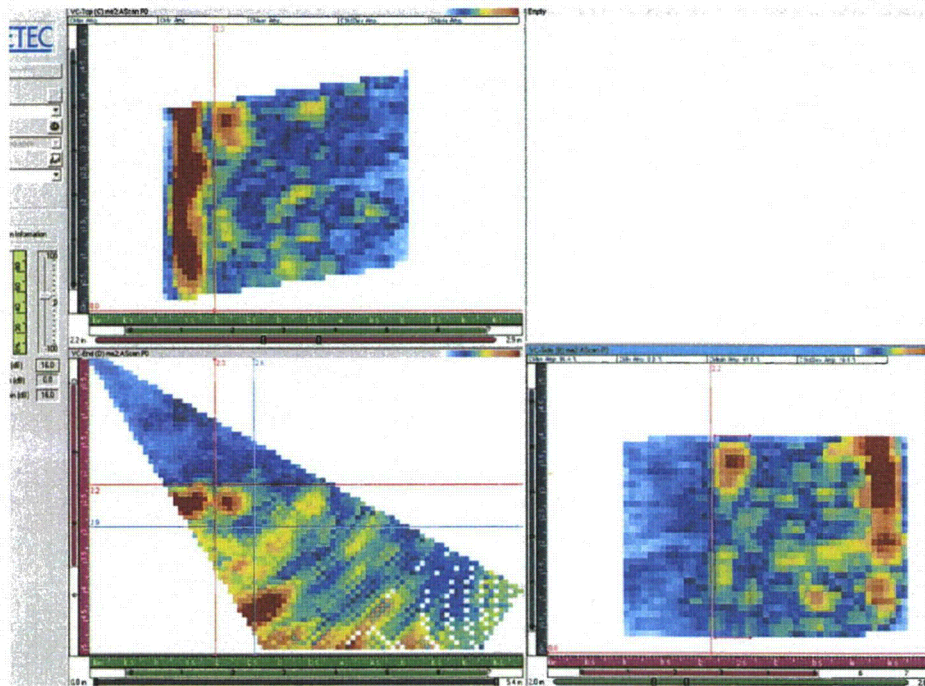


Figure C.51 B520 as Inspected from the Columnar Side of the Weld with Merged Data, Showing a Yes Detected

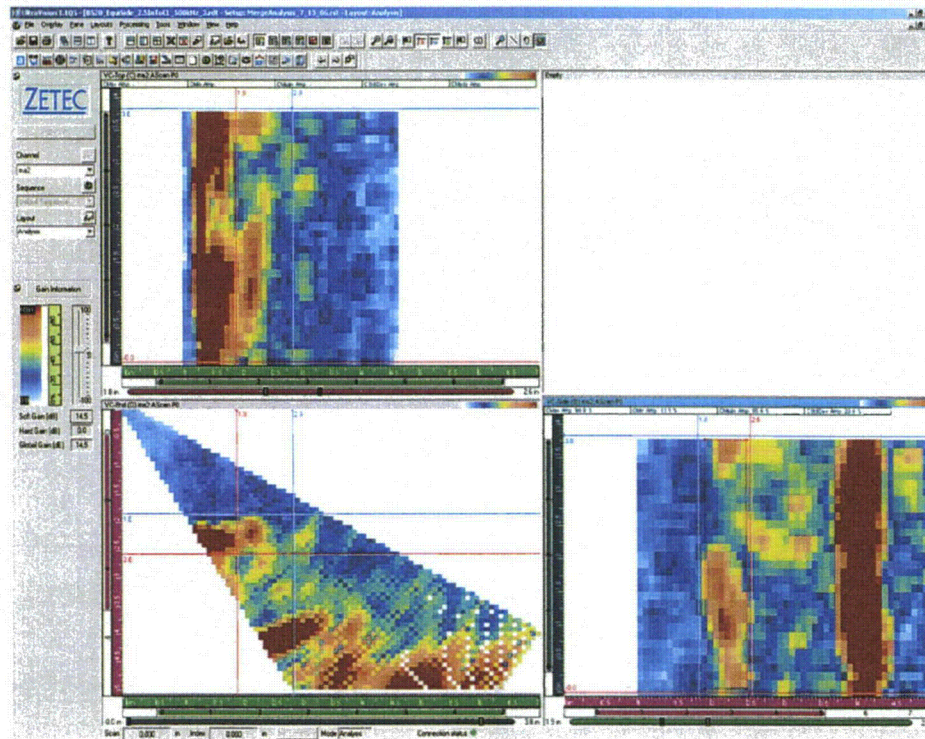


Figure C.52 B520 as Inspected from the Equiaxed Side of the Weld with Merged Data, Showing a No Detection

NRC FORM 335 (9-2004) NRCMD 3.7		U.S. NUCLEAR REGULATORY COMMISSION		1. REPORT NUMBER (Assigned by NRC, Add Vol., Supp., Rev., and Addendum Numbers, if any.) NUREG/CR-6933	
BIBLIOGRAPHIC DATA SHEET (See instructions on the reverse)					
2. TITLE AND SUBTITLE Assessment of Crack Detection in Heavy-Walled Cast Stainless Steel Piping Welds Using Advanced Low-Frequency Ultrasonic Methods				3. DATE REPORT PUBLISHED	
				MONTH March	YEAR 2007
5. AUTHOR(S) M. T. Anderson, S. L. Crawford, S. E. Cumblidge, K. M. Denslow, A. A. Diaz, S. R. Doctor				4. FIN OR GRANT NUMBER NRC Job Code Y6604	
				6. TYPE OF REPORT Technical	
8. PERFORMING ORGANIZATION - NAME AND ADDRESS (If NRC, provide Division, Office or Region, U.S. Nuclear Regulatory Commission, and mailing address; if contractor, provide name and mailing address.) Pacific Northwest National Laboratory P.O. Box 999 Richland, Washington 99352				7. PERIOD COVERED (Inclusive Dates)	
				9. SPONSORING ORGANIZATION - NAME AND ADDRESS (If NRC, type "Same as above"; if contractor, provide NRC Division, Office or Region, U.S. Nuclear Regulatory Commission, and mailing address.) Division of Fuel, Engineering and Radiological Research Office of Nuclear Regulatory Research U.S. Nuclear Regulatory Commission Washington, DC 20555-0001	
10. SUPPLEMENTARY NOTES D.A. Jackson and W.E. Norris, NRC Project Managers					
11. ABSTRACT (200 words or less) Studies conducted at the Pacific Northwest National Laboratory in Richland, Washington, have focused on assessing the effectiveness and reliability of novel approaches to nondestructive examination (NDE) for inspecting coarse-grained, cast stainless steel reactor components. The primary objective of this work is to provide information to the U.S. Nuclear Regulatory Commission on the effectiveness and reliability of advanced NDE methods as related to the inservice inspection of safety-related components in pressurized water reactors (PWRs). This report provides progress, recent developments, and results from an assessment of low frequency ultrasonic testing (UT) for detection of inside surface-breaking cracks in cast stainless steel reactor piping weldments as applied from the outside surface of the components.					
12. KEY WORDS/DESCRIPTORS (List words or phrases that will assist researchers in locating the report.) nondestructive examination cast stainless steel inservice inspection pressurized water reactors surface-breaking cracks low-frequency ultrasonic testing safety-related components				13. AVAILABILITY STATEMENT unlimited	
				14. SECURITY CLASSIFICATION (This Page) unclassified	
				(This Report) unclassified	
				15. NUMBER OF PAGES	
16. PRICE					



Federal Recycling Program